Theses and Dissertations	1. Thesis and Dissertation Collection, all items

1972

The dependence of compressor face distortion on test cell inlet configuration.

Tower, Philip William.

Monterey, California. Naval Postgraduate School
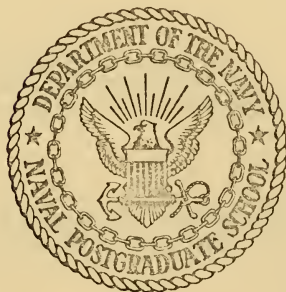
http://hdl.handle.net/10945/16062

THE DEPENDENCE OF COMPRESSOR FACE DISTORTION
ON TEST CELL INLET CONFIGURATION

Philip William Tower

NAVAL POSTGRADUATE SCHOOL
Monterey, California

THESIS

THE DEPENDENCE OF COMPRESSOR FACE DISTORTION
ON TEST CELL INLET CONFIGURATION

by

Philip William Tower

Thesis Advisor: Allen E. Fuhs

December 1972

T153111

THE DEPENDENCE OF COMPRESSOR FACE DISTORTION ON TEST CELL

INLET CONFIGURATION

by

Philip William Tower
Lieutenant, United States Navy
B. S., United States Naval Academy, 1965

Submitted in partial fulfillment of the
requirements for the degree of

AERONAUTICAL ENGINEER

from the

NAVAL POSTGRADUATE SCHOOL
December 1972

T 783

ABSTRACT

The aircraft turbine engine has evolved to the point that current
static test facility designs require modification to provide adequate
service and growth potential. Current design procedures are inadequate
in that they do not provide methods for the prediction of flow uniform-
ity at the increased thrust and air flow rates now being required.
Through the testing of a multiplicity of inlet models the effect of test
cell inlet configuration on engine distortion level is evaluated. A
method is developed for the correlation of inlet design characteristics
with experimentally observed distortion levels. Together with the eval-
uation of augmentor performance in an associated thesis by Lt. David L.
Bailey, this tentative correlation provides a basis for the development
of a practical system for the prediction of the performance of proposed
test cell designs.

TABLE OF CONTENTS

LIST OF TABLES

LIST OF FIGURES

7

ACKNOWLEDGEMENT

I. INTRODUCTION

The design of sea level test facilities for aircraft gas turbine
engines is a demanding and expensive enterprise. Introduction of the
turbofan engine configuration and the continuing demand for increased
thrust have made the uniformity of the engine inlet air flow a critical
design parameter. Techniques are available for the prediction of acous-
tic, thermal, and, to some extent, atmospheric emission characteristics
of proposed test cell designs.

Many industrial concerns whose products are used in test cell con-
struction offer consulting services which can provide pre-construction
analysis of these characteristics. Several architectural engineering
companies have experience in the design of efficient and durable test
cells and can predict many of the details of their operating conditions.
One factor which cannot be realiably predicted is the pressure or velo-
city profile which will exist at the compressor face when a future engine
is operated at various power levels in a proposed test facility.

Test cell inlet aerodynamic design can be described as rule-of-thumb.
As might be anticipated, this results in occasional, expensive failures,
and consistently uneconomical conservatism in design practice. This
research was intended to provide a foundation for the application of
modern aerodynamics to this current and practical problem.

The air flow through a test cell inlet is of low subsonic velocity
and ambient temperature. The lack of a comprehensive, practical method
of analysis (such as the USAF DATCOM provides for airframe design) is,
therefore, not due to the nature of the aerodynamics involved but rather
to the fact that one was not required in the past. Only in recent years

have cases of cell-engine mismatch become relatively frequent occur-
rences. Test cells designed without concern for the inlet aerodynamics
were adequate if sufficiently large. With the generation of aircraft
which included the 747 and the C5A, construction of test cells with the
required excess of flow capacity became impractical.

Inlet aerodynamics have thus become increasingly critical considera-
tions in facility design, and research became necessary. Many avenues
were open for the initiation of this research, and the choice of alter-
natives received careful consideration.

II. BACKGROUND

A. THE CHARACTERISTICS OF FUTURE ENGINES

Sea level engine test facilities designed and constructed in the near future will be expected to provide satisfactory service for twenty years or more. Economically sound test cell design requires the best available information about the characteristics of future engines. Many industrial and governmental planning agencies have direct responsibilities for the maintenance of engine development forecasts. Appendix C, Section II, provides a summary of these forecasts and the information required to obtain timely updates.

These forecasts and Fig. 1 illustrate the changes in engine design which have already resulted in premature obsolescence of many current test facilities. This trend toward increasing thrust, and correspondingly increased air flow rate, which is evident for all engine types, is in many cases coupled with an increase in exhaust temperature. Higher exhaust temperatures increase the quantity of cooling air required in the test cell and further emphasize the need to provide an aerodynamically designed inlet. Future engines will thus require total air flow rates which cannot be provided at the low flow velocities possible in the past. Increasing velocity in the inlet will emphasize its distortion producing characteristics and require proportionally greater flow length for the damping of generated distortion. Additionally, current engines and those proposed to follow them are less able to tolerate distortion than were similar engines in the past.
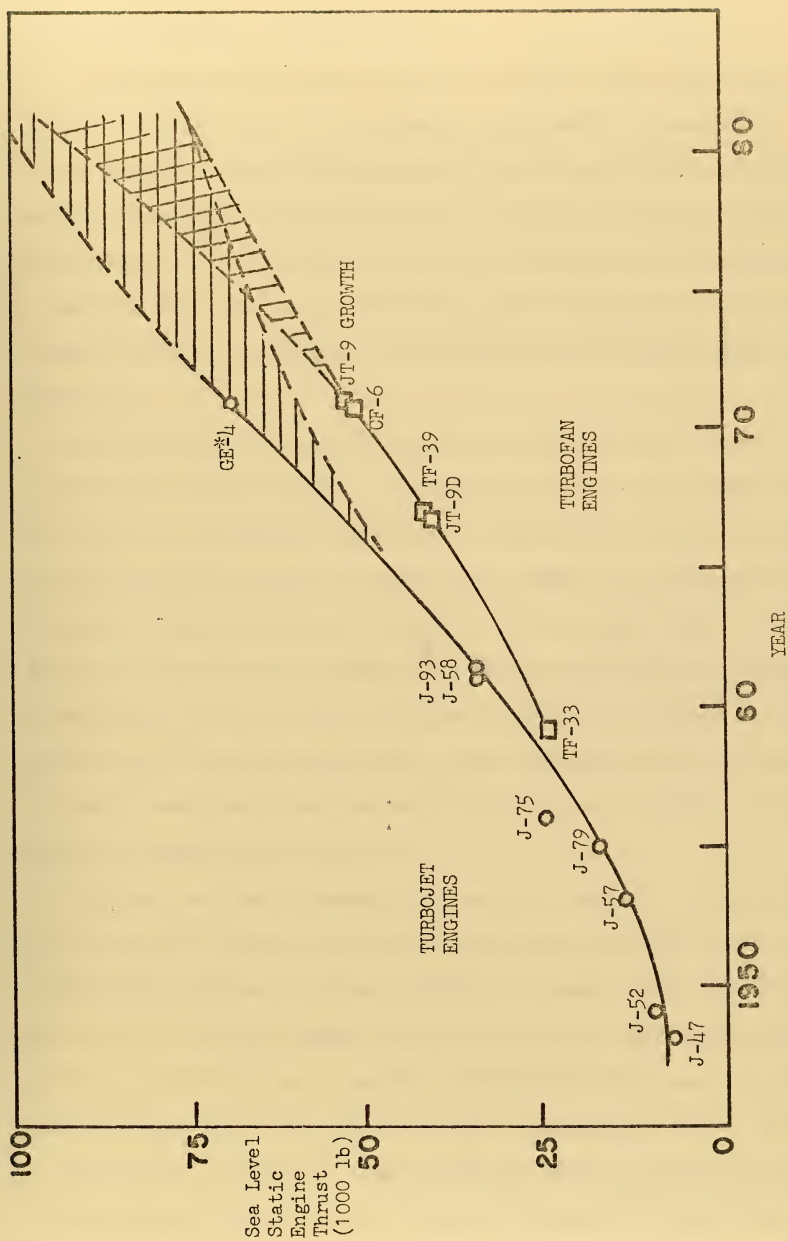
Figure 1. MILITARY AIRCRAFT ENGINE GROWTH

13

B. TEST CELL DESIGN REQUIREMENTS

If uniformity of the inlet air flow were the only consideration, test cell design would be a relatively simply matter. Complicating the design process are other considerations each conflicting to some extent with the requirement for uniform flow. Appendix C contains a complete discussion of the factors which must be considered in the evolution of a complete test plant design proposal. Those which most directly influence the inlet design may be classed as structural and environmental /Ref. 1/.

Included in the structural category are considerations of real estate costs and availability. Most engines of the turbine type must be tested in the horizontal position. A horizontal cell inlet would contain the fewest sources of distortion. However, this arrangement requires a larger building site than one with an equal length of inlet duct, a portion of which is vertical. The horizontal inlet also adds a requirement for a screened clean area in front of the inlet for protection again foreign object damage. Flow contract devices to improve the inlet aerodynamics must be compatible with the structural requirements for access routes and doors.

A third structural limitation on the inlet layout is the requirement for duct shut off doors to seal the inlet during operation of the fire extinguishing system. This shut off hatch is more simply installed at one side of the ninety degree corner in a vertical inlet configuration than in a horizontal one. Appendix C includes a discussion of the inlet configurations which meet these structural requirements and are in use at current test facilities. Construction techniques and economic considerations also limit the inlet design. An inlet of circular cross

section constructed of polished stainless steel may contribute to good
aerodynamic performance; but since experience indicates that less ex-
pensive designs can suffice, such a design is impractical.

The other restrictions on the inlet which complicate the analysis
and design process are environmental. Nearly all test cell sites require
some attenuation of the engine generated acoustic power propagating
through the inlet stack. Most of the available means of providing this
attenuation involve subdividing the inlet flow, with the attendant
mutiplication of distortion sources. Acoustic considerations also in-
dicate the use of the vertical inlet stack since this directs the un-
attenuated sound in the least damaging direction. Proper inlet design
must not only account for the effect of the acoustic treatment on inlet
uniformity but must provide space and a structurally sound position for
their installation. Flow control devices required for the conditioning
of the inlet flow will alter the performance of installed acoustic
treatment. Close coordination of inlet acoustic and aerodynamic design
is necessary for the development of designs satisfactory in both respects.

Environmental considerations also take the form of protection of the
test cell from its environment. In addition to screens for FOD (foreign
object damage) protection, which through type and placement may contri-
bute to the uniformity of the flow, test cells in some locations have
found it advantageous to filter the cell air supply. Removing dust and
other atmospheric pollutants improves the service life of cell instru-
mentation, but filter design and positioning must be considered in light
of its effect on flow uniformity as well   /Ref. 2/.

The exterior environment may also affect the cell operation directly,
and inlet design must account for the variation in wind direction,

15

velocity profile, and humidity /Ref. 3/. Most vertical inlets are
covered with rain caps of some type, and some are shielded from prevail-
ing winds. Either may radically change overall inlet aerodynamics
/Ref. 4/.

Considering the number and variety of factors which must be accounted
for in inlet design, it is apparent that the goal of the inlet aerody-
namicist must be adequacy rather than perfection. Rather than the de-
velopment of new and highly refined inlet components, the result of a
practical improvement in inlet analysis methods will be a rational
method for the arrangement, sizing, and modification of components now
being used in test cell construction.

C. INLET DISTORTION

1. Sources

The air entering an aircraft engine during inflight operation
is not perfectly uniform. Changes in angle of bank, pitch, and yaw as
well as altitude, configuration, and velocity alter the intensity and
pattern of this existing distortion. Much effort has gone into the de-
velopment of aircraft inlets which minimize these effects, but perfect
uniformity is not required. As a result, discussion of test cell inlet
distortion is confined to consideration of the ways in which the non-
uniformity of the flow into the first compressor stage differs in extent
and character from that encountered in flight.

The basic properties of the flow through the test cell duct are
fixed by the shape and dimensions of the inlet. The most common charac-
teristic of current test facilities is the rectangular cross section of
the inlet. Eckert /Ref. 5/ provides a summary of current theory of flow
of a gas in a rectangular duct. One common conclusion of all investigators

16

is that sharp corners produce, at all flow rates, extensive distortion effects which persist downstream of the corner for a distance well in excess of that found in test cells.

Cursory examination of typical dimensions for current test cells demonstrates the virtual impossibility of delivering a laminar air stream to the engine (a condition which has been specified in some recent construction proposals, such as Ref. 6). If an inlet cross section of twenty by twenty feet is considered typical, the hydraulic radius (defined as the ratio of duct cross sectional area to duct perimeter) is five feet. An engine requiring just 50 pounds of air per second (typical of the J37 helicopter engine) would produce a velocity of 16.4 feet per second at standard atmospheric density. This results in a duct flow Reynolds number of 2.06×10^6 in the open duct and higher values in restricted sections. Considering the natural roughness of typical concrete construction and the natural vorticity of the ambient air supply during windy conditions, it is reasonable to conclude that the transition Reynolds number will be at or near its mean value of 2000.[1] Thus turbulent duct flow is to be expected as well as turbulent boundary layers, on duct surfaces and all flow dividers.

Alternately, the large cross section of the inlet duct might encourage consideration of the flow as equivalent to that over flat plates. At a typical inlet mean velocity of 30 feet per second, a Reynolds number based on length of 3.5×10^5 corresponds to a length of

---

[1] Eckert and Irvine /Ref. 5/ summarize experimental works reporting transition Reynolds numbers varying from 800 to 6000 with duct shape, surface roughness, and vorticity of the ambient air supply.

1.10 feet. Although boundary layer transition may be delayed to some-
what higher Reynolds number values by careful conditioning of the flow,
the above value is considered typical for a test cell flow /Ref. 7/.
Thus a turbulent boundary layer will exist along nearly the entire flow
length even if a rough, square leading edge or lip separation produced
by external winds do not trip it at the upstream end of the inlet.

Turbulence does not necessarily contribute to the distortion of
the compressor flow and can in some cases act to redistribute energy in
a manner which smooths out variations in the velocity profile. Both
the interaction of the boundary layers in the square corners of the duct
/Ref. 8/ and the growth on all surfaces immersed in the flow produce
momentum deficiency which becomes distortion at the compressor face when
the test cell is operated with zero augmentation, i.e. all inlet flow
passing through the engine. The extent of this deficiency will be pro-
portional to the total surface area exposed to the flow, and its dis-
tribution will depend upon the inlet configuration and position of the
engine relative to the inlet components. Coupled with this effect is
the development of the velocity profile in the duct flow.

Eckert and Irvine /Ref. 5/ report varying estimates of the flow
length required to produce a fully developed velocity profile in rectan-
gular ducts. At a minimum, a flow length twenty-five times the hydraulic
diameter of the duct has been observed. Current test cells are typically
from 8 to 15 hydraulic diameters in length from inlet lip to compressor
face. At any power setting then, a developing velocity profile and
attendant vorticity are inducted into the engine. Additionally, the
development of the velocity profile varies with the mean duct velocity,
and distortion so produced will therefore vary with the power setting
of an engine under test.

18
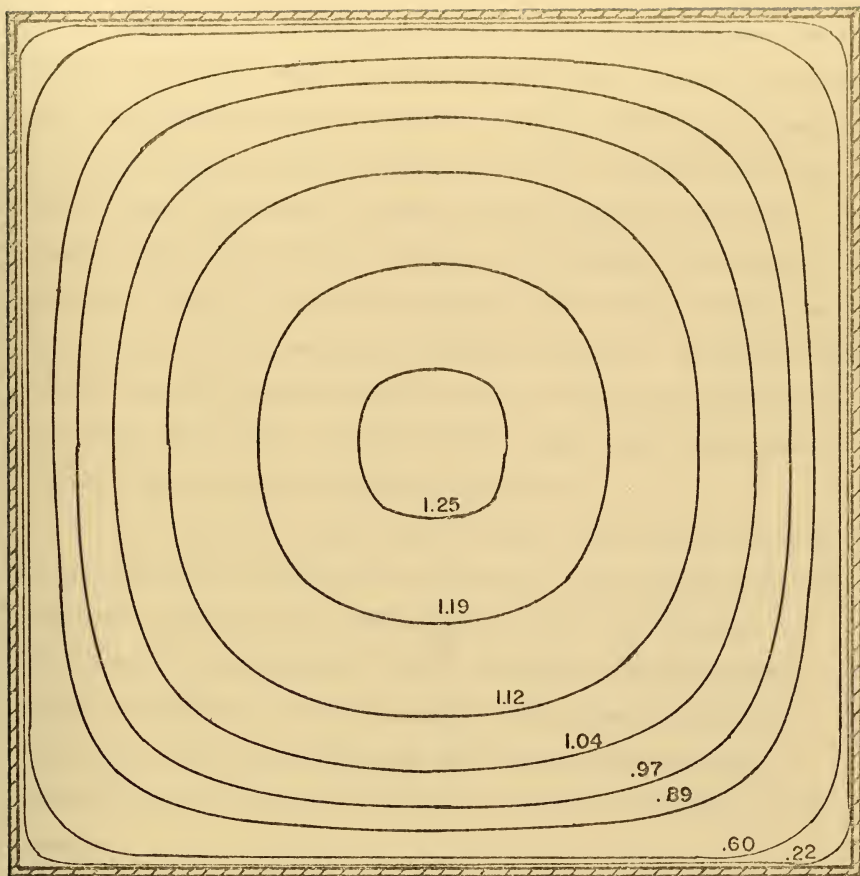
Indicated values are for the ratio $\dfrac{V_{local}}{V_{mean}}$

Figure 2. THE DISTRIBUTION OF VELOCITY IN A NONCIRCULAR DUCT WITH FULLY DEVELOPED VELOCITY PROFILE.

These considerations apply to flow in an open duct. Most practical inlet designs require acoustic treatment which subdivides the inlet duct into numerous straight or sinuous passages. Within these passages individual velocity profiles develop, and at the trailing edges of the baffles wakes are produced. Acoustic baffles normally have rounded leading edges and streamlined trailing ones to minimize the extent of distortion /Ref. 9/, but even the smoothest flat airfoil produces a wake which can persist for considerable distance downstream. To perform their acoustic damping function the surface of most baffles are constructed of perforated sheet metal, an aerodynamically rough surface which enhances boundary layer growth and turbulence generation.

For the typical design shown in Figure 3, the hydraulic radius of the passages between baffles is 0.48 feet. A flow length of 24 feet represents a common average and with this length fully developed flow will occur in these passages. The air discharged from the acoustic baffles will exhibit a highly irregular velocity profile with zero velocity at the baffle surface and, with fifty per cent blockage, a maximum of at least twice the open duct velocity at the center of each passage.

In addition to the acoustic treatment, there are usually other wake generators in the inlet flow duct. These may include structural members for an overhead engine transport system, lights, plumbing for CO_2 injection nozzles, frames for air filters and screens, and observation cameras or windows. If the center line of the inlet duct is not a straight line additional sources of distortion are introduced.

The evolution of secondary velocity components perpendicular to the duct axis is an inevitable result of a change in the direction of a
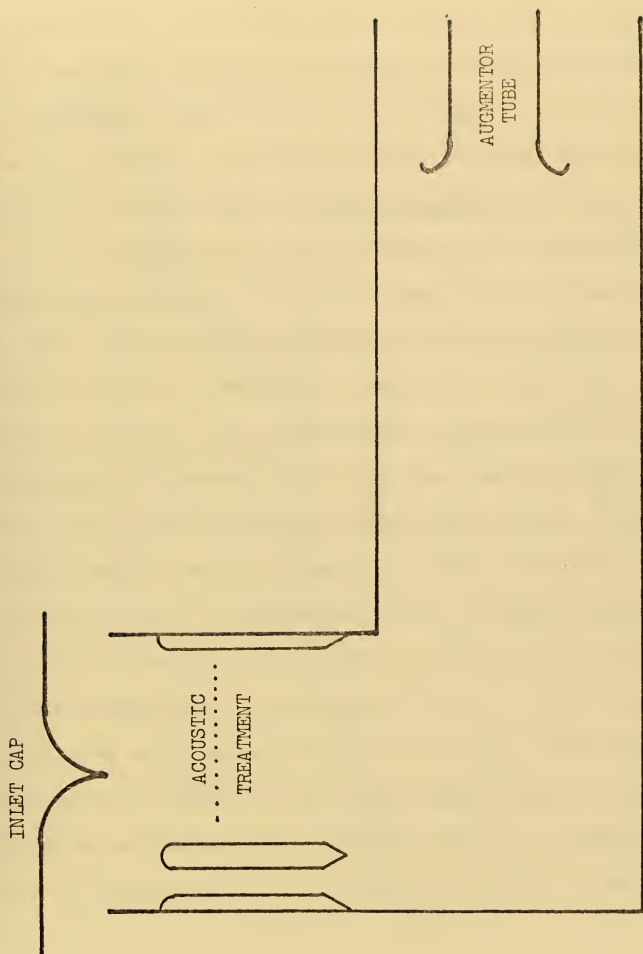
Figure 3. TYPICAL DIVISION OF INLET DUCT BY ACOUSTIC TREATMENT

INLET CAP

ACOUSTIC
TREATMENT

AUGMENTOR
TUBE

flowing viscous fluid. Figure 4 illustrates the process of production. Though in some analytical work the effect of this secondary flow is neglected,[1] this can be the case only when the concern is with average flow properties. In the investigation of distortion, the transfer of even one per cent of the flow energy into secondary components will have a significant effect on the detailed shape of the velocity profile. One per cent distortion persisting to the compressor face would use up one half of the stall margin allowed in current engines /Ref. 10/.

"In a straight duct with a developing velocity profile the flow possesses axial symmetry. This is no longer true for flow in bends." /Ref. 10/. A velocity profile which is not axially symmetrical at the compressor face is, by definition, distorted. Additionally, while it is common to assume, in the ducted flow of incompressible fluids, that static pressure is constant for a duct cross section perpendicular to the flow, this is not the case for flow around a bend. The construction techniques used in production test cells further complicate the effects of turning the inlet flow since the corner is commonly square at both the minimum and maximum radius. This is, in effect, a variation of the duct area expanding and contracting the flow as it enters and leaves the turn. The sharp corner at the inner radius of the turn can also produce an area of separated flow which causes additional contraction of the flow leaving the turn. The effectiveness of unguided square corners in producing distortion is confirmed in Ref. 10 where a reduction

---

[1] "Measurements on a bend of square cross section showed that the energy in the secondary flow after a 90° bend was only about one per cent of the energy associated with the axial velocity distribution " /Ref. 11/.

PG $\longrightarrow$ PRESSURE GRAD.

CF $\longrightarrow$ CENTRIFUGAL FORCE
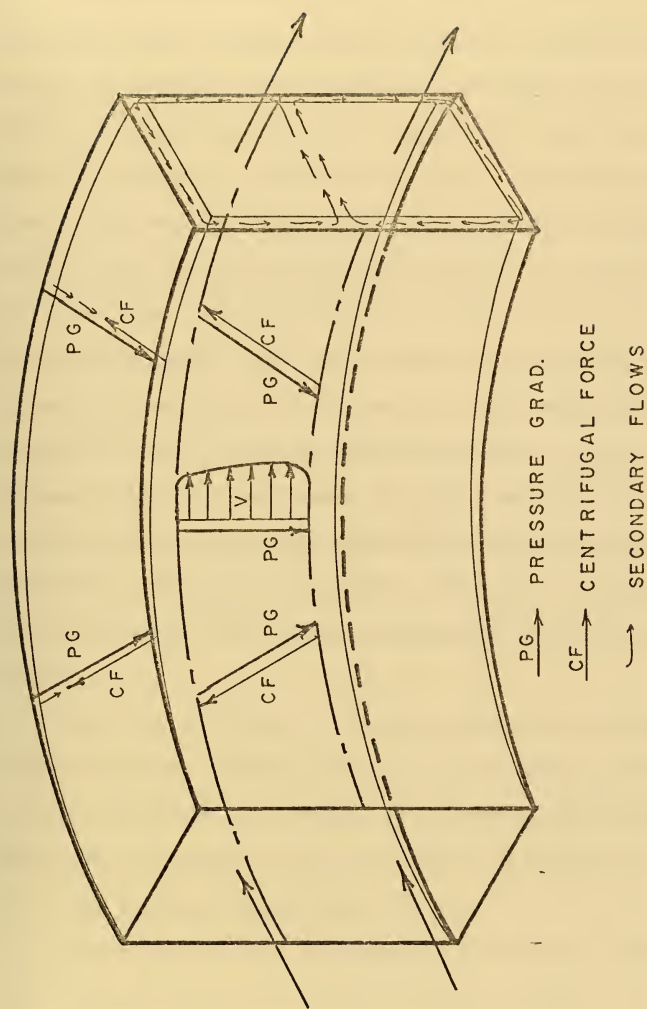
$\longrightarrow$ SECONDARY FLOWS

Figure 4. THE GENERATION OF SECONDARY FLOW IN TURNS BY THE IMBALANCE OF CENTRIFUGAL AND PRESSURE GRADIANT FORCES IN THE BOUNDARY LAYER

23

in distortion from 8 to 2 per cent was observed to result from the installation of turning vanes in the corner.

Augmentation of the engine air supply by routing some of the incoming air past the engine might be expected to reduce distortion by providing an alternate path through the test section for the low velocity flow near the duct walls. Two counter effects leave the final result of increasing augmentation uncertain. The augmentation naturally increases the mean inlet velocity and the consequent probability and extent of flow separation. Also, the addition of a flow past the engine inlet renders the engine susceptible to distortion from another source, the inlet vortex /Ref. 12/. The formation of this vortex, which produces intense localized distortion, is dependent upon many factors including the ratio of inlet and surface velocities and that of inlet diameter to distance from the duct surfaces. An engine undergoing test is at various distances from large plane surfaces and operates in a flow which may contain numerous sources of vorticity. This vortex, normally invisible, may be the source of some otherwise unexplained test cell data discrepancies.

The possible sources of distortion are numerous and to a large extent interrelated. Some variation of the velocity profile will exist in even the best test cell design. The effect of this variation on the engine must be understood before its control is undertaken.

2.   The Effects of Distortion

The effect of inlet distortion is to cause the blades of the first compressor stage to encounter varying velocities, either along their length (radial distortion) or at various positions during revolution (circumferential distortion). The blade is then at other than

design angle of attack at some position. Compressor blades are designed to tolerate some variation in angle of attack. The stall margin is the expression of this tolerance and represents the maximum variation in angle of attack, lateral extent of the variation, and its position. A distortion of the test cell inlet flow which exceeds the tolerance of the engine is unacceptable and one which is near this limit leaves no margin of safety for occasional transient fluctuations. In the aircraft...

"This distortion may result from the ingestion of hot exhaust gases or low energy boundary layer air from the fuselage or wing surfaces, boundary layer separation within the inlet, inlet lip separation at high angles of yaw or attack, or clear air turbulence " /Ref. 13/

The propagation of these distortions through succeeding stages is highly dependent on the design of the particular engine. Exhaustive testing of a fully instrumented turbofan TF30-P-3 reported in Ref. 13 produced the following picture of distortion history.

A circumferential distortion of 10 per cent[1] was attenuated to less than one per cent at the compressor discharge. Radial distortion of 17 per cent at the compressor face produced no significant distortion of the flow into the combustor but did reduce the absolute pressure level at this position. The circumferential distortion caused a 4.5 per cent loss in fan hub compression efficiency, a 3.6 per cent loss in the core compressor, and a 1.5 per cent decrease in pressure ratio.

"In summary, radial inlet pressure distortion effects on compressor component performance were greatest at the fan and attenuated

---

[1]
Defined as the difference between maximum and minimum total pressure divided by the compressor face average.

downstream, whereas, circumferential inlet pressure distortion showed
least effect at the fan but an increasing one on downstream components "
/Ref. 13/

Extensive research and developmental engineering effort goes
into the determination of distortion sensitivity of every new power
plant. References 14 to 20 provide summaries of the work accomplished
and underway in the analysis of engine-inlet matching in which distor-
tion is of primary concern. Many of the recent difficulties in the
development of the F 111 fighter were the result of excessively dis-
torted velocity profiles being delivered to the compressor. The result
of advances in engine technology in the past decade has been the develop-
ment of engines with greater propulsive efficiency, power, and operating
ranges of altitude and speed. One side effect of these improvements has
been the reduction of the stall margin in many engines. This condition
is responsible for increased research in aircraft inlet design and has
two important consequences for the test cell designer and operator.
The first of these, as outlined in Section II, is an increase in total
cell air requirements, with the overall effect of intensifying the
distortion produced in current test facilities. The second is reduc-
tion of the permissible distortion level. The total effect then of
nonuniformity of the inlet flow is to alter the engine operating condi-
tion and the results of static tests. In the extreme case, stall occurs,
and the engine cannot be tested safely. In any case, distortion reduces
the validity and utility to test results. Inlet design must then reduce
distortion to the lowest level consistent with economic, acoustic, and
maintenance restrictions.

III. ANALYSIS METHODS

A. REQUIREMENTS

To justify the analysis effort, it must be possible to anticipate a result which will either further the understanding of the natural phenomena involved or be of practical use in the application of existing theory to problems of engineering interest. The nature of the flow through the test cell inlet (low velocity, viscous, ducted, and turbulent) makes it somewhat unlikely that any analysis, however thorough, will contribute substantially to the theory of gas dynamics. The phenomena involved in the production of distortion are, individually, well understood and adequately documented.

It is then a basic requirement that the method of analysis employed be such that its results are amenable to direct engineering application. With regard to test cell design, this implies a flexibility for application to a large number of possible configurations, sizes and flow rates. A complete analysis would involve the accurate prediction of all flow properties at every point in or near the test cell for each possible engine power level and augmentation ratio combination. The ultimate aim of such an analysis system would be the specification of the optimal inlet for any established set of parameter engines, permissible acoustic levels, and land availability. There is, theoretically, no reason why such an analysis system cannot be developed. Some of the possible approaches to the development of such a system are considered in the following paragraphs with a discussion of the probability for success and projected cost of each method.

27

B. AVAILABLE ALTERNATIVES

1. Direct Integration of the Navier-Stokes Equations

The motion of real fluids and the spatial and temporal variation
of flow properties are completey described by the full Navier-Stokes
equations. The nature of any Newtonian flow system, including that of
air through a test cell inlet, could theoretically be determined by a
solution of Navier-Stokes equations. Two characteristics of the inlet
flow simplify the form of the equations required to describe this flow.
One is the relatively low velocity which permits the assumption of in-
compressibility to be applied throughout the flow field. The second is
the absence of significant heat transfer to or from the inlet flow,
which allows its treatment as an adiabatic system.

Given these simplifications and access to a digital computer one
might anticipate success in what was once considered an unlikely prospect.

"The theoretical method involves the integration of the
equations for unsteady motion in a way which has never been
accomplished and which, considering the general intractability
of the equations is not promising."
Reynolds (1883)

Several methods for the accomplishment of this unpromising inte-
gration are now available $\sqrt{R}$efs. 21, 22, 23, and 24$\sqrt{\ }$, and one might
consider their application to the prediction of inlet distortion. Two
difficulties are quickly evident, and one is the enormously complex
nature of the required boundary conditions. Not all inlet surfaces are
solid (acoustic treatment usually requires perforated surfaces), and
these surfaces are vastly more extensive, numerous, and interactive
than any of the combinations found in current literature. Given suffi-
cient talent and resources, it may be possible to overcome this difficul-
ty, but the second peculiarity of this analysis must first be considered.

The duct which comprises the test cell inlet is one of the largest encountered in aeronautical engineering applications. The turbulent nature of the resulting flow does not eliminate the theoretical solution of the Navier-Stokes equations. But, in spite of the computational capacity of the digital computer, it cannot yet approach the almost infinite complexity of nature.

Corrsin /Ref. 23/ provides an excellent review of the nature of turbulent flow and the techniques which have been developed for its exact and approximate analysis. The most basic factor in the exact analysis which employs the method of finite differences is the size of the computational grid established within the flow volume. In turbulent flow it is essential that the spacing of these grid points not be greater than the size of the smallest significant motion. The best estimate of the average turbulent eddy size is 1/10 the characteristic dimension of the duct /Ref. 23/. If the Reynolds number is greater than 10^4 (which it will be in nearly all test cells), the size of the smallest turbulent eddies will be 10^{-4} times the typical test cell characteristic length, or 0.005 feet. "This is the maximum allowable spacing of the lattice points; actually there is significant flow structure which is smaller." /Ref. 21/

Given that adequate numerical methods are available to permit integration of the equations of motion between points, a test cell duct (taking the volume to be the cube of the characteristic dimension) must contain a minimum of 10^{12} lattice points. At each of these, three velocity components and pressure gradients must be evaluated. Even when the cell flow is macroscopically steady, it is decidedly not so on a microscopic scale; hence, temporal variation must also be accounted for.

Additionally, even efficient differencing methods require that fifty to one hundred iterations be made at each point. Computation will then utilize some 4×10^{14} computer storage sites. This is well in excess

29

of the capacity of even the most advanced current system. It must be clear that while a solution might be attempted by subdivision of the flow system, the effort involved would be enormous, the results short of a complete analysis, and the cost unjustifiable relative even to the cost of a modern jet test facility. No other method is theoretically capable of determining all flow properties at every point so the goal of a full numerical analysis is presently unattainable.

2. Simplified Navier-Stokes Equations

If mean flow properties were of sufficient value, the time dependence of the equations of motion might be eliminated and the flow treated as completely steady. Perhaps the greatest simplification would result from the assumption of laminar flow throughout the duct since a large body of theoretical analysis techniques could be used in the analysis. Unfortunately the flow lengths involved in the test cell are so long that the difference between turbulent and laminar boundary layer thicknesses at the downstream end of the inlet approaches the total duct height.

Of perhaps equal assistance would be the assumption of inviscid fluid behavior. Valentine /Ref. 25/ provides a complete procedure for the analysis and design of two dimensional ducts for subsonic inviscid fluids. The thickness of the boundary layers which are present in the cell, the wakes of all cross duct obstructions, and viscous damping effects make it unlikely that the results of such an analysis would be useful in distortion prediction. Burggraf /Ref. 23/ provides a thorough explanation of the reasons that inviscid analysis cannot account for ducted turning flow phenomena and proposes a form of viscous correction factor. Dwyer /Ref. 22/ proposes a method for including viscous effects

30

in a rapid calculation procedure but points out that the analysis is then restricted to flow upstream of the first separation point. Even in the most carefully designed inlet, areas of separation will occur and cannot be ignored since they will contribute significantly to the distortion level.

The analysis of separated flows has been investigated /Ref. 23/, and presumably the established techniques could be combined with a linearized solution of the equations of motion for the flow in the remaining unseparated areas. Again the practical limitations are formidable. Burggraff /Ref. 23/ reports a computation time of 30 minutes for the analysis of the flow past a single circular cylinder at a Reynolds number of 400. He observes that as this number is increased, convergence slows, increasing the number of iterations required, and that the mesh size must be decreased to maintain accuracy. In a qualitative manner, this indicates the effort involved in analyzing a flow at a Reynolds number of the order 10^6 passing through the 50 to 100 interacting flow regions of the typical cell inlet.

It thus appears that while theoretically possible, no complete solution of the exact flow equations is practical even when all possible simplifications have been made.

3. Approximate Theoretical Methods

A summary of approximate analysis methods applicable to subsonic flow, a portion of which is reproduced in Table I, is presented in Ref. 25. In addition, this reference provides an annotated bibliography with a brief description of the available methods. A review of these makes it apparent that none of these methods can be directly applied to the total cell inlet flow. The following restrictions apply to one or more of these approximate methods:

31

METHOD	APPLICABLE CONFIGURATIONS	RESULTS
1-D Isentropic gas relations	Symmetric 2-D or axisymmetric shapes with low divergence angles	Inviscid, uniform stream props. and adequate 1st order est. for boundary layer calculations.
Valentine's geometric /Ref. 26/	2-D shapes with bends and/or con-divergence	Inviscid flow props. and wall pressure and velocity distribution
Kline and Johnson	Symmetric, non-turning, 2-D 3-D if conical or annular	Pressure recovery for unstalled diffusers, includes entrance B.L. and corner effects
Shin and Johnston	Curved 2-D diffusers	Performance efficiency as function of turn angle and area ratio
Crosthwait	General shapes	Guidelines for geometrical parameters within which acceptable performance can be expected, based on past test results.
Stanitz	2-D ducts with known wall velocity distributions	Complete inviscid flow field velocity distribution

Table I.   SUMMARY OF SUBSONIC FLOW ANALYSIS METHODS

32

1. One dimensionality

2. Two dimensionality

3. Inviscid flow

4. Uniform flow velocity

5. Straight ducting

6. Fully developed duct flow

7. Purely laminar flow

8. Unseparated flow

9. Circular ducts

10. Potential flows

Any of these restrictions prevent application of the method to the total inlet flow. There remain some general methods dealing with turbulent boundary layer growth and subsonic flow in non-circular ducts. These may be divided into two categories. The first class is based on application of the momentum theorem; and while directly applicable to the inlet, they yield only average flow properties /Refs. 25, 27, 28 and 29/. These are useful in the prediction of test cell depression;[1] however, as detailed in appendix C, this value is usually far less critical than the level of distortion. Since these handbook methods are available for the evaluation of duct pressure losses in the types of components used in test cells, the application of these analytical methods is not justified.

The second class of applicable approximate methods includes those based on turbulent boundary layer theory. Schlicting in Ref. 31 provides as introduction to the theoretical development for these methods and

---

[1] Defined as the difference between ambient static pressure and that measured at the engine bellmouth.

additionally provides a comprehensive guide to the available research results. The complex nature of the interior duct surface is again the difficulty in attempting this application. Semi-empirical boundary layer theories are available for the treatment of external flows past flat and curved surfaces and internal flows in unobstructed ducts /Refs. 7, 30, 31, 32, and 33_7; however, none of these includes a theoretical development for the region in which the boundary layers of perpendicular surfaces intersect. Additionally, the majority of the empirical data used to determine the values of the exponents in these proposed equations were obtained for areas with fully developed velocity profiles.

Before these boundary layer methods could be applied to the inlet flow, it would be essential to divide the flow into regions which could be treated separately. This division would require prior knowledge of streamline placement and areas of flow separation. The effect of turning, expansion-contraction, screens, and damping lengths could then be individually assessed using available techniques, provided the complete approach velocity profile were available at each component /Refs. 11, 26, 34, 35, 36, and 37_7 The validity of this approach would be highly dependent on the division system used. Several methods might be employed to predict the required streamline position data.

4. Electrostatic Modeling

Though it has many inherent limitations, the use of this simulation is so rapid and inexpensive that it must be carefully evaluated. Figure 5 illustrates the type of information available from this method. The most basic limitation is the two-dimensional nature of the technique. The flow is naturally potential; and while streamline spacing may be taken as indicative to 2-D property variation, the effects of turbulence, boundary layer, and circulation are absent.
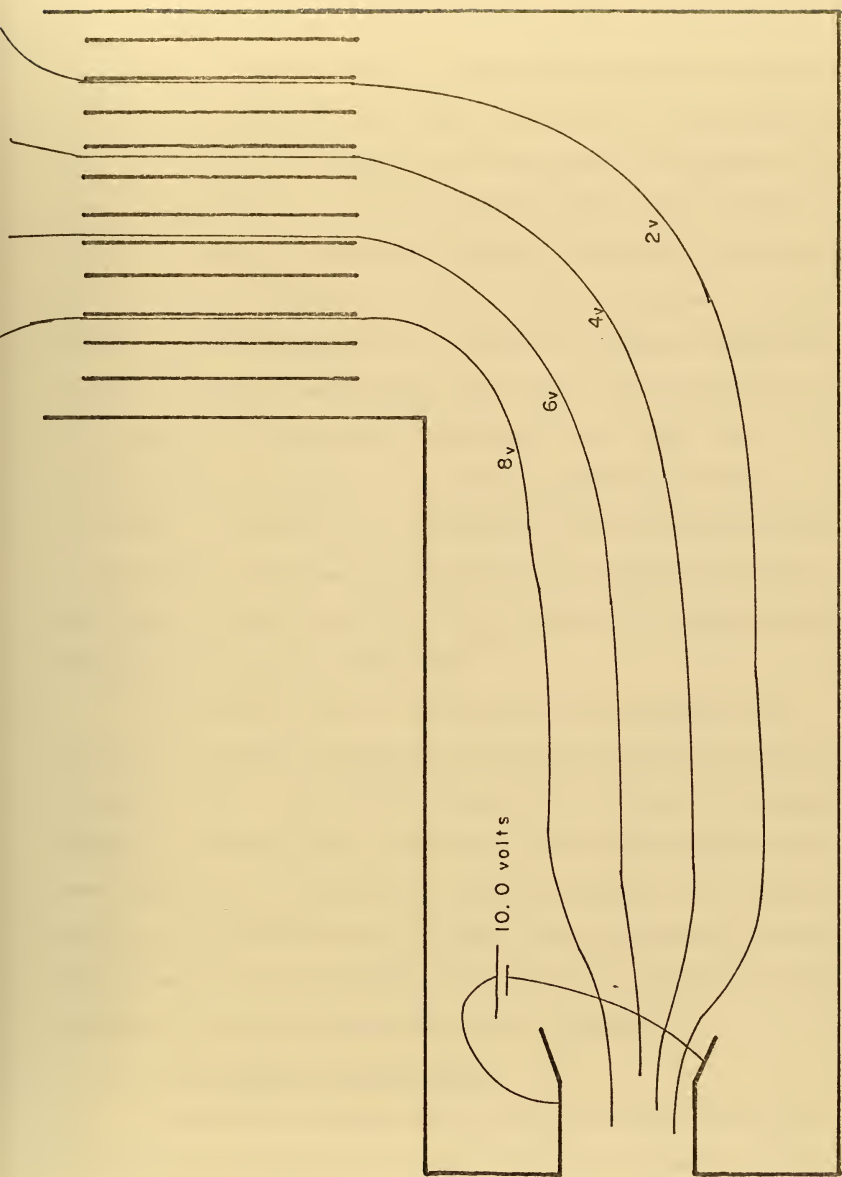
Figure 5. ESTIMATION OF STREAMLINE POSITION BY MEASUREMENT OF ELECTROSTATIC POTENTIALS ON A SLIGHTLY CONDUCTIVE SURFACE

35

For a first estimate of streamline patterns, this method provides a relatively simple solution with inexpensive equipment and might be used to divide the inlet duct into similar flow regions. Also, a general picture of the effect of component size and position is available through repeated application. By suitable repositioning of the electrode lines and the inclusion of equipotential surfaces in the plot of each duct, it is possible to observe the results of length variation on the uniformity of the velocity profile. With some refinement, namely the inclusion of multiple power sources, the effect of cell augmentation may be included in the study, and an estimate of its effects made. It is possible that the analysis of the inlet flow might be furthered by the comparison of streamline and equipotential surface positions obtained in this manner with those resulting from other theoretical methods. The change of position might be used to evaluate the changes produced by viscosity and vorticity of the flow.

The greatest practical difficulty in this analysis is the necessity to produce an entirely new conductive drawing for each configuration tested. The ability to assemble the layouts from component pieces would simplify the procedure and is considered feasible with some modification of commercially furnished equipment. The classroom instructor kit manufactured by the Pasco Scientific Company was used in the evaluation of this procedure and should provde adequate for initial attempts to continue investigation with this method.

5. Three Dimensional Scale Models

Construction and operation of inlet scale models offers the opportunity to include in the analysis the natural effects of geometry, viscosity, and turbulence which contribute to the character of the

36

velocity distribution in the actual cell. Model studies by-pass the
difficulties of the theoretical mathematical treatment, but in doing so
create other difficulties. Without a theoretical basis to predict the
results, the analyst must develop a system which permits the test re-
sults to be generalized. In specific cases, where a single proposed
design is of interest, an instrumented model is the most efficient means
of analysis currently available. Even in this single configuration case,
careful consideration must be given to the selection of instrumentation,
scaling factors, and the simulation of power settings and augmentation
ratios. Reference 38 is typical of the results that can be obtained
through this type of analysis. Many of the considerations necessary
for this effort are similar to those involved in wind tunnel operation.
The numerous references available in this field and the utilization of
personnel experienced in tunnel design and operation can be expected to
simplify this form of inlet analysis and increase confidence in the
results.

    While an analysis of model inlet test data cannot be expected
to meet the goal of full understanding of all flow properties, it can
meet the analysis requirement of permitting direct engineering appli-
cation. Properly conducted, this analysis also can approach the goal
of inlet design optimization. The following section considers the
questions which must be resolved in the design of an inlet model test
program before results can be applied to inlet configurations in general.

IV. INLET MODEL TESTS

A. GENERAL CONSIDERATIONS

Perhaps the most general concern in model studies is that of economy. This takes many forms, and one of these is generality of the results. The models must be designed, constructed, and operated in such a way that the results permit valid conclusions to be reached concerning full scale systems. The fewer the restrictions on the application of the results to a wide variety of possible configurations, the greater the economy of the operation.

It is necessary to test a multiplicity of configurations to achieve any degree of generality. Minimization of cost and effort in the construction of necessary number of models will be furthered by the utilization of interchangeable modular components. Economy also is necessary in the handling of the experimental data. Even with minimum instrumentation, the requirement for tests of numerous configurations and operating conditions can be expected to produce a large quantity of data. Processing methods must be planned to efficiently handle this data while providing the flexibility required for the establishment of correlation and prediction methods.

B. CONSTRUCTION

1. Selection Criteria

Prior to the design of the model several decisions were necessary concerning: scale, materials, configuration, and assembly methods. Single piece models have been constructed for use in test programs conducted to evaluate the performance of specific proposed inlet designs

38

/Ref. 38/. Interchangeable model components reduce greatly the cost of providing the required number of different inlet configurations.

The ability to repeatedly assemble the model components required the utilization of a construction material other than the cast concrete used in actual cell construction. Sheet metal was a logical alternative since it is low in cost, and assembly was possible in the available laboratory work shops. The models constructed for the tests reported in Ref. 38 were constructed in this manner. The pressure loss of the inlet flow results in an inward force on the model walls which will deform the duct cross section if the construction material lacks sufficient stiffness. With sheetmetal this requires a wall thickness which could result in a total model weight in excess of that which would be encountered if a concrete model were built. The metal models referred to above utilized exterior stiffeners to meet the deformation requirements and avoid excessive weight. Addition of this bracing to the components of a modular design would greatly complicate the design of the required subassemblies.

This design was simplified by the use of lighter, stiffer material. In selecting this material it was recognized that since model tests are empirical in nature, circumspection required that no prior assumptions be made as to the type of test information which would be significant. The metal models used included glass viewing windows which permitted both still and motion picture records to be made of the motion of flow visualization tufts. Construction of the entire model from transparent material was a logical extension of this technique. The use of glass would have required refined assembly techniques not readily available, though this material would be suitable in other respects. The acrylic resin material, commerical Plexiglas, was also considered. In addition

39

to transparency, Plexiglas is relatively low in cost and can be machined
by experienced model makers. Its stiffness makes external bracing un-
necessary for most span widths, and it is tougher than glass which was
of considerable importance in lengthy test programs where extensive
handling would be required. Construction experience sufficient to meet
the requirements for accuracy of dimension and alignment was available
at the Naval Postgraduate School model shop, and Plexiglas was, there-
fore, selected as the primary construction material for the present
investigation.

In the selection of required model configurations, a brief ex-
amination of the available specifications for current test cells made
it clear that even an ambitious test program could not include all
possible designs. Since no claim of optimality had been advanced for
any current design, a truly complete test program would have to include
every practical configuration not yet utilized. The model construction
had to include as many of the major variations in inlet design as
possible. However construction of more configurations than could be
tested during the proposed program duration was avoided. The limited
number of components constructed for this investigation were sufficient
to assemble 718 inlet configurations of practical significance. Multi-
plying these by the number of power levels and augmentation ratios which
were selectable, more than sufficient combinations were available for
investigation.

Most critical to the acquisition of valid test results was the
choice of model scale factor. Practical considerations limited this
choice, since a large model is difficult to reassemble frequently and
requires a power source approaching the capacity of the jet engines

tested in the actual test cells. Large models also increase material costs, and the increased span of the walls makes the requirement for external stiffeners more probable, depending upon the material and the wall thickness. On the opposite end of the scale, size limits are imposed by the extent of the necessary instrumentation because miniaturization rapidly increases both cost and complexity. As the scale factor increases, there is also increased fineness of detail required along with precision of construction methods.

For construction from Plexiglas the duct cross section was considered to be limited between 6 x 6 inches and 3 x 3 feet. Besides those effects mentioned above, variation of the model scale results in alteration of the Reynolds number of the inlet flow. Since this dimensionless flow parameter is a function of both flow velocity and duct size, it can be held constant only if flow velocity is increased inversely to the reduction in duct dimensions. Thus a model using air as the fluid and having a 12 x 12 inch duct cross section would require a flow velocity 24 times that occurring in a 24 foot square test cell. Exact Reynolds number similarity between model and cell could be expected to eliminate one source of possible test discrepancies. Many experiments in gas dynamics have been conducted to determine the importance of this similarity in flows over a wide range of Reynolds numbers.

In the case of the test cell model this requirement for flow Reynolds numbers equal to those of the full scale cell would reduce rather than increase the validity of the test results. In the test cell, flow velocities are normally limited to a maximum of 50 feet per second in the open duct. This low subsonic velocity (Mach number less than 0.05) is the primary characteristic of the flow and the type of components

which can affect the distortion level. If the model were to be operated at an equal Reynolds number, the Mach number of the model flow would be 0.96. In the portions of the duct where flow area are reduced, this would cause supersonic flow, and even in the open duct, compressibility effects would alter the nature of the flow.

It is then necessary that the flow in the model, if it is of the same fluid and occurs in the same Mach number regime, be at a different Reynolds number. Although exact similarity is not possible, it is necessary that the nature of the boundary layer and wakes formed in the model be the same as those found in the cell. In this regard, Kays /Ref. 7/ provides a complete summary of the flow regimes for air. For a sea-level test facility with a 24 foot square cross section and a mean flow velocity of 35 feet per second, the Reynolds number based on hydraulic diameter is 5.32×10^6. For a one twentyfourth scale model of this cell operated at 20 feet per second, this number is 1.27×10^5. Schlichting /Ref. 31/ demonstrates that the duct flow type which includes the flow in the actual cell extends down to at least 10^4 and under conditions of initial flow vorticity, to 5×10^3. Thus, while this scale factor does not permit Reynolds number equality to be maintained at this velocity, it does produce a flow which has the same character and is subject to the same major distorting effects. Sherman /Ref. 39/ provides experimental confirmation of Reynolds number independence.

These decisions, made individually to meet the existing selection criteria for model testing, collectively establish the model design requirements. The resulting design for the one twentyfourth scale model components is detailed in the following section.

2. Component Descriptions

The horizontal portion of the inlet duct included test sections and a horizontal flow straightening section which were used in all tested configurations. Upstream of these was the convertible turning section which made the inlet either a horizontal or vertical one. The test section housed the instrumented engine model and static depression ports for the measurement of cell depression. With the turning section assembled for vertical flow, either a straight vertical stack or a double bend, back and up, section could be placed on top of it. Three inlet caps could be placed on top of the vertical stack, and three types of acoustic treatment models were available. These treatments were designed to permit their installation in the horizontal flow straightening section, the vertical stack, or between the second and first turns of the triple bend configuration.

A turning vane model was available which could support seven equally spaced vanes or any combination of lesser numbers. This assembly could be placed either in the single turn of the vertical inlet configurations or in the second or third turn of the S curve inlet. The hex section flow straightening assembly permitted its use in any of the horizontal or vertical duct sections. Figures 6 through 21 provide photographic views of these components and dimensioned sketches of each, together with views of typical assembled configurations. Except where otherwise noted, the construction material was Plexiglas 0.25 inches thick.

43
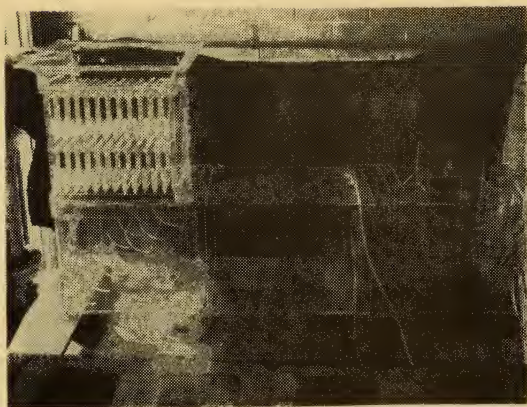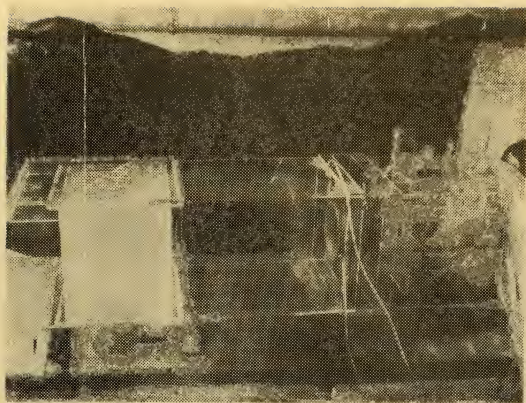
Figure 6.   ASSEMBLED MODELS, NON-AUGMENTED FLOW
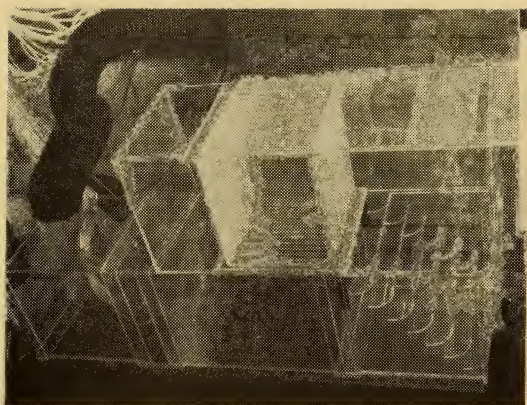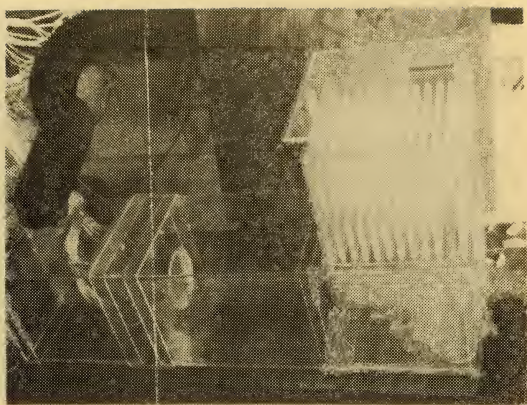
Figure 7. ASSEMBLED MODELS, AUGMENTED FLOW

45
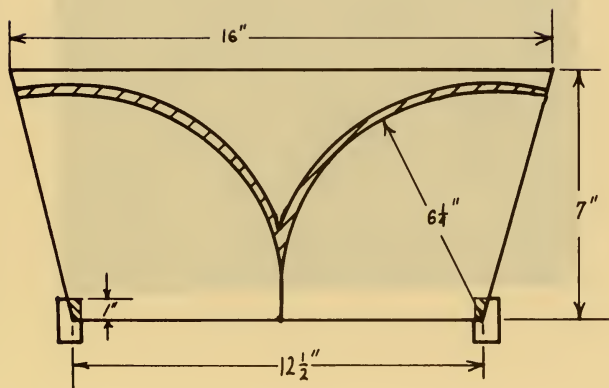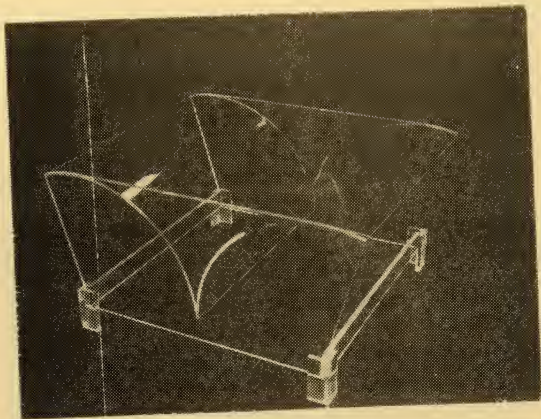
Figure 8. BI-DIRECTIONAL INLET CAP
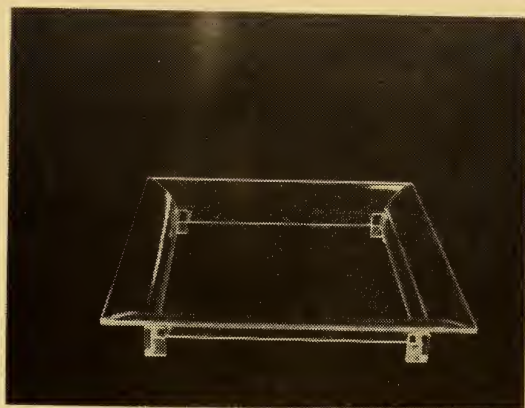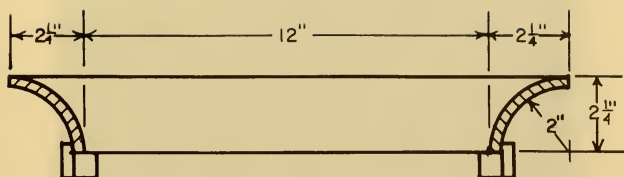
Figure 9.   FAIRED INLET CAP
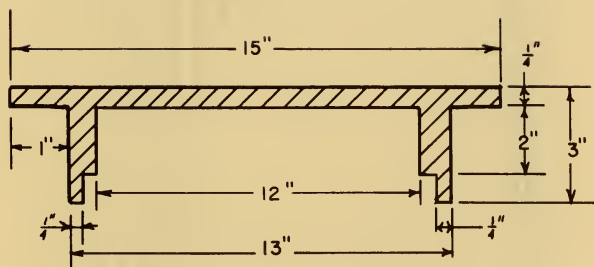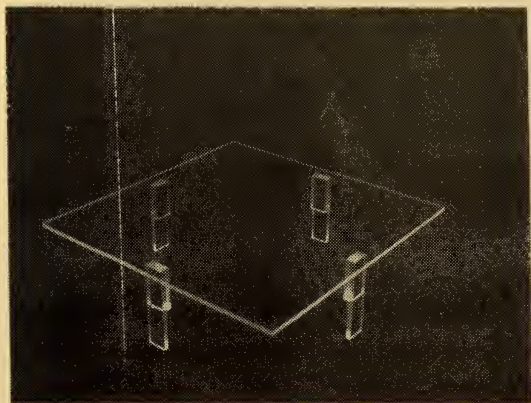
Figure 10. FLAT PLATE INLET CAP
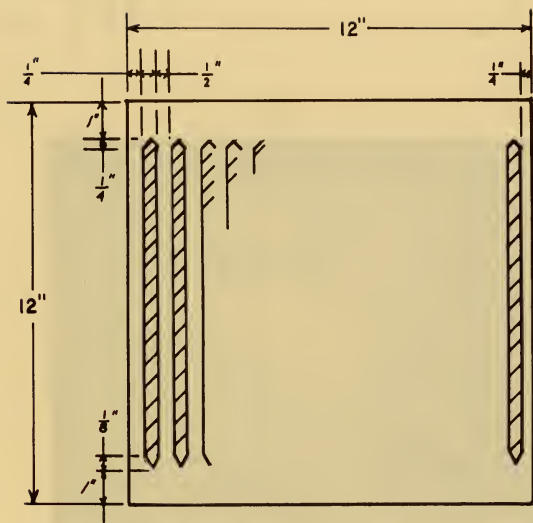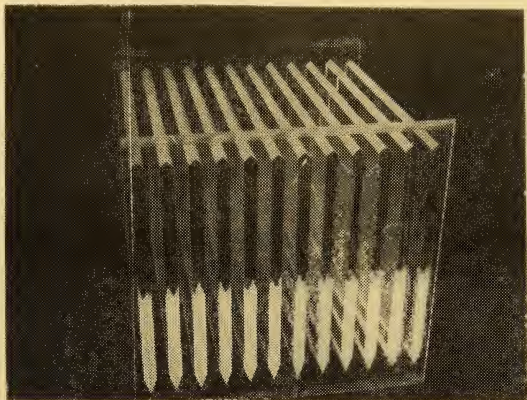
Figure 11. FLAT BAFFLE ACOUSTIC TREATMENT
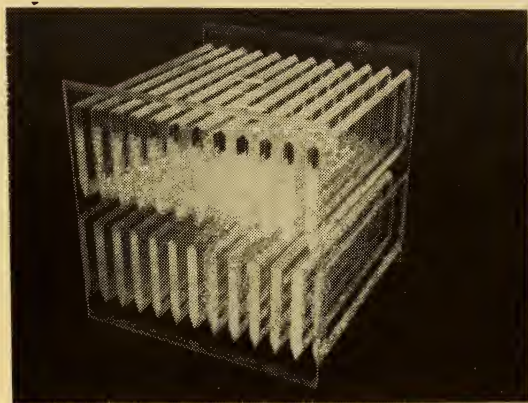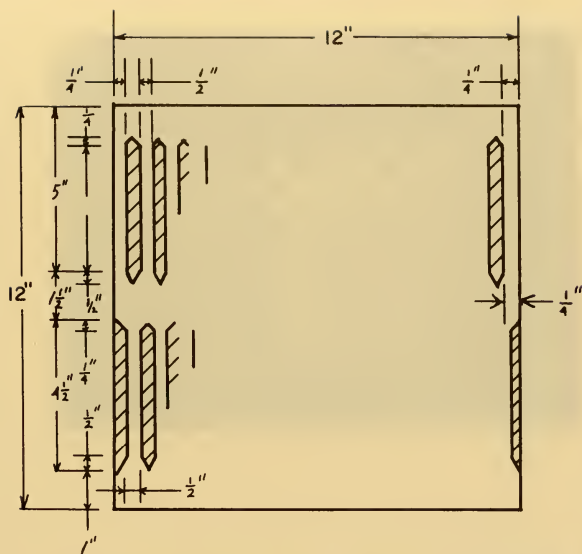
Figure 12. STAGGERED BAFFLE ACOUSTIC TREATMENT
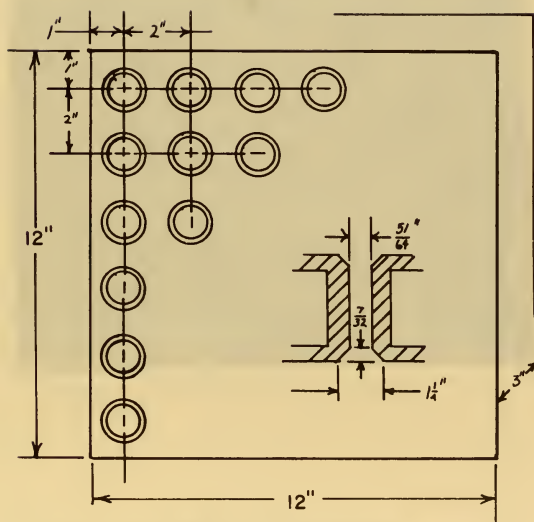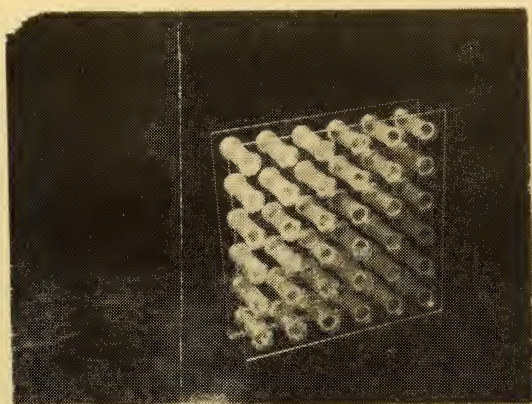
Figure 13. TUBULAR ACOUSTIC TREATMENT
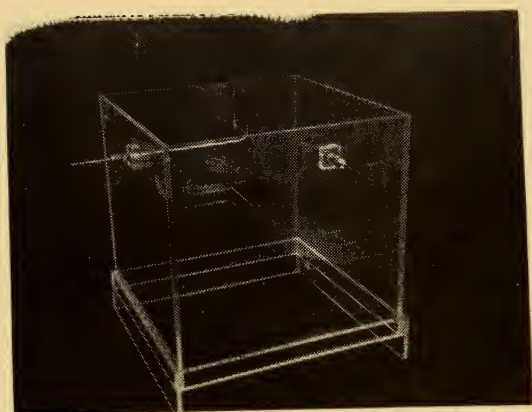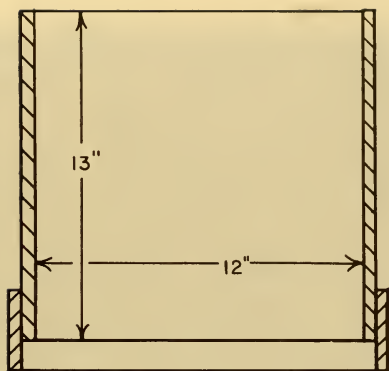
Figure 14. VERTICAL INLET STACK
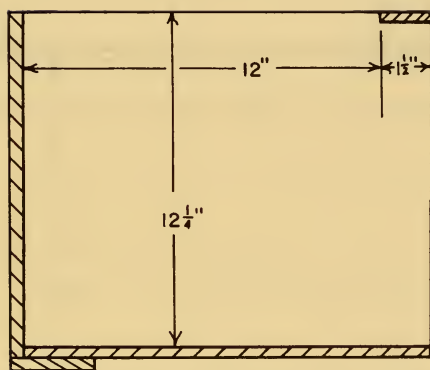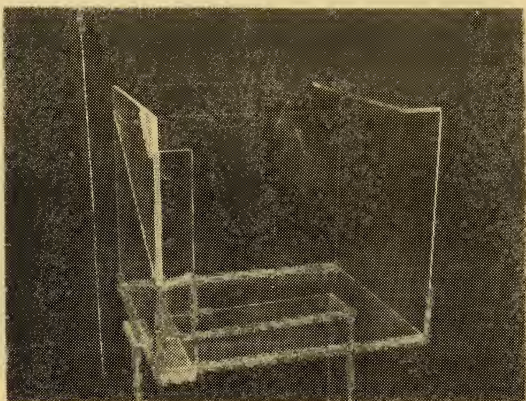
Figure 15.   CONVERTIBLE DUCT BEND
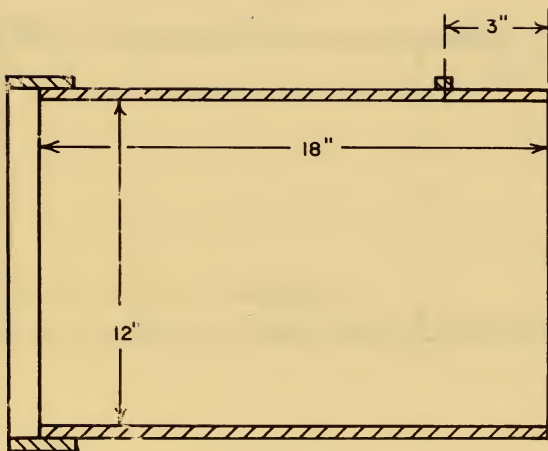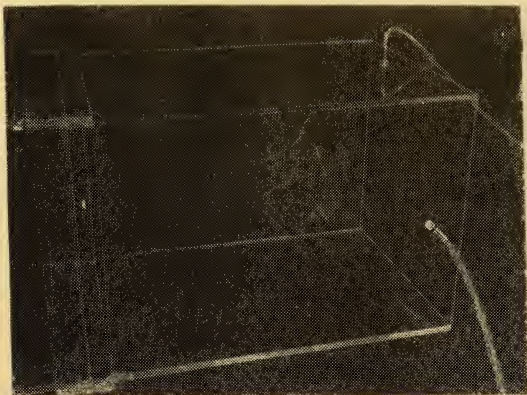
Figure 16. FLOW STRAIGHTENER COMPONENT
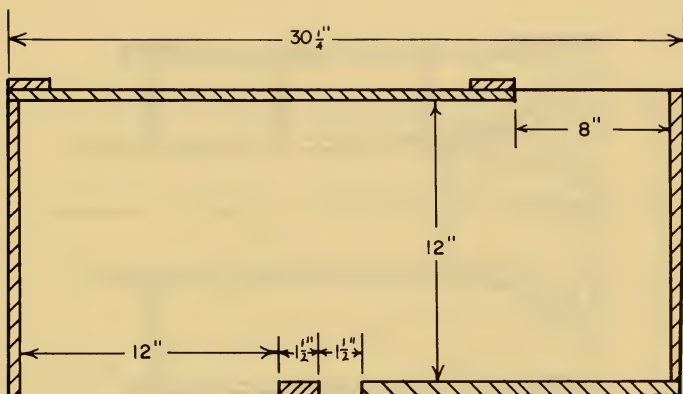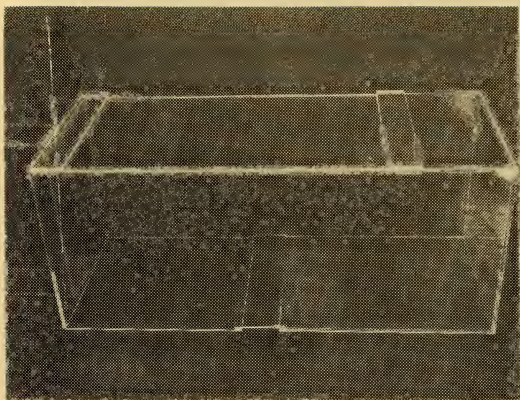
Figure 17. TRIPLE TURN INLET BOX COMPONENT
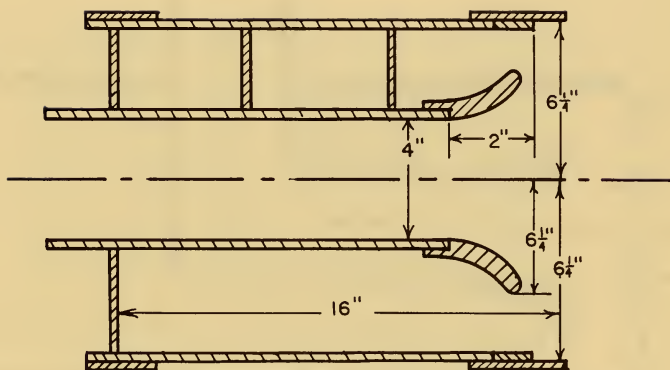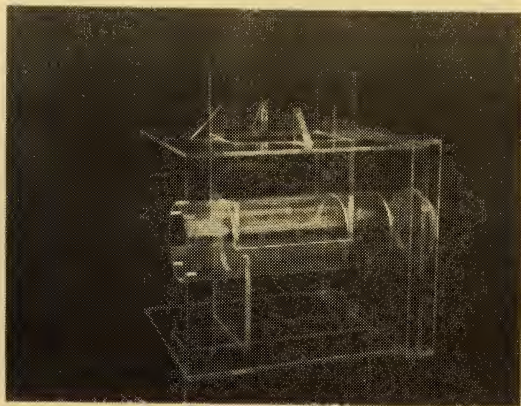
Figure 18. ZERO AUGMENTATION TEST SECTION
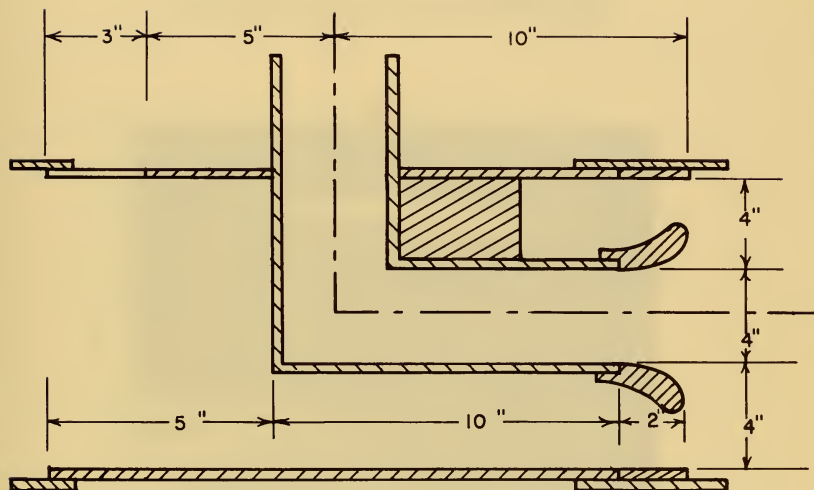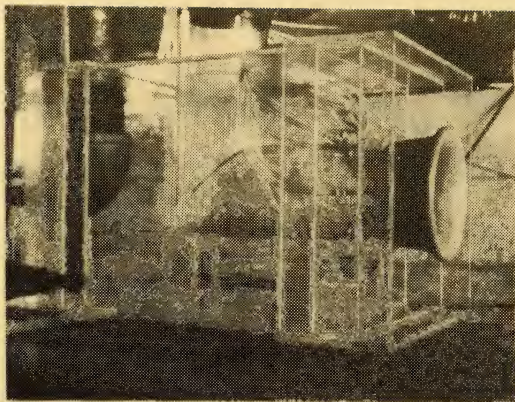
Figure 19. DUAL POWER TEST SECTION

57
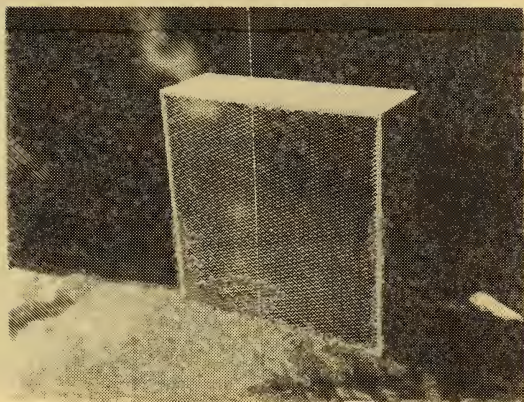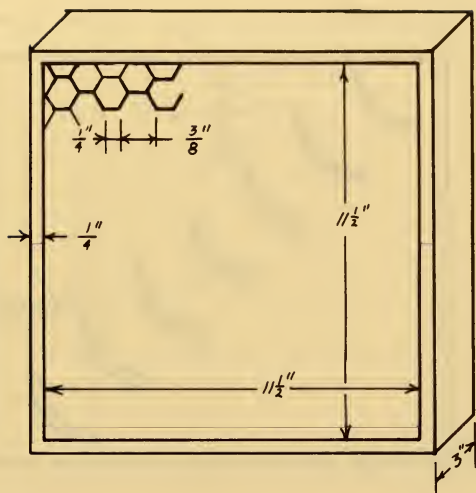
Figure 20.   HEX SECTION FLOW STRAIGHTENER
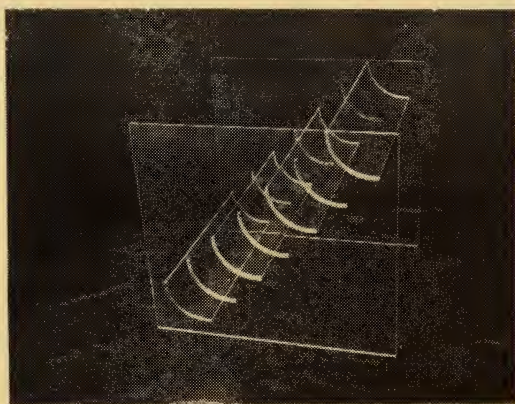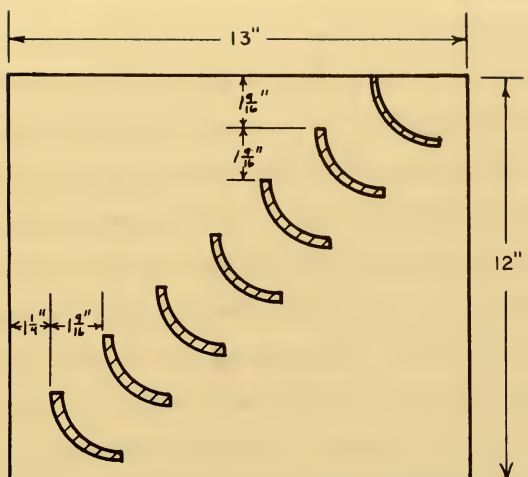
Figure 21.   TURNING VANE ASSEMBLY

C. POWER SUPPLY SELECTION

   1. Requirements

      The critical requirement for the model power supply is that it
be of a size appropriate to the scale of the model. Flow in both the
test cell and the model will be turbulent even at very low velocities.[1]
This is due to the relatively large cross section of the duct compared
to that of a typical turbulent eddy. Also, as detailed in previous
sections, the flow through the test cell will not approach full velocity
profile development. Typically, cell flow lengths vary from 3 to 6
times the hydraulic diameter of the open duct. It was thus considered
reasonable to scale the length of the model in a similar manner. This
has the effect of producing a flow which occupies the same fraction of
the duct entrance length and permits the same analysis methods to be
applied to both situations. The selection of the model power source
must be based on the flow velocity required in the model for maximum
similarity of distortion.

      Distortion of the engine air supply results from the existence
of regions of momentum deficiency. Boundary layer theory includes the
definition of a momentum thickness which is developed as a specific
measure of this deficiency /Refs. 7 and 31/. At any duct cross section
the percentage of the flow which has lost momentum due to surface fric-
tion is equal to the percentage of the duct area within the momentum
thickness of the boundary layers. If the test cell and model consisted
of sharp lip, straight, open ducts, the percentage distortion existing

---

[1]Reference 6 includes a design requirement that laminar flow be
delivered to the engine. In a 24 foot duct with a 100 foot flow length,
delivery of laminar flow could be accomplished at a maximum velocity of
0.003 feet per second if the transition Reynolds number is taken as 2000.

at any position, including the critical compressor face, would be ex-
actly equal if the ratio of momentum boundary layer area to duct area
was the same in the two ducts. Test cells and their models are not
ducts with this simplicity of arrangement and contain many secondary
surfaces which also form boundary layers and produce pressure gradients
affecting layer growth in their vicinity. Still maintenance of this
area ratio at equal values in cell and model will insure that one major
source of distortion will be available for measurement in the laboratory.

Figure 22 is a schematic representation of open duct flow where
D is the momentum thickness of the boundary layer. For a square duct
with side length of L feet and total area L^2, the area of the Momentum
Boundary Layer (MBLA) is

$$MBLA = L^2 - (L - 2D)^2$$

The distortion percentage or distortion area ratio is

$$\frac{MBLA}{A} = \frac{L^2 - (L - 2D)^2}{L^2} = \frac{4D}{L} - \frac{4D^2}{L^2}$$

The condition for similarity of distortion in cell and model is that
this ratio be equal in each case or

$$\left(\frac{D}{L} - \frac{D^2}{L^2} \right)_{MODEL} = \left(\frac{D}{L} - \frac{D^2}{L^2} \right)_{CELL}$$

The thickness of this momentum boundary layer is a function of
flow velocity and length, assuming that surface roughness is held
approximately constant. Kays /Ref. 7/ reports this expression as the
best approximation of this thickness:

$$\frac{D}{x} = 0.037 \left(\frac{\nu}{Vx} \right)^{0.2}$$

where x is the flow length, V is the duct center line velocity, and

61
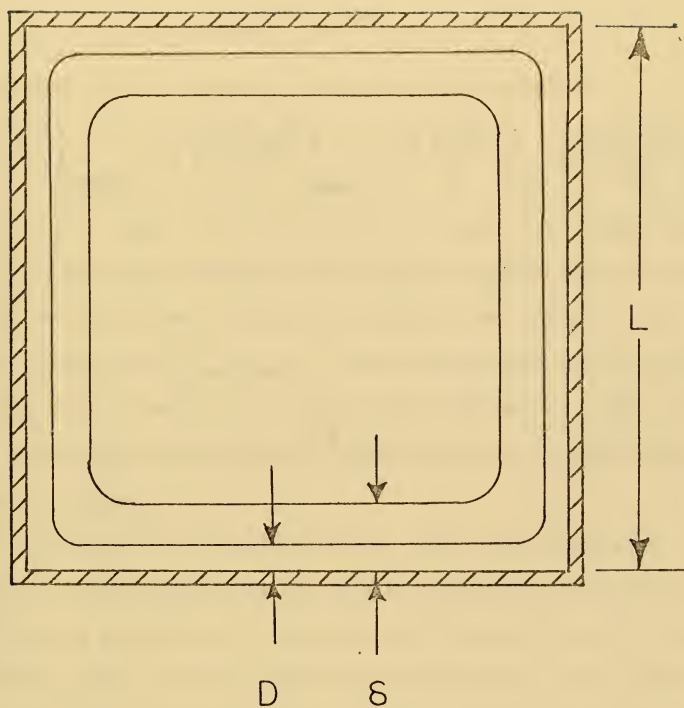
D - Boundary Layer Momentum Thickness

δ - Boundary Layer Thickness

L - Duct Height

Figure 22.   SCHEMATIC DUCT FLOW CROSS SECTION

ν is the kinematic viscosity coefficient. At sea level ν = 1.5757 x 10^{-4} ft^2/sec. Thus taking

$$B \equiv 0.037 \, \nu^{0.2} = 0.1741$$

the displacement thickness is:

$$D = B \, V^{-.2} \, X^{0.8}$$

The requirement for similarity of flow may thus be written as

$$B \left(\frac{V^{-.2} X^{.8}}{L} \right)_{MODEL} - B^2 \left(\frac{V^{-.4} X^{1.6}}{L^2} \right)_{MODEL} = B \left(\frac{V^{-.2} X^{.8}}{L} \right)_{CELL} - B^2 \left(\frac{V^{-.4} X^{1.6}}{L^2} \right)_{CELL}$$

Fixing V_{cell} at a common value of 40 feet per second, and having fixed L_{model} : L_{cell} at 1.24, examination of the above relation revealed that the selection of the power which sets the model flow velocity, also fixes the length ratio x_{model}/x_{cell}. The selected power source was required to produce a realistic value for this length ratio. Figure 23 presents the results of the complete analysis and the full development is included as Appendix A.

The selected power source also had to meet requirements for flexibility. Engines operate in test cells at idle power and at max thrust including afterburner. The air flow in the inlet duct is a function of engine power and also of cell augmentation ratio, AR, defined as the ratio of mass flow rate past the engine to the flow rate through it. Commonly, this ratio varies from zero (close coupled exhaust) to three (in facilities treating the exhaust gases for introduction into pollution control devices). The above analysis utilized the open duct velocity as the independent variable and must be somewhat extended to assess the effect of power variation.

63
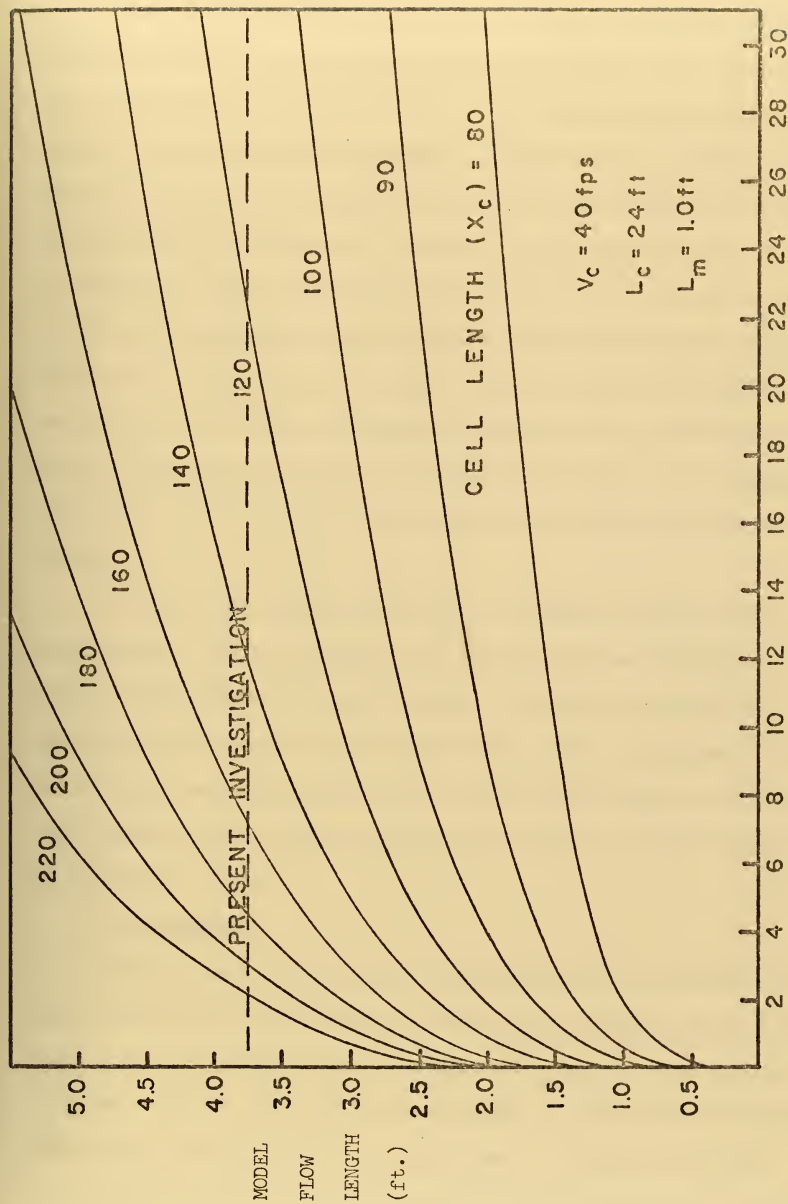
Figure 23. VARIATION OF LENGTH SCALE FACTOR WITH MODEL VELOCITY

64

The model length ratio is fixed utilizing maximum predicted air flow for the test cell and the corresponding maximum flow velocity. Then, referring to the previous form of the similarity expression, the length ratio is observed to be fixed. In this case, the effect of model velocity variation is to change the velocity scale factor of the test in accordance with Figure 23. The power source must therefore be capable of varying the model flow velocity in increments the size of which are available from the desired cell velocity variation increment size and Figure 23. In the case of the tests conducted during the present investigation, the change in compressor face distortion resulting from a one foot per second variation in velocity was desired. This implies a requirement that the power source be able to provide a sensitivity of 0.6 fps.

This is the limiting sensitivity criterion for the suction power source. Figure 23 shows that a source with low capacity can simulate only extremely long test cells. Practical considerations also limited this selection since the power unit would be required to operate for extended test periods and for a total usage in excess of 300 hours. Total program economy was best served by considering inherent durability as a selection factor.

2. Alternatives

Four primary power sources were considered for use with the inlet model. Reference 38 is a report on model tests conducted using a scale model turbine engine operated by compressed nitrogen. Both hot and cold gas models have been used in the development of methods for simulating engine power effects in wind tunnel testing. In nearly every case satisfactory simulation required complex, sensitive models. The cost

of most model engines with the capacity to operate a cell inlet model
was high enough to make their use impractical except for an organization
which has them internally available. Model studies conducted for the
investigation of other cell flow phenomena may require the use of scaled
engine models; but for the purpose of inlet studies, simpler and less
expensive power methods are available.

A vacuum or high pressure source may be used to induce the re-
quire flow in the model. Suction, when applied to an appropriately
scaled model bellmouth, has the advantage of natural similarity with
test cell flow. The application of high pressure air to the inlet would
have involved considerable difficulty in the simulation of the natural
environment of a test cell. Simulation of the turbulence level of the
atmosphere would have required extensive treatment of the power supply
outlet flow by screening and/or contraction-expansion sections /Ref. 40/.
To permit natural streamline patterns around the cell model, it would
have been necessary to submerge the inlet deeply within a pressure
supply plenum to prevent interference effects from the plenum walls.

A suction powered model avoids these complications by permitting
the model to use air from ambient room conditions and simplifies the
simulation of external wind conditions if desired.[1]   The suction power
supply could have been either a type of vacuum pump or the intake of a
rotating blower. The choice in this case was a function of availability
and model scale. Most vacuum pumps of reasonable cost have flow capa-
cities which limit their use to models of the smallest size unless a

---

[1] Leef /Ref. 4/ reports the dependence of distortion on external wind
direction and velocity and examines in depth some methods of its reduc-
tion.

sizeable holding tank system is employed and testing is scheduled to meet the required recharge time. The rotating blower is available in sizes to meet much larger model flow requirements. They are typically low in maintenance cost and provide unlimited test run time in most cases. With either the pump or blower it is necessary to provide ducting which permits the flow to be divided between primary (engine) and secondary (augmentation) flows. High pressure supply systems would have to be confined to the testing of zero augmentation configurations since no provision for this division is readily available.

Another method of providing power to the model was to use a simplified engine model in the form of an injector nozzle supplied from a high pressure source using the nozzle discharge to induce both primary and secondary flows. The quantity of flow required of the supply source imposes an additional limit on model size by the dimensions of the supply piping required. The greatest difficulty anticipated in the use of this arrangement was the provision of adequately sensitive control of the two flow rates.

3. The Selected Power System

This investigation was conducted in conjunction with the research reported in Ref. 41. As that investigation of test cell augmentor flow required accurate simulation of the engine exhaust, a pressure fed ejector nozzle was constructed. To overcome the difficulty of providing control of the flow rate and permit a more uniform exhaust flow, an additional power source was used to provide engine flow. A rotary cage blower with a flow capacity of 0.7 pounds per second was separately ducted to the model engine bellmouth. Thus in the dual power mode, the air passing through the compressor face was exhausted through the blower

67

discharge and the augmentation air together with the nozzle supply flow
exited through one of a variety of instrumented augmentor ducts.

At an augmentation ratio of 3.0 a total inlet flow of 1.94
pounds per second was measured in the model. In this condition, the
open duct velocity was 22.02 feet per second. Since the model center-
line flow length (vertical configurations) was 3.75 feet, Figure 24
indicates that a test cell flow length of 120 feet was simulated, and
this was considered typical of many sea level test facilities. Figure
24 shows that at full engine power and zero cell augmentation the power
source had to be capable of producing a duct velocity of 8.8 feet per
second. Test data included in the computer output section of this
report indicate that this value was closely approached by the selected
blower unit when connected directly to the horizontal engine duct.
Power system layout is illustrated in Fig. 25, and system performance
is evaluated in Section VI (A).

D. INSTRUMENTATION

1. Requirements

The correlation of inlet configuration and distortion required
information on the existing distortion, the model operating condition,
and the makeup of the inlet. A survey of the compressor face velocity
profile could have been made either with a positionally fixed set of
probes or a single probe which could have been located at varying
positions. Any of the numerous velocity measuring systems designed for
subsonic flow could have been utilized, and the choice was dependent
upon the aim of the test program. Investigation of dynamic distortion
effects would require response time consistent with the anticipated
fluctuations. This investigation, being confined to the effect of

Cell Length, X_c, Simulated at Full Power (ft.)
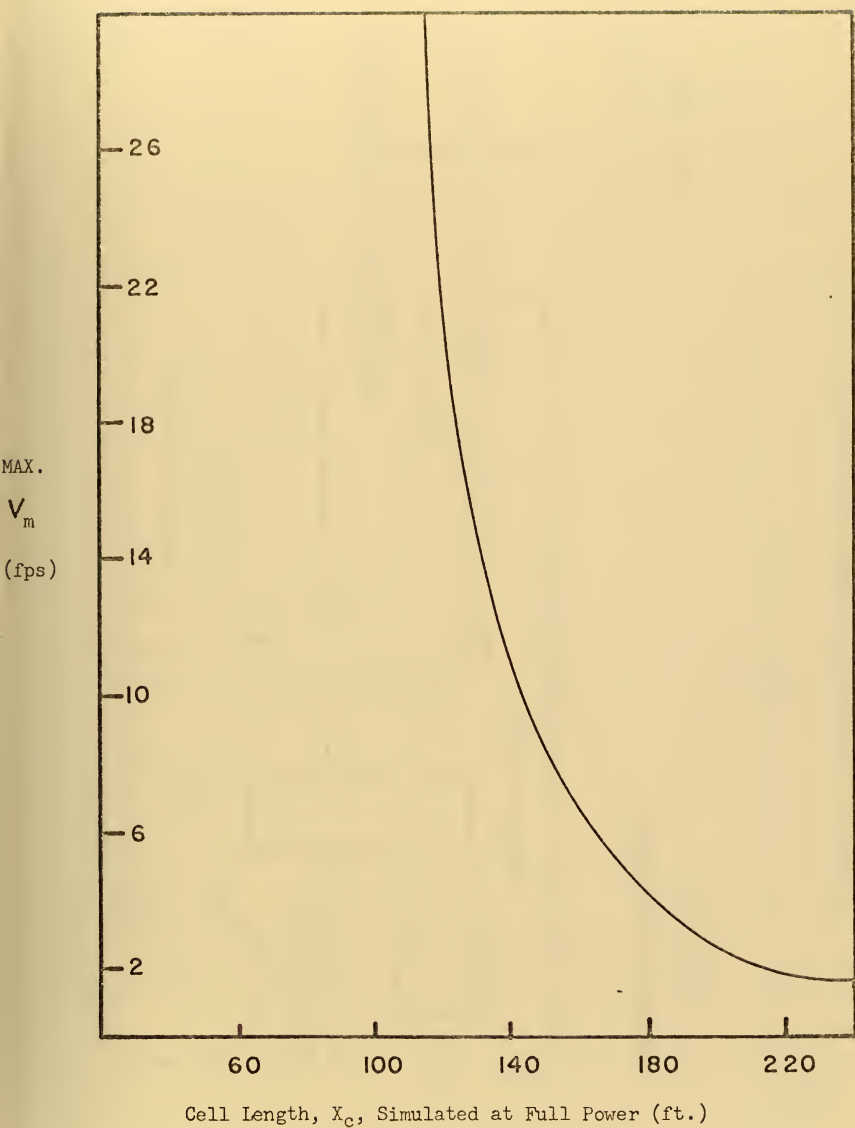
Figure 24. THE VARIATION OF SIMULATED LENGTH WITH
MAXIMUM MODEL FLOW VELOCITY

METERED COMPRESSED
AIR SUPPLY

AUGMENTOR VELOCITY
SURVEY PLANE

ENGINE EXHAUSTER

COMPRESSOR FACE VELOCITY
SURVEY PLANE
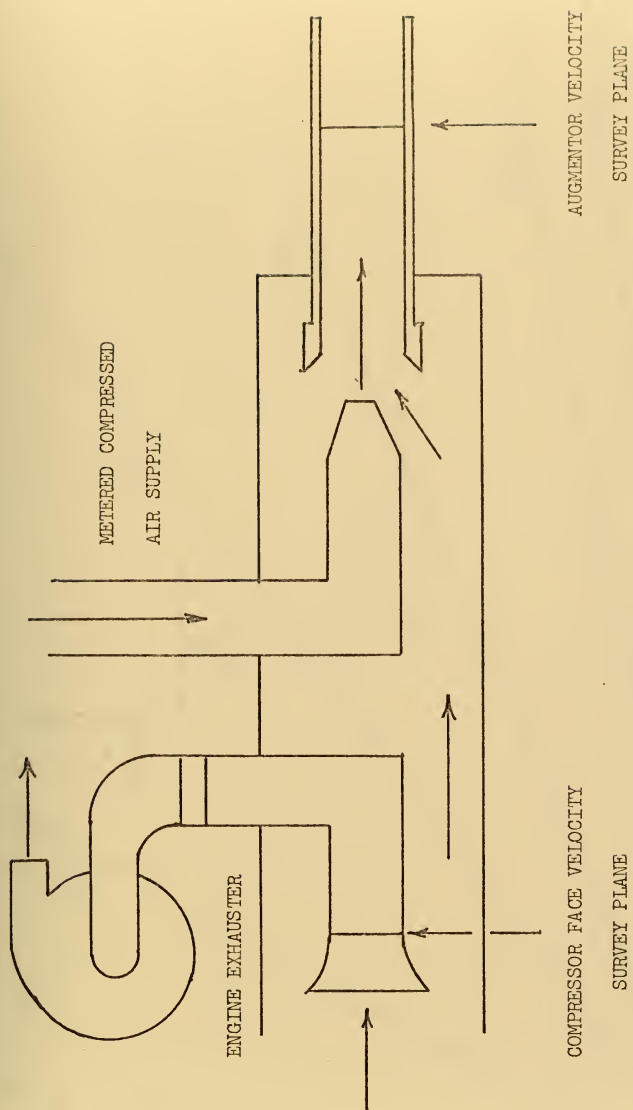
Figure 25. AUGMENTED FLOW POWER SYSTEM LAYOUT
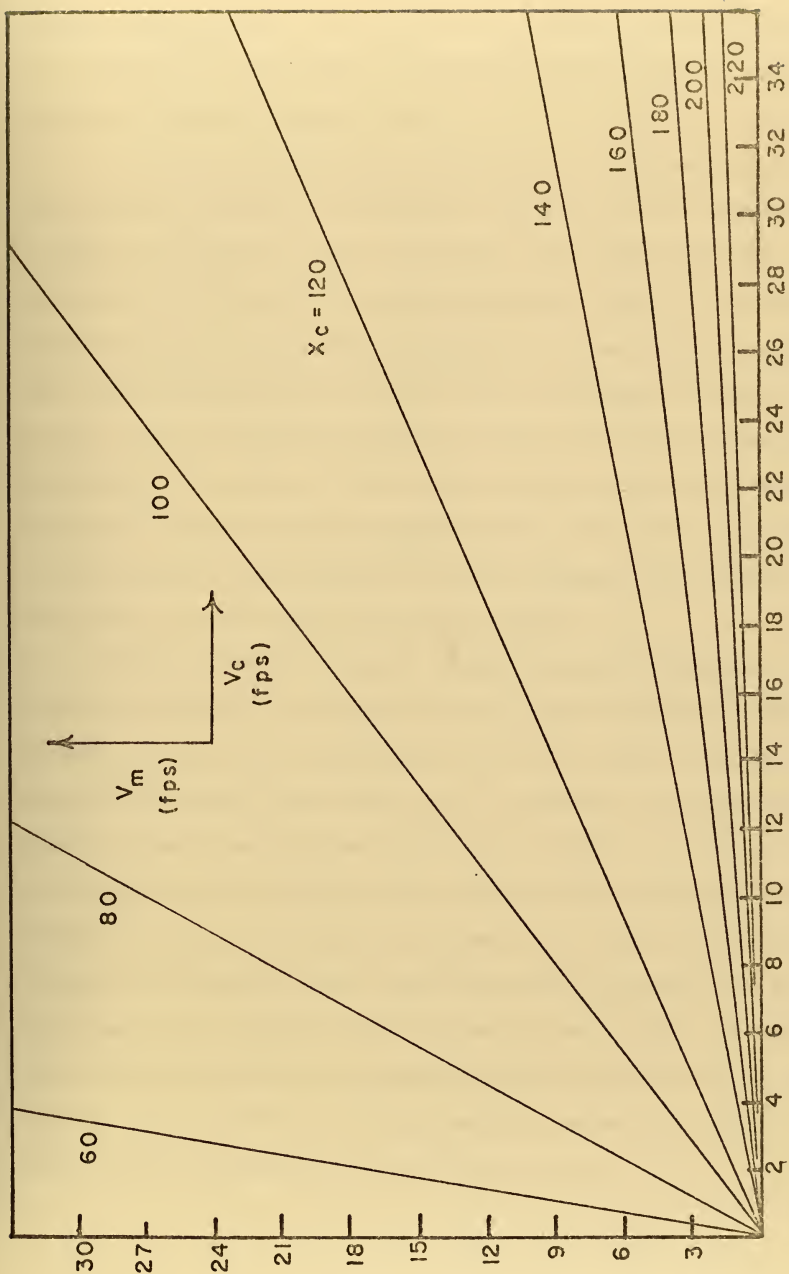
Figure 26. VARIATION OF LENGTH SCALE WITH TEST CELL VELOCITY

71

steady distortion, made the use of slower responding instruments possible and eliminated the requirement for simultaneous measurement of model vibration stressed by Jansen in Ref. 15.

Practical considerations entered the selection problem since large numbers of tests were anticipated, and the total time required to complete the program was largely dependent on the effort required to record the distortion data for each configuration. While it was possible that provision of a measurement probe which could be located at any position within the inlet could contribute to a full analysis of the flow system, this was considered impractical in tests for direct engineering application. The number of runs required and the desire to reduce data acquisition time to a minimum suggested that a fixed survey rake located at the compressor face would have definite advantages over a single probe which had to be relocated between readings.

Either pitot static probes or those using electromagnetic pressure transducers are well suited to the requirements of a subsonic velocity survey and were considered for use in the model. The pitot static system offered lower cost, and the transducers were more easily adapted to use in an automated data recording system. In addition to the measurement of distortion, it was necessary that instrumentation be provided for the determination of cell mass flow rates. This would establish the simulated engine power level and the effective cell augmentation ratio. Practical considerations of cost and speed of operation confined the selection to standard methods suited to the low speed, low flow rate anticipated. The instrumentation selected as a result of these factors is described in the following section.

2. Description

For the determination of distortion twenty five total pressure
probes were built into the model engine. Probe positions were selected
to permit the measurement of both radial and circumferential distortion.
Location and identification are detailed in Figure 27. Initially,
alignment was parallel to the engine axis. This was adjusted for in-
dividual inlet configurations where evidence of misalignment was en-
countered in the form of excessive total pressure difference between
adjacent probes. The effect of the velocity survey rake assembly on
the flow was considered and limited the number and size of the probes
employed. The twenty five probes at the compressor face had an outside
diameter of one eighth inch so that total blockage area was 0.202 square
inches. This was 1.6 per cent of the total flow area and was considered
consistent with the blockage of the inlet guide vanes in current engines.
At the plane of the probe stems, the blockage was 1.125 square inches or
9 per cent, and this is less than the solidity of most first stage com-
pressor stators. Two static pressure taps were inserted on opposite
sides of the engine duct at the plane of the velocity survey. While
the assumption of uniform static pressure across the duct was borne out
in the observed data, the individual static pressure values were asso-
ciated with the closest total pressure heads for reduction of the data
to velocity. This arrangement considerably simplified construction of
the survey rake since the assembly of twenty five pitot static probes
of the required shape would have been a formidable task.

Total and static probes were connected with flexible plastic
tubing to an inclined manometer board, so marked as to permit a resolu-
tion of 0.02 inches of water in gage pressure. Since the maximum

73
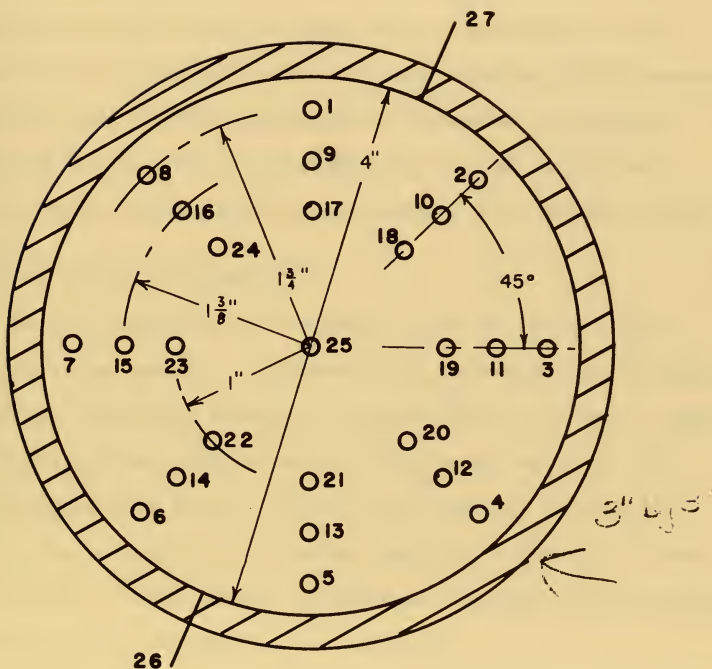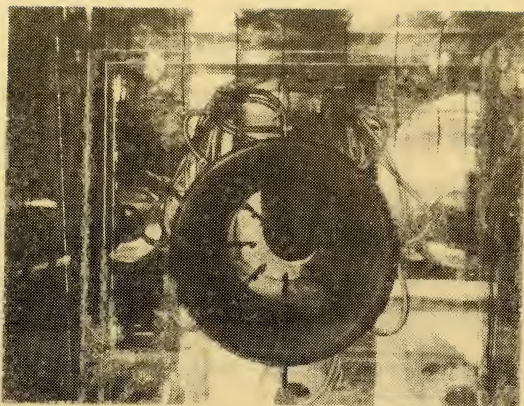
Figure 27. THE ARRANGEMENT OF COMPRESSOR FACE INSTRUMENTATION

anticipated compressor face Mach number was less than 0.2, it was possible to assume atmospheric density at the plane of the velocity survey. The pressure information was thus sufficient to determine the engine mass flow rate. A variety of methods for the averaging of the velocity data were used and are detailed in the following chapter.

Additional instrumentation consisted of static pressure taps in the duct walls foreward of the engine bellmouth for the determination of cell depression and that associated with the augmentor flow system. A standard throttling plate and required instrumentation were installed in the high pressure supply line, and provisions were made in the aug- mentor tubes for the operation of velocity surveying traverses. Prior to the testing of fully assembled inlet models, instrumentation was installed in the vertical inlet stack to permit velocity profile measure- ment at that position. This instrumentation consisted of two pitot static probes inserted through the stack walls at right angles and secured in a manner which permitted adjustment of their extended length.

E. SELECTION OF TEST CONFIGURATIONS

With the interchangeable duct components constructed for this in- vestigation, it was possible to construct 3240 different inlet configur- ations without introducing frames for different kinds of screens. Each of these configurations could be operated at a wide variety of power levels and augmentation ratios. Since it was necessary to limit the duration of the testing phase, it was not possible to test all, or even a large portion, of these possible arrangements. Several factors affected the selection of the configurations to be tested.

In the construction of the model components the vertical inlet stack and the inlet caps were completed first, and during the construction of

the other components, tests were made to determine the effect of the
inlet cap on the initial velocity profile in the vertical duct. As a
result of these tests, it was concluded that sufficient difference
existed in these profiles to substantially effect the overall inlet
performance

An additional constraint was the fact that the design and fabrica-
tion of the augmentation system was more complex and time consuming than
that of the inlet components. It was thus possible to test first those
configurations not requiring augmentation. Also since the major differ-
ence existing in current test cell designs, other than their augmentation,
is the presence or absence of turning vanes, the initial test phase was
divided into two portions.

The horizontal inlet configurations were tested first with the
various acoustic treatments, engine power levels and zero augmentation
flow. The vertical inlets were then tested for all combinations of
acoustic treatment and inlet caps. These were tested at full and re-
duced power levels though the observed trend of increasing distortion
with increasing flow rate was found to be consistant throughout this
phase. The effect of installed flow straightener sections was studied
through their addition to previously tested configurations.

This full set of vertical configurations was then retested with each
of four different combinations of turning vanes, still without augmenting
flow. Then, from the analysis of the data accumulated to this point,
configurations were selected for testing with nonzero augmentation
ratios. The majority of those selected were at the extremes of the dis-
tortion spectrum observed during the tests of unaugmented configurations.
Additional configurations were selected to insure the inclusion of all

components and each major configuration type. This was considered necessary since configurations composed of components which generated little distortion at low flow rates might show disproportionately higher distortion potentials if an increase in the flow rate caused separation of the flow to occur in some component. A total of 213 different configurations were tested and an additional 22 test runs were made to check on the repeatability of the test results.

V. INLET MODEL TEST PROCEDURES

A. CONFIGURATION IDENTIFICATION

Each inlet model test was identified by a ten digit code number which indicated the included components, their arrangement, and the settings of the engine and augmentor power supplies. The code used is. indicated in Table II. The use of numerical identification numbers facilitated computer sorting and grouping of the processed test data and permitted changes and additions to be made without making it necessary to reidentify the data sets previously collected. This was a significant advantage since as the test data was accumulated, it became possible to identify significant distortion sources and refine the test parameters to investigate the persistence of these characteristics over a range of similar configuration and operational conditions.

B. FLOW VISUALIZATION METHODS

An initial attempt was made to secure a photographic record of smoke traces injected into the inlet of the model. The record of streamline behavior provided by these records would have been of value if the deflection of an initially uniform flow by the various inlet components could have been correlated with the total distortion of the engine air supply. The turbulent nature of the flow in the inlet was confirmed by the observation of the almost immediate and complete diffusion of the initially thin, uniform smoke streams. No smoke source tested provided a stream trace which persisted more than three inches into the inlet. It was therefore necessary to utilize alternate means of visualization.

Table II. CONFIGURATION IDENTIFICATION

Configuration Codes: ABCD.EGFHIJ

A INLET	B INLET CAP	C ACOUSTICS	D ACOUS. POSIT.
1 vertical	1 none	1 none	1 before turn, transverse
2 horizontal	2 faired	2 flat baff.	2 after turn
3 none	3 bi-direct.	3 staggered baffles	3 none
4 vert. w/o stack	4 flat plate	4 tubular	4 before turn, axial
	5 bi-direct. sideways	5 stag. baff. X-ways	5 top of stack

E TURN VANES	F FLOW GDS.	G ENG/BELL	H AUGMENT.
1 none	1 none	1 neither	1 none (end plate)
2 one (#3)	7 hex section	2 eng w/o bell	2 none poss.
3 four		3 eng+bell	3 low
4 seven			4 medium
5 one (#5)			5 high
6 one (#1)			6 zero
7 four in turn #2			
8 one (#3) in turn #2			
9 seven in turn #2			

I POWER	J ENGINE PWR
1 test sect- blower	1 max
2 eng-blower	2 mid
3 eng+aug- blower	3 min
4 dual mode	

Yarn tufts were secured to the interior surface of the inlet duct forward of the engine in the test section and in upstream areas not occupied by the acoustic treatment models. In another effort to provide some indication of streamline positions lengths of light weight black thread were fed into the inlet from various positions and extended through the inlet components to the compressor face. At low flow rates the flow velocity was insufficient to support the weight of the tracer, and it was consistently carried toward the bottom of the duct from all entry positions.

At higher flow rates the turbulence of the flow was such that the results of this tracing were time dependent with different paths being followed from identical entry positions. It was not possible to produce permanent streamline position records, but useful qualitative information was obtained in this way. Through observation of trace motion, particularly the portion close to the free tip of the thread, it was possible to obtain comparative information about the scale of the turbulent macro-eddies generated by the components of the inlet duct. This information was utilized in the development of the correlation method and provided some feeling for the nature of the interaction of the various duct components. This trace method was also of value in the alignment of the total pressure probes at the compressor face and in confirming that the presence of the survey rake in the engine did not alter the bare engine flow characteristics to any observable degree. The use of this technique is recommended for future model test programs since it is of minimal cost and required only that caution be exercised to prevent ingestion of the trace by the power source.

C. TEST METHODS

1. Inlet Flow Velocity Profiles

For these tests the flow straightener, turning corner, and
vertical stack components were assembled with the downstream end of the
straightener section connected directly to a suction power source. Each
of the four inlet caps was tested at three flow rates. For each operat-
ing condition, two pitot static probes were traversed perpendicularly
across the inlet in a plane level with the top of the vertical stack.
At each of the positions shown in Figure 28 the manometer displacement
of the total and static pressure ports were recorded. Prevailing atmos-
pheric pressure and ambient temperature were recorded from standard
laboratory instruments at the beginning and end of each test period.

2. Distortion Baseline Tests

With the instrumented engine model installed in the test section
and connected to the blower intake, the upstream duct components were
removed. With the power set at various levels the manometer deflections
for the twenty five total and two static pressure ports were recorded.
Initial tests were made with the test section and power source supported
in the center of a solid laboratory table. With the bellmouth in place
on the engine, the velocity profile observed clearly indicated that the
table surface influenced the velocity in the lower third of the test
plane. With the test section reoriented to overhang the table edge,
this effect was removed. With this arrangement, uniform velocity was
observed at all power levels within the 0.02 in. H_2O accuracy of the
inclined water manometer system. These tests also served to provide
calibration of the power source regulator for all unaugmented configura-
tion tests.
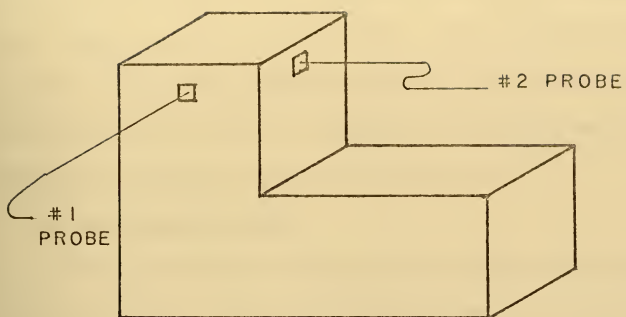
PROBE POSITIONS
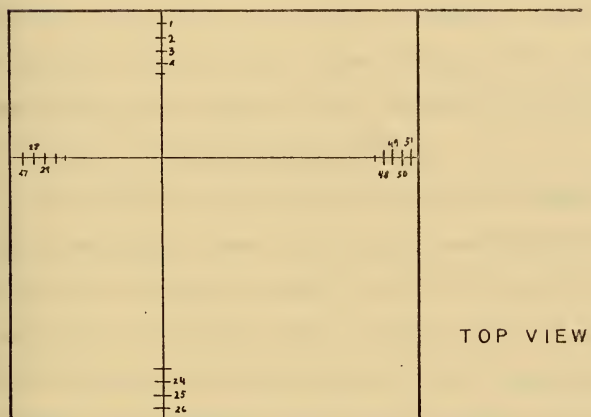
DATA POSITIONS

Figure 28.   INLET VELOCITY SURVEY PLAN

When construction of the dual power source test section was completed, these tests were repeated with the additional ducting in place between engine model and blower. This provided calibration of the power supply for augmented tests and confirmed the presumption that the necessary 90° turn in the engine model ducting would not observably affect the uniformity of the test plane flow.

3. Non-Augmented Tests

Each of the inlet configurations tested without augmented flow was assembled with a duct end plate in place at the downstream end of the test section component. The power source blower was throttled in accordance with the calibration obtained during the baseline tests and activated. When uniform flow had been established (manometer displacements constant), the data sheet shown in Figure 29 was completed. Laboratory pressure and temperature were recorded from standard instruments.

4. Tests of Augmented Configurations

In addition to the procedure followed for those configurations without augmentation, these tests required measurement of the total mass flow through the augmentor exhaust duct and the mass flow rate of the air supplied to the ejector nozzle. Bailey in Ref. 41 supplies a complete description of the methods used in these measurements. His data processing method produced a flow rate, in pounds per second, of inlet flow by-passing the engine bellmouth, and this was entered on the data record prior to processing of the distortion data.

D. DATA PROCESSING METHODS

1. Goals Established

The most general aim of the processing methods developed during this investigation was to establish the basis for a consistent correlation

83

DATE_____

		CONFIGURATION CODE				
		PROBE 1				
		2				
		3				
		4				
		5				
		6				
		7				
		8				
		9				
COMPRESSOR FACE	Patm - Ptot	10				
		11				
		12				
		13				
		14				
		15				
		16				
		17				
		18				
		19				
		20				
		21				
		22				
		23				
		24				
		25				
	Patm-Ps	26				
		27				
Cell Depression						
Upstream Tufts						
Downstream Tufts						
Test Plane Dynamics						

Patm _____ in. Hg   Tatm _____ ^{o}F Maug _____ lbm/sec

Figure 29. INLET TEST DATA SHEET

84

between inlet configuration and engine distortion level. This imposed several requirements on the selection of processing techniques. Since many different methods were available and no prediction could be made as to which would most readily provide the desired correlation, a primary requirement for the processing system was that it be able to use all the available methods and compare the results. This requirement and that of limited project completion time implied the necessity for machine processing of the collected data. The information from the test data sheets was transferred to punch cards and processed by the programs described in the following sections. This technique met the additional requirement which is inherent in correlation methods; that is, the repeated processing of large amounts of data as different correlation parameters were tested.

2. Vertical Inlet Velocity Survey

The program developed for the processing of this survey data is included in the computer program section of this report. This program was written in the FORTRAN IV language for the Naval Postgraduate School's IBM system 360 and had as its primary aim the evaluation of inlet cap effect on initial inlet velocity profile. Secondarily, it was desired to evaluate the proposal that one or two pitot static probes properly located in the vertical inlet stack would make accurate determination of total inlet mass flow rate possible.

The average velocity measured along the line of each probe traverse was computed directly from manometer readings of $P_t - P_s$ and the assumption of constant density. This required the averaging of the velocity at each adjacent pair of measuring stations and the weighting of this average value with the lengthwise separation of the points.

These length weighted velocities were then summed and divided by the total length of the traverse to obtain a quantity identified within the program as the "slice average velocity." The velocity profile obtained in this manner was then adjusted by a constant factor, the value of which was determined as that necessary to cause the adjusted value at the point of intersection with the second trace to equal the observed velocity at that point. Figure 30 schematically illustrates this process. In this manner slice average velocities were obtained on both sides of the measured one, one for each data point on the second crosswise trace. These slice averages were in turn averaged and weighted by the lateral distance between sections and then divided by the total flow area to obtain the final average flow velocity.

This complete procedure was then repeated with the two sets of survey data points in opposite roles with the results of both calculations being presented in tabular form for comparison. Figure 31 shows a typical pair of measured profiles. The processed data was also examined in an attempt to select probe positions, which for each inlet cap accurately measured a velocity near the calculated average at all power levels. As the power source used in this test program was different than that to be used in the testing of complete inlet models, no attempt was made to calibrate the blower throttle position with mass flow.

3. Distortion Tests

This program accepted the information from the data sheet shown in Figure 29. All recorded manometer data was converted to absolute pressure, and the minimum and maximum total pressure readings were identified. The average total pressure at the compressor face was

86
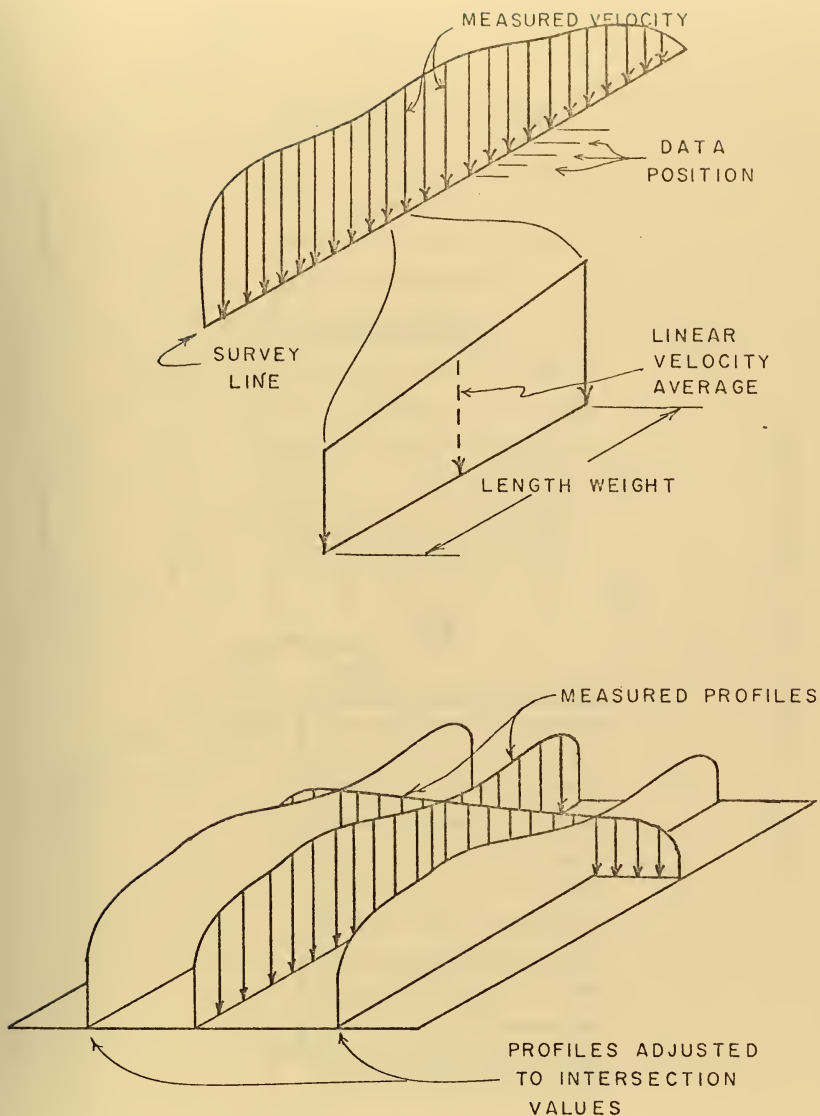
Figure 30. INLET VELOCITY AVERAGING PROCEDURE
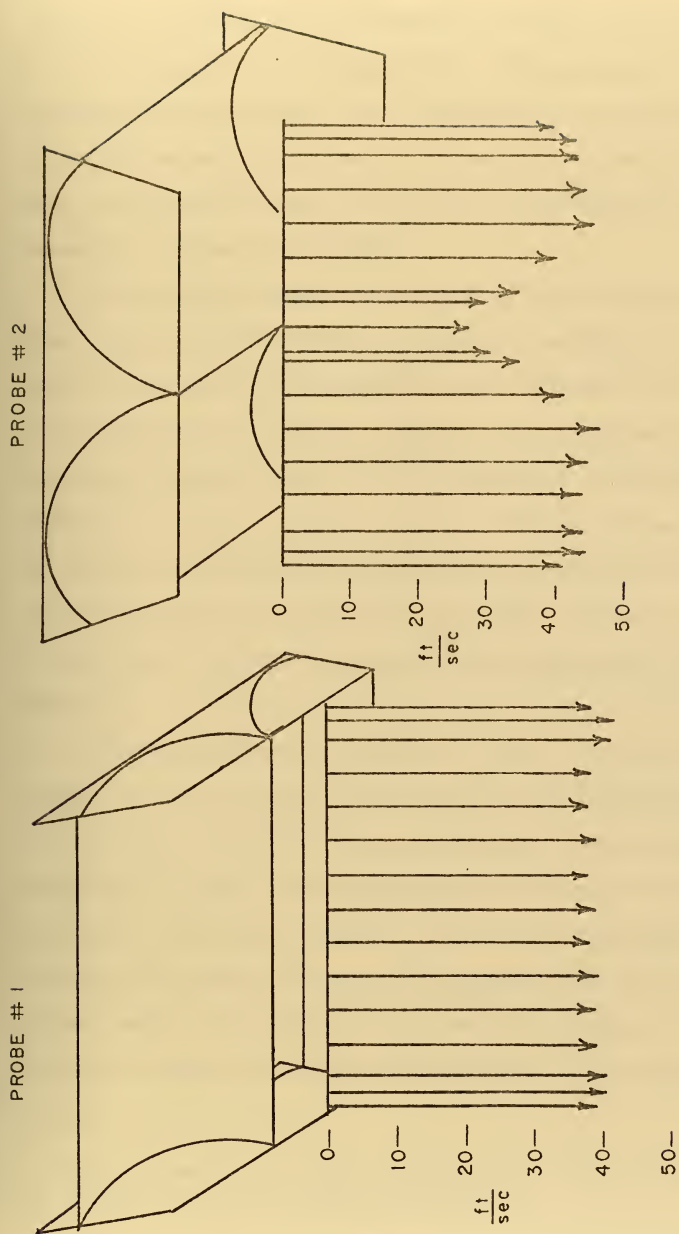
Figure 31. TYPICAL INLET VELOCITY SURVEYS

88

computed by numerical and area weighted averaging, and the mass flow averaging technique which Ferguson /Ref. 27/ demonstrates to be the only theoretically valid method. This computation also provided the average velocities and mass flow rates for the engine using the static pressure data from the probe nearest to each total pressure position and the assumption of atmospheric density.

Average total pressures for each 45° sector of the compressor face plane was then evaluated using mass flow weighting. If any sector was more than one per cent below the overall average in total pressure, it was identified as spoiled. Adjacent sectors were then examined to determine the angular extent of the low pressure area by linear inter- polation of the sector average values.[1] With this information the Naval Air Propulsion Test Center's circumferential distortion factor used by the Arnold Engineering Development Center /Ref. 36/ was also evaluated at this point along with other common distortion measures shown in Table III.

These factors were considered to apply to a typical current turbojet (first stage compressor rpm of 8320 and high pressure stages at 14,154 rpm). Where known limits existed for the initiation of engine stall or surge, these distortion indices were evaluated as sat- isfactory for this typical engine. If the inlet configuration produced unsatisfactory distortion levels, the limiting type was identified (either radial or circumferential). Where the limiting distortion was radial, the program indicated whether the stall would originate in the

---

[1] This procedure is identical to that used in Ref. 21 except that 30° sectors were used in that investigation.

Table III. MEASURES OF DISTORTION

NAME	SOURCE	DEFINITION
K	Ref. 11	$$\dfrac{\left[(\bar{\Theta}/2\pi)(q/P)^{1/2}\right]_{ref.}}{(q/P)^{1/2}/(\bar{q}/\bar{P})^{1/2}}$$ Where $\bar{\Theta} \equiv$ radial extent of spoiled sector.
K_r	Ref. 42	$$\left\{(\bar{r}/r_{\bar{c}})(r_2-r_1)/\left[r_2 Z_2(r) - r_1 Z_1(r)\right]\right\} \times$$ $$\left[\left\{\left[1-(\Delta P/\bar{P})\right]/\sqrt{(q/P)/(\bar{q}/\bar{P})'}\right\}-1\right] \times$$ $$\left[1 + (q/\gamma P)\right]$$ where Z is a complex function of position formed from eigenvalues of appropriate momentum equations and a linear combination of Bessel functions of the first and second kinds.
K_D	Refs. 7 and 10	$$100\sum_{n}\dfrac{\left[\left(\dfrac{P_{ring(avg)} - P_{ring(min)}}{P_{ring\,(avg)}}\right)\bar{\Theta}_{ring}\,C_{ring}\right]}{\sum C_{ring}}$$
D_I	Ref. 43	$(P_{T_{max}} - P_{T\,min})/P_{T\,avg}$
D_{I2}	Ref. 43	$(P_{T_{avg}} - P_{T\,min})/P_{T\,avg}$
D_{I3}	Ref. 43	$(P_{T_{max}} - P_{T\,min})/P_{T\,avg}$

RADIAL DISTORT.
BAND LIMITS

PROBE

AREAS

(minus probe
blockage)

ⓐ   0.5964 in^2

ⓑ   0.38935 in^2

ⓒ   0.4399 in^2

ⓓ   0.7698 in^2

Figure 32. SURVEY PLANE SUBDIVISIONS

91

the hub or tip area of the compressor blades. When circumferential

distortion caused unsatisfactory performance, the program output in-

cluded the rpm below which the compressor could operate unstalled in

the inlet being evaluated $\boxed{\text{Ref. 41}}$. Intermediate values required in

the calculation procedure and all results were printed for each con-

figuration. At the end of each processing run, a summary table was

produced which had the form of the tables included in this report in

the computer output section.

A modified form of this program was also developed which elimi-

nated the complete data for each configuration and produced a punch

card output containing the summary data. Two sorting routines were

then used to assist in the organization of the test data. Both sorted

the summary data cards and produced tables containing this data arranged

in sets having configuration code numbers with a common digit in any

desired position. This permitted the test results to be collected into

groups having common inlet components or operating conditions.

The sorting programs differed in the ordering of the tabular

data. The first produced tables in which the configuration code numbers

were arranged in numerical order. The second type of tables were

arranged in order of increasing distortion level. Primary ordering was

dependent on the value of the NAPTC circumferential distortion index.

Where differences in this value were not significant, the data lines

were ordered using values of the radial index. Both included optional

commands to permit the production of complete summary tables ordered in

the same manner as the grouped ones. The numerically ordered tables

permitted rapid location of the data for any desired configuration

number and grouped the results of repeated tests for comparison. Those

ordered by distortion level simplified the selection of high and low distortion configurations and components. Ordering of the test data in this manner was instrumental in permitting rapid testing of the various proposed correlation methods since any system which radically altered the order of the configurations could be discontinued.

VI. TEST RESULTS

A. MODEL PERFORMANCE

Construction methods and materials proved to be satisfactory in all
respects. Two inlet components were damaged during the test program,
but repairs required minimum time and were affected without alteration
of the duct dimensions or finish. Measurable distortion of the duct
components occurred only during the tests in which the cell depression
exceeded two inches of water. Maximum deflection was less than one
per cent of duct height, and no attempt was made to correct the data
for the three tests in which depression in excess of two inches was
observed.

The jet pump exhaust simulator provided more than adequate augmen-
tation flow in the model, but the number of variables (augmentor geometry
and placement, cell depression, and primary flow rate) controlling this
flow rate was such that it was not possible to predict in advance the
augmentation ratio which would exist during each run. This resulted in
variations between tests which precluded the possible quantitative
evaluation of the effect of augmentation on distortion level.

The limited capacity of the suction source placed an additional
limitation on the variety of configurations tested. The losses produced
in the ducting between blower and compressor face, when the model was
assembled for augmented flow tests, were of a magnitude to produce an
engine power level similar to that produced by direct connection of the
engine to the blower with the maximum flow restrictor in place. Future
extension of the test results reported here will require the addition
of a more powerful and directly adjustable suction power source.

Performance of the test instrumentation was acceptable. The automation of the data processing task would have made the use of a manometer board with variable inclination readily feasible and would have improved the accuracy of the test data by providing an adjustment for the wide range of pressures encountered. No attempt was made to directly assess the effect of test section blockage by the instrumentation leads; but their effect could be observed during flow visualization, and streamlining of this area should be considered in future tests.

The design of the model used in this experimental investigation was fundamentally sound and provided reproduceable data of the required type and quantity. The time required per test run was considered excessive; approximately one hour for non-augmented configurations and two for those in which both power systems were required. This was due primarily to the necessity for hand recording of the data and subsequent transfer to punched cards. Extensive future use of this model should involve the installation of at least semi-automatic data acquisition equipment.

B. COMPONENT PERFORMANCE

1. Acoustic Treatments

Of the models tested, the tubular type proved to be the least satisfactory with only 5 of 27 configurations exhibiting acceptable distortion levels. All of those which were satisfactory required that the tubular treatment be located in the horizontal flow straightening section; a highly impractical arrangement for actual test cells. Additional testing of this treatment with varied flow length and blockage models will be required before it is completely evaluated, but initially it does not appear to be competitive. It was not possible to discriminate

clearly between the other tested acoustic alternatives as they exhibited
approximately equal percentages of satisfactory performances.

2. Inlet Caps

Through the testing of numerous configurations which differed
only in the type of inlet cap, it was possible to make a fairly clear
determination of their effect on inlet distortion. In general, the
faired cap produced minimum distortion at the compressor face, followed
by bi-directional, open end, and flat plate caps. This order was con-
sistent (within the accuracy of measurement) for all configurations in
which the acoustic treatment was located in the vertical stack portion
of the inlet duct. For those vertical configurations without acoustic
components (the lined wall concept of Appendix C) or those with the
treatment in the horizontal duct section, cap performance was less pre-
dictable and highly dependent on the type of turning vanes included.
With four or seven present in the duct bend, the performance of the
open ended vertical inlet was greatly improved. Seven turning vanes
acted with the uncapped inlet to provide less distortion than with any
of the other caps, regardless of acoustic type. The flat plate cap
also improved the uniformity of the flow produced when at least one
vane was present in the corner. With four or seven vanes in use, this
cap was superior in performance to the bi-directional one. Using one
or three vanes, it was better than the open inlet though not quite equal
to the bi-directional.

3. Duct Orientation

The effect of duct shape was the clearest and most easily pre-
dictable. Only one of eight horizontal inlet configurations (that
without flow straighteners and with the staggered acoustic baffles

inserted horizontally) was found to be unsatisfactory. Conversely, 29
of the 34 triple turn configurations exhibited unsatisfactory distortion
levels. Although it was not possible to test this arrangement with
turning vanes in all three corners, several combinations of vane numbers
and positions were investigated without finding one which could reduce
distortion to an acceptable level over a range of flow rates. Vertical
inlet configurations were of intermediate value with the distortion
level being dependent upon the other duct components. No vertical con-
figuration was better than the best horizontal one or worse than the
worst three-turn model.

C. CORRELATION METHODS

1. Distortion Measurement

The first decision necessary in the establishment of a correla-
tion method was the selection of the distortion measurement index to
be used. Any of those listed in Table III could have been selected.
The choice was made on the basis of the evaluation of these and other
indices reported by Brunda and Boytos in Refs. 42 and 44. It was their
conclusion, based on extensive experimental research, that of the avail-
able distortion indicators only the NAPTC circumferential and radial
indices could be consistently related to engine performance. They
additionally determined that for the majority of current and future
jet engines, performance is most often limited by the extent of the
circumferential distortion. The NAPTC circumferential distortion factor
was selected as the measure of distortion level with which inlet con-
figuration would be correlated.

2. Inlet Correlation Parameters

a. Alternatives

It must be considered possible that the distortion level measured at the engine compressor face of a jet engine might be related to any of the following factors either singularly or in any combination:

1. Average flow length.

2. Total wetted area.

3. Difference between maximum and minimum streamline length from inlet cap to compressor face.

4. Number of distinct wetted surfaces.

5. Total degrees of turning.

6. Percentage of duct length obstructed.

7. Maximum local velocity or position.

8. Separated flow volume or area.

9. Number, volume, or surface area of cross duct obstructions.

10. Engine position relative to duct center.

11. Ratio of duct height to width.

12. Number, position, or size of turning vanes.

13. Shape, length, or blockage of flow straighteners.

14. Shape of inlet cap.

15. Relative component lengths or areas.

16. Number and ratio of convergent-divergent flow sections.

17. Surface roughness.

18. Position or shape of screens.

19. Engine or augmentation flow rates.

20. Augmentation ratio.

21. Engine bellmouth shape or size.

22. Cell depression.

23. Exhaust back pressure.

24. Size or ratio of turn radii.

b. The Selected Correlation Method

Eleven separate correlations were attempted between indivi-
dual configuration characteristics included in the above list and the
selected distortion indices. In none of these was there evidence of a
consistent relationship. As a result, the following rational approach
to the analysis of the interactive effects was developed. This initial
correlation development was confined exclusively to vertical inlet con-
figurations. This is an extension of the method used in Ref. 15 for
the correlation of aircraft inlet effects.

The components considered were the inlet cap, the type of
acoustic treatment, its position, and the number of turning vanes present.
For each of these components, distortion producing contributions were
considered possible from seven characteristic properties:

1. Distance from the upstream component.

2. Component length.

3. Percentage of duct area reduction.

4. Number of flow subdivisions produced.

5. Degrees of turning.

6. Alignment with upstream components.

7. Alignment with next downstream component.

For each type of duct component, the available alternative models were
rated according to the possible contribution of each of the above factors.
The initially assigned values are shown in Table IV. The configuration

99

Table IV. INITIAL PENALTY WEIGHTS

COMP CODE	DIST	LTH	%BL	#DIV	^{o}T	AL UP	AL DW
B = 1	0	2	0	4	45	0	0
2	0	0	0	3	20	0	0
3	0	3	10	2	100	0	4
4	0	4	40	4	135	0	0
5	0	3	10	2	100	0	2
C = 1	0	8	0	0	0	0	0
2	0	8	50	12	15	0	0
3	0	8	60	24	30	0	0
4	0	3	75	64	45	0	0
5	0	8	60	24	30	2	2
D = 1	16	5	0	0	0	0	10
2	8	0	0	0	0	0	5
3	2	0	0	0	0	0	0
4	16	5	0	0	0	2	5
5	16	0	0	0	0	0	2
E = 1	0	3	0	0	90	5	20
2	5	0	4	2	90	5	0
3	5	4	16	5	90	5	10
4	15	5	28	8	90	5	10
5	10	2	4	2	90	5	10
6	15	1	4	2	90	5	0
COL. TOT.	108	72	401	208	1060	32	71
SIGNIF.	80	70	100	20	60	40	30
FACTOR	.75	.97	.25	.10	.0566	.8	.422

component codes used in this table are the same as those established in Table II. These values were considered penalty factors with higher values designating greater distortion potentials. To normalize these penalty values an initial estimate was made of the relative importance of the seven selected distortion characteristics. This estimate is shown in Table IV as the SIGNIFICANCE line. The multiplication factors necessary to reduce the column totals to the desired significance level were determined and applied to each of the penalty factors in that column. This produced the adjusted factors shown in Table V. The total estimated penalty factor for each configuration component was then available in the ROW TOTAL column.

These component factors were applied to a random selection of configuration codes, first through the addition of the penalty weights and secondly by the multiplication of these values. The selected configurations were then ordered according to their total penalty value and the resulting ranking compared with that produced by sorting the same configurations according to distortion level. These ordered lists were examined to discover components or combinations of them which were present in configurations found to be out of order. The distortion penalty weights assigned to these components were then adjusted by the amount necessary to correct this order. The penalty totals for all configurations required re-evaluation after each such adjustment. When excessive corrections were applied, the resulting disorder was often greater after correction than before.

This process was then repeated with the object of producing a set of component penalty weights which when either added or multiplied together ordered the configurations according to their distortion level.

101

Table V. NORMALIZED PENALTY WEIGHTS

COMP CODE	ROW TOT	DIST	LTH	%BL	#DIV	$^{\circ}$T	AL UP	AL DW
B = 1	4.94	0	2	0	.4	2.54	0	0
2	1.43	0	0	0	.3	1.13	0	0
3	13.06	0	3	2.5	.2	5.66	0	1.7
4	21.9	0	4	10	.4	7.5	0	0
5	12.2	0	3	2.5	.2	5.66	0	.844
C = 1	8.0	0	8	0	0	0	0	0
2	22.55	0	8	12.5	1.2	.85	0	0
3	27.1	0	8	15	2.4	1.7	0	0
4	30.69	0	3	18.75	6.4	2.54	0	0
5	29.54	0	8	15	2.4	1.7	1.6	.84
D = 1	21.22	11.8	5	0	0	0	0	4.22
2	8.11	5.96	0	0	0	0	0	2.11
3	1.5	1.5	0	0	0	0	0	0
4	20.71	11.8	5	0	0	0	1.6	2.11
5	12.84	11.8	0	0	0	0	0	.84
E = 1	20.54	0	3	0	9	5.1	4	8.44
2	14.05	3.75	0	1	.2	5.1	4	0
3	25.57	3.75	4	4	.5	5.1	4	4.22
4	37.37	11.25	5	7	.8	5.1	4	4.22
5	19.8	7.5	2	1	.2	5.1	4	0
6	24.66	11.25	1	1	.3	5.1	4	2.11

In applying this method it became apparent that the summation technique required fewer iterations, and it was adopted as the preferred technique. Multiplication totals were kept for reference, but iteration was terminated once the additively ordered list matched the distortion ranking.

Beginning with a set of 10 vertical configurations, the ordering was completed after 5 iterative adjustments of the penalty weights. Ten additional configurations were then added to the ordered set and the adjustment procedure repeated if necessary. This procedure was continued until all of the 176 vertical configurations tested were included in the ordered set.

Several times during the execution of this phase progress was arrested when a cycle of repetitive adjustments were established. In some of these cases it was possible to identify one or more of the most recently added configurations which were responsible for the untracking of orderly progress. These suspect configurations were reassembled in the lab and the distortion measurement tests repeated. In 12 such cases significant changes in distortion level were observed. If a second retest confirmed this new result, the original data was deleted from the summary file and replaced with the improved measurement.

In 8 of the required retests the originally measured distortion level was confirmed. These configurations were assigned an EXCEPTION label and examined after each subsequent adjustment of penalty values. If this examination found the new set of weights ordered this configuration properly, it was returned to the ordered set. Otherwise, it remained in the exception file and was not considered in determining the acceptability of subsequent weight sets.

It was recognized that measurement accuracy was a necessary consideration in the distortion order ranking. Appendix B demonstrates that the assumed limit of total pressure measurement accuracy of 0.01 inches of water represents a possible variation of from three to eleven rank positions depending upon overall position in the distortion spectrum. Thus, as the number of configuration included in the ordered set increased, it became more improbable that any set of weights would order the list exactly as it was arranged by the data processing program. This was accounted for by considering only the first three non-zero digits of the circumferential distortion factor value to be significant. A set of penalty weights which properly ordered this index value rounded to the third digit was considered satisfactory.

A total of 275 different sets of weight values were considered before further progress was considered to require a change in the original distribution of distortion contributions. The final "best" set of component weights is shown in Table VI. The extent of the correlation between configuration and distortion is shown in Figure 33 where each point represents a tested configuration located by its distortion level and total additive configuration penalty weight.

This final set of penalty values was transferred to the initial distortion factor estimate table (Table V), and the adjustment required to bring each row total to the final penalty value was applied to each weight in that row. The relative size of the column totals then reflected the observed importance of the distortion characteristics included in the study. These values comprise the SIGNIFICANCE line of Table VI and represent the final results of this investigation. The effectiveness of this correlational development technique is dependent

Table VI. FINAL PENALTY WEIGHTS

COMP CODE.	ROW TOT.	D	L	%	#	o	UP	DW
B=1	22	0	8.9	0	1.78	11.3	0	0
2	22.5	0	0	0	4.75	17.8	0	0
3	25	0	5.75	4.8	.38	10.8	0	3.25
4	30	0	5.5	13.7	.55	10.3	0	0
5	26	0	6.4	5.3	.43	12.1	0	1.8
C=1,D=3	51	8.1	4.3	0	0	0	0	0
C=2,D=1	51	13.75	15	14.6	1.40	.99	0	4.9
C=2,D=2	34	6.7	8.8	13.8	1.33	.94	0	2.34
C=2,D=4	45	12.3	13.5	13.0	1.25	.88	1.66	2.2
C=3,D=1	47	11.5	12.6	12.2	1.2	1.65	0	4.1
C=3,D=2	45.5	7.7	10.5	19.4	3.1	2.2	0	2.73
C=3,D=4	50	12.4	13.5	15.7	2.5	1.8	1.73	2.2
C=4,D=1	60	13.7	15	21.7	7.4	2.96	0	4.9
C=4,D=2	43	6.6	3.33	20.8	7.1	2.82	0	2.33
C=4,D=5	60	16.7	4.23	26.4	8.9	3.58	0	1.18
C=5,D=2	41.5	6.6	8.8	16.5	2.64	1.87	1.76	3.25
E=1	32	0	4.7	0	0	8	6.25	13.1
2	29	7.75	0	2.06	.41	10.6	8.25	0
3	28	4.1	4.38	4.38	.55	-5.6	4.38	4.62
4	25	7.53	3.34	4.68	.53	3.4	2.68	2.82
5	32	12.1	3.23	1.61	.33	8.25	6.46	0
6	33	15.1	1.34	1.34	.27	6.83	5.36	2.82
SIGNIFICANCE FACTOR		162.6	144.9	211.9	46.8	124.6	38.5	58.5

105
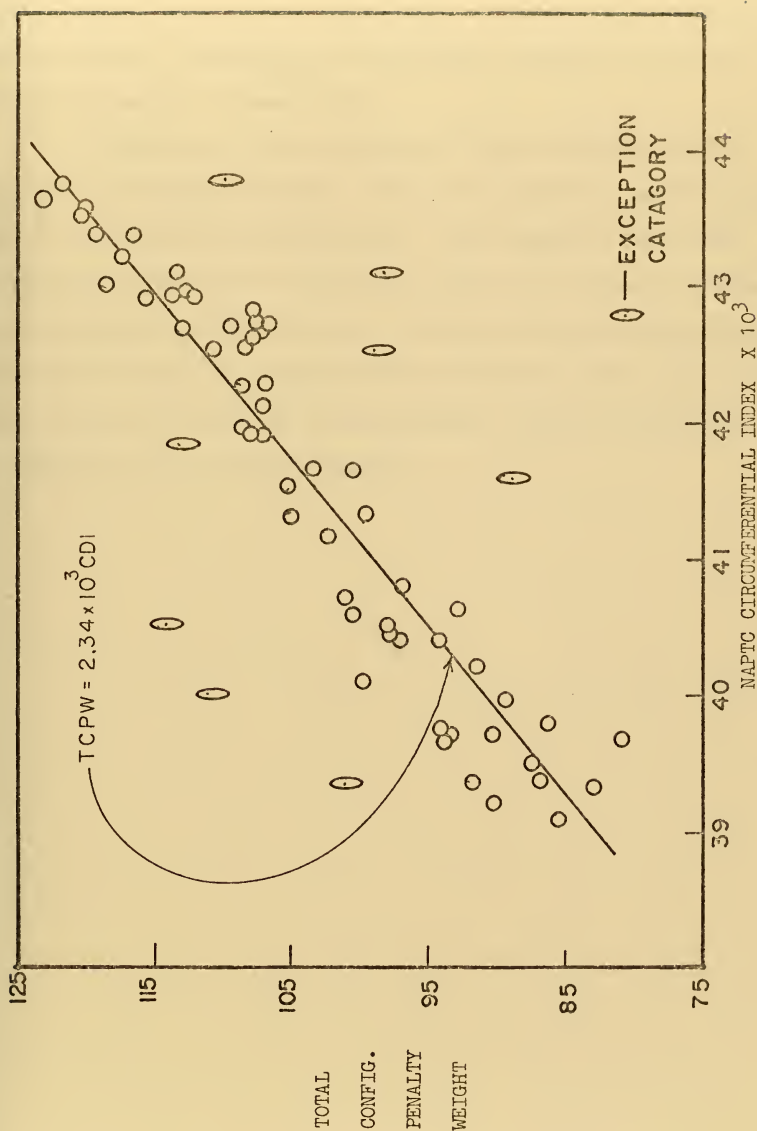
Figure 33. THE CORRELATION OF CONFIGURATION AND DISTORTION

TCPW = 2.34 × 10³CDI

⊖ — EXCEPTION CATAGORY

NAPTC CIRCUMFERENTIAL INDEX X 10³

TOTAL CONFIG. PENALTY WEIGHT

upon the initial selection and distribution of contributing distortion geometry factors. Improvement of correlational accuracy will require iterative alteration of these factors.

Adaptation of this technique to fully automatic machine processing is considered feasible. This is the next step toward development of a fully unified analysis system. This adaptation would make possible the evaluation of refined and expanded sets of component geometry and operating condition factors. Further extension would be necessary to confirm the effect of component sizing properties as well as the shape effects determined here. The steps necessary to execute this expansion are considered in the following chapter.

VII. GUIDELINES FOR RESEARCH EXTENSION

The experimental techniques, data treatment procedures, and correla-
tional development method validated through this research require ex-
tension to establish a fully inclusive empirical theory of large duct
aerodynamics. Experimentally it will be necessary to construct addi-
tional component models designed to provide variation in size and spacing
parameters in the same manner that the components used here differed in
basic geometry. The necessity for conversion of the instrumentation to
automatic data processing has been discussed and should include in its
planning provisions for the reduction of the mean measurement error.
The redesign of the power system to permit wider variation and more
direct control of primary and secondary flow rates has also been de-
tailed in previous sections.

To fully establish the validy of this experimental analysis method
it will also be necessary to observe the effect of varied duct cross
section dimensions since many non-square sections are in common use.
Similarly it will be necessary to make provisions in future model test
sections for the vertical variation of engine position and augmentor
location.

In the processing of experimental test data the results obtained in
this investigation will have a simplifying effect. Sufficient evidence
is available to conclude that the NAPTC circumferential and radial in-
dices are sufficient distortion measures, and the computation of the
others described in this report is unnecessary. Additional refinement
of the sorting methods used here should provide the capability for
sorting on more than one configuration code digit simultaneously. This

would simplify the identification of significant component performances
and reduce the number of steps required in the determination of component
distortion weights during correlation refinement.

The necessity for automation of the correlation refinement procedure
was pointed out in the discussion of the present development. This
adaptation should be relatively straightforward as far as duplicating
the efforts reported here. Once the optimum set of initial contribu-
tions of each distortion factor has been determined, it will be neces-
sary to extend the experimental portion of the investigation to include
components of similar geometry and varying dimensions and spacings.
This will permit confirmation or adjustment of the relative importance
of the included distorting factors for each type of component. The
correlation method will then be expanded to account for additional
effects including: inlet types other than vertical, engine position
in the duct, duct cross section shape, inlet flow rate, and augmenta-
tion ratio. Complete correlation will require adequate provision for
the EXCEPTION configurations discovered in this project. It will be
necessary to predict their unique character and account for their un-
expected performance. It is possible that a close examination of these
inlets and careful variation of their configuration geometry will
greatly assist in the estimation of the significance of geometric
characteristics.

It may be desirable to include in future studies additional com-
ponent designs for inlet covers and acoustic treatments. This will be
particularly true if it is found to be feasible to extend this analysis
to other applications such as the inlet ducting for shipboard gas tur-
bine power plants /Ref. 45/. Completion of the development to this

point will constitute one half of the total effort as it will still be necessary to account for dynamic distortion effects.

If the conversion of the instrumentation includes the addition of low response time total pressure transducers in the survey rake, dynamic data may be acquired simultaneously with that required for the above refinements. NAPTC has developed dynamic distortion indices similar to those employed in this development, and it is to be expected that a parallel test program will produce a correlation between inlet configuration and dynamic distortion levels.

Finally, it will be necessary to present the complete research results in easily applied handbook form for distribution. This phase is of paramount importance; and until it is successfully accomplished, the research, however complete, will have failed to meet its ultimate goal and justify its costs.

VIII. CONCLUSIONS

Based on the results of this investigation, it can be concluded that
testing of three dimensional flow models is a viable method for the
analysis of test cell inlet flow. It appears that relatively unsophis-
ticated experimental methods and standard, widely available, data re-
duction techniques can, with sufficient effort, produce substantial
improvements in future test cell designs. Pending completion of corre-
lational development and comparison with full testing of actual cells,
it is reasonable to expect that experimentally determined configuration-
to-distortion correlations will accurately predict cell distortion
performance. Completion of the research initiated in this project will
provide the means to determine optimum inlet configurations for test
facilities with known operational requirements.

No attempt was made to evaluate the effectiveness of the distortion
indices in predicting engine performance, but no correlation with con-
figuration was possible with any distortion index other than those
furnished by the Naval Air Propulsion Test Center. Currently available
handbook methods for the prediction of total pressure losses in ducted
flows were found to be adequate for use with test cell inlet models.

The data collected in the course of this investigation may be
utilized in the prediction of cell performance for configurations
having components similar to those described in this report. These
configurations are listed in the Computer Output section. To utilize
these results, consult Table II and determine the coded designation of
the configuration which is of interest; locate this code number in the
numerically ordered data summary and note the indicated value of the

circumferential distortion index. This value will permit rapid location of the configuration code in the table which is ordered according to distortion level. The position of the configuration code in this list will permit initial estimation of inlet performance. Those located in the upper or lower third of this ranking will provide satisfactory and unsatisfactory performance, respectively. For those configurations having indices which place them near the middle of this list, it is necessary to identify the range of compressor rpms which will be tested and compare it with those assumed in the determination of satisfactory performance.

This investigation was the first step in a lengthy development. It provides the basis for continuation of this development, and the results support the contention that complete success is possible with sufficient support.

APPENDIX A

COMPUTATION OF THE MODEL LENGTH SCALE FACTOR

The similarity condition for the model is that

$$\frac{B \, V_m^{-.2} \, X_m^{.8}}{L_m} - \frac{B^2 \, V_m^{-.4} \, X_m^{1.6}}{L_m^2} = \frac{B \, V_c^{-.2} \, X_c^{.8}}{L_c} - \frac{B^2 \, V_c^{-.4} \, X_c^{1.6}}{L_c^2}$$

For this investigation:

$$L_m = 1.0 \text{ feet}$$
$$L_c = 24.0 \text{ feet}$$
$$B = 0.1741 \text{ ft}^2/\text{sec}$$
$$V_c = 40.0 \text{ ft/sec}$$

Evaluating this condition in an iterative manner, treat x_c as a constant and define

$$C \equiv \frac{B \, V_c^{-.2} \, X_c^{.8}}{L_c} - \frac{B^2 \, V_c^{-.4} \, X_c^{1.6}}{L_c^2}$$

and

$$y \equiv \frac{V_m^{-.2} \, X_m^{.8}}{L_m}$$

With these, the similarity requirement becomes

$$B \, y - B^2 \, y^2 = C$$

or

$$B^2 y^2 - B y + C = 0$$

Then, taking

$$E = \frac{C}{B}$$

this becomes

$$By^2 - y + E = 0$$

Applying the quadratic formula,

$$y = \frac{1 \pm \sqrt{1 - 4EB}}{2B}$$

For a selected value of x_c, the value of x_m is then available from

$$x_m^{.8} = y\, L_m \Big/ V_m^{-0.2}$$

or

$$x_m = y^{1.25}\, L_m^{1.25}\, V_m^{0.25}$$

The model length ratio is thus:

$$\frac{x_m}{x_c} = \frac{y^{1.25}\, V_m^{0.25}}{x_c}$$

In a similar manner, the variation in simulated cell velocity with changes in model flow rate may be determined with

$$C \equiv \frac{B\, V_m^{-.2}\, x_m^{.8}}{L_m} - \frac{B^2\, V_m^{-.4}\, x_m^{1.6}}{L_m^2}$$

$$y \equiv \frac{V_c^{-.2}\, x_c^{.8}}{L_c}$$

so

$$C = By - B^2 y^2 \qquad\qquad E = -\frac{C}{B}$$

and

$$By^2 - y^2 + E = 0$$

As before
$$y = \frac{1 \pm \sqrt{1.0 - 4BE}}{2B}$$

This relation is then evaluated at selected combinations of V_m and model length ratio. From these y values, the effective cell velocity is then available

$$V_c^{-.2} = 24.0 \, y \, X_c^{-.8}$$

or

$$V_c = (24y)^{-5} \, X_c^{4}$$

where

$$X_c = \frac{X_m}{\text{Model Length Ratio}}$$

APPENDIX B

ESTIMATION OF EXPERIMENTAL ERROR

The experimental measurements in this investigation were subject to three kinds of errors: systematic errors, mistakes, and random errors. Systematic errors were reduced by careful debugging of the instrumentation system and data reduction techniques. The procedures followed in this investigation were initially designed and continuously revised in an effort to minimize these errors. The results of final comparisons and standardization checks confirmed the virtual absence of systematic errors, and these are neglected. Errors due to mistakes were minimized by the length of the experimental program which permitted the accumulation of considerable experience. Early operation revealed several common mistakes in both data acquisition and processing techniques. Checks were then incorporated to guard against their repetition. The data processing programs were developed with intrinsic error checks and for rapid reprocessing of accumulated data when errors were detected.

Random errors were mainly due to random behavior of the system and the inherent inaccuracy of the instrumentation. The magnitude of these errors may be estimated in the following manner:

The velocity vectors were calculated from the equation,

$$V = \sqrt{\frac{2(P_0 - P_s)g_c}{\rho}}$$

where, V = Magnitude of the total velocity
                        vector, ft/sec

                    P_o = Total pressure, lbf/ft^2

                    P_s = Static pressure, lbf/ft^2

                    g_c = Proportionality factor, $32.17 \frac{lbm-ft}{lbf-sec^2}$

                    ρ = Local density, lbm/ft^3

The local density, ρ , was computed from the perfect gas law equation

$$\rho = P_s / R T_s$$

where

                    P_s = Local static pressure
                        (absolute), lbf/ft^2

                    R = Gas constant for air, 53.34
                        ft-lbf/lbm-F

                    T_s = Static temperature, deg.
                        Rankine

In terms of the measured quantities, this is

$$V = \sqrt{\frac{334.42\,(h_s - h_o)\,SG}{\rho}}$$

where h_s = Measured manometer deflection
                        for static pressure, inches

                h_o = Measured manometer deflection
                        for total pressure, inches

                SG = Specific gravity of the
                        manometer fluid

The logarithmic differential of this equation is

$$\frac{\Delta V}{V} = \frac{1}{2}\left(\frac{\Delta(\Delta h)}{\Delta h} + \frac{\Delta \rho}{\rho}\right)$$

assuming that the error in the specific gravity is negligible. The error in density is

$$\frac{\Delta \rho}{\rho} = \frac{\Delta P_s}{P_s} + \frac{\Delta T_s}{T_s} \quad .$$

Assuming the maximum variation in the absolute static pressure and the static temperature to be 0.05 in Hg and 2°, the maximum error in the density is

$$\frac{\Delta \rho}{\rho} \times 100 = \left(\frac{0.05}{29} + \frac{2}{530} \right) \times 100 = .17 + .38 = 0.6\%$$

For a manometer deflection of 2.5 inches, the observed reading error was about 0.2 inches. The error in the total velocity is therefore

$$\frac{\Delta V}{V} \times 100 = \frac{1}{2} \left(\frac{0.2}{2.5} + .006 \right) \times 100 = 4.3\%$$

For several sample data sets the recorded data was adjusted by this amount and then reprocessed with the result that a variation of 0.00006 to 0.00012 was produced in the circumferential distortion factor. This 0.15 to 0.3 per cent error in the magnitude of the distortion factor corresponds, for the collected data of this investigation, to from three to eleven positions in the distortion order ranking.

APPENDIX C

Pages 120 through 200 constitute Appendix C and are a reprint of
NPS-57Ba,To72061A which was written after the completion of the back-
ground research which established the aims of this investigation.
Reference and Figure numbers apply to the listings which appear within
the appendix. To simplify the use of page number references in this
reprint the original page numbers appear in parenthesis.

NAVAL POSTGRADUATE SCHOOL
Monterey, California
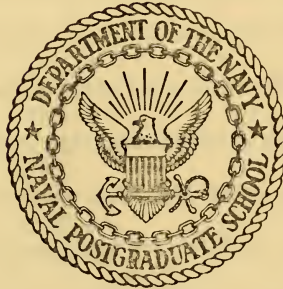
PRODUCTION TEST FACILITIES FOR TURBOJET
AND
TURBOFAN ENGINES - 1975 to 1995

D. L. Bailey LT, USN

P. W. Tower LT, USN

May 1972

NAVAL POSTGRADUATE SCHOOL

Monterey, California

Rear Admiral A. S. Goodfellow, Jr., USN   Milton U. Clauser
Superintendent   Provost

ABSTRACT:

A review is made of test cell design options in order to identify

characteristics of jet engine test facilities to be constructed in the

1970's and designed to be operable for a minimum of twenty years.

The necessity of providing replacements for many current facilities

is documented, and the factors which will ensure future production

capability and economic feasibility are detailed. Present turbine

engines are reviewed and projections of future engines and aircraft

are made. A confidential supplement is included for qualified receivers.

Experimental investigations of inlet flow patterns and engine

exhaust-augmenter relationships are being carried out. Results will be

published in thesis form in October 1972, by the Naval Postgraduate

School, Monterey, California.

ACKNOWLEDGMENT

TABLE OF CONTENTS

LIST OF FIGURES

I. INTRODUCTION

Through the 1960's satisfactory engine test facilities consisted
of large rainproof buildings located and constructed in such a manner
that the nearest neighbors were not permanently deafened. Today, the
evolution of aircraft propulsion systems has rendered some of these
installations unuseable long before their physical deterioration would
have done so. Turbojet test cells constructed during the next decade
will be required to meet a greatly expanded and refined definition of
satisfactory performance. Factors such as increased thrust, use of
high bypass turbofans, proliferation of special-purpose turbine engines,
inflation of real estate and utility costs coupled with reduced availabil-
ity and the recognition of the need for environmental protection will
increase the cost and the challenge of designing test facilities operable
through the 1990's.

It is the purpose of this report to identify the essential character-
istics of the jet engine test facilities to be constructed during the 1970's
and to provide a summary of the techniques available to meet these
requirements. In the following sections the necessity of providing
replacements for current facilities is documented, and the factors
which will ensure future production capability and economic feasibility
are detailed.

II. ENGINES

A. PRESENT

Aviation Week and Space Technology magazine, in its annual inventory issue, presents a comprehensive summary of the types and sizes of aircraft propulsion systems in use with operational aircraft. The largest in each class is of primary interest to the test cell designer but account must be taken of the wide variation within classes. Within the class of turbojet engines, thrust varies from 30,000 pounds (J58 in the SR 71) to 170 (WR24-7 in drones) and the corresponding lengths vary from 22 to 2 feet.

The facility designed to service turboshaft engines would have to handle variations in shaft horsepower from 5000 SHP (J56-A-15) to 300 SHP (TSE 36) as well as length and weight changes. Similarly, turbofan engines in military use come in one to nine-foot diameters (Harpoon and C5) and have weights of 100 to 7500 pounds. Review of current engine useage makes it obvious that the facility mission must be carefully established prior to initiation of design.

B. FUTURE

In the past, varied aircraft types were powered by similar engines. New technology developments have changed matters dramatically, as evidenced by the present differences between

characteristics of high bypass turbofans and afterburning turbojets. Future changes and developments will require more precise matching of engines and airframes for specific missions [Refs. 1, and 2].

The Navy of the future will move strongly towards utilization of gas turbine powered surface vessels. These may be surface effect vehicles (SEV), or standard design vessels, but their propulsion systems will need overhaul and repair facilities similar to those of a Naval Air Rework Facility (NARF).

Because of the vast differences of engine types, it may not prove feasible to build a single test cell capable of testing all engines. Present Navy policy is to assign the overhaul and repair responsibility of a particular type engine to each NARF. The purpose of this section is to correlate engine characteristics and projected aircraft performance.

The first advanced technology engines for Navy fighter aircraft will be used in the F-14 Tomcat. Early versions will utilize the Pratt and Whitney TF-30 412 engine, and F-14B models will be equipped with the more powerful F401 PW 400 engines. The latter engine is in the 20-30,000 pound thrust class and will have an air flow rate at full power of about 300 pounds per second. If an augmentation ratio of 2:1 is chosen a test cell flow rate on the order of 900 pounds per second will result. Other engine manufacturers are also developing afterburner equipped engines in the 25,000 pound thrust category [Ref. 3].

Further fighter aircraft developments will bring to the Navy the ADLI, or Advanced Deck Launched Interceptor. The ADLI will utilize

(3)

an advanced technology engine with turbine inlet temperatures in excess of 3,000⁰ F. Also, advanced hybrid multicycle engines are being developed and will be introduced to operational use during the life of test cells built in the present decade [Ref. 4]. Turboramjets or supercharged ejector ramjets (SERJ) are also being developed. Discussion of these engines are contained in the confidential supplement to this publication.

Future attack aircraft must combine the capability of high subsonic cruise speeds with the ability to loiter for long periods over target areas. Non-afterburning turbofan engines are presently in use and their continued development and refinement is predicted.

The U.S. Marine Corps presently have the Harrier (AV-8A) in operational use. The Navy may move toward procurement of Harrier aircraft in the near future and advanced vectored thrust V/STOL aircraft within the next ten or fifteen years. The Harrier utilizes the Pegasus turbofan engine with variable nozzles which is built by Rolls Royce. The advanced Pegasus 15 will have 25,000 pounds thrust and an airflow requirement of 450 pounds per second. A requirement for testing these engines is that shrouds and ducts be installed for directing the exhaust streams of the individual nozzles into a common exhauster [Ref. 5]. Total cell requirements for this engine will also be 900 pounds per second with a 1:1 augmentation ratio.

The Navy is currently developing the S-3 carrier based ASW aircraft, which is powered by the General Electric TF-34 turbofan

engine. This is a 9,000 pound thrust engine with an airflow capacity

of about 300 pounds per second, and will be the first engine that the

Navy operates that will be tested in the same configuration as it is

mounted on the aircraft. That is, it will be pylon mounted, thereby

requiring an overhead thrust bed. Because of the large mass flow

through the turbofan engine any pressure variations in the cell acting

across the fan exhaust will cause errors in thrust measurement. The

TF-34 has a bypass ratio greater than 6:1. Because of the exhaust

characteristics of turbofan engines care must be taken in matching

the engine and augmenter to avoid excess air entrainment over that

which is required for cooling purposes, thereby increasing the cell

depression [Ref. 6].

Future patrol aircraft developed to be introduced in the 1980's

may utilize large fan engines. Other aircraft using the same type

engines may be those developed to replace the Navy's present trans-

port fleet. Military transports with STOL capability will require

turbofans in the 25-30,000 pound thrust category [Ref. 7]. The air-

flow through an engine of this size will be on the order of 1,000 pounds

per second and total cell airflow could run as high as 2,000 pounds per

second, depending on the augmenter design.

Smaller logistic aircraft, successors to the C-2 COD aircraft,

may use turbofans in the 5-10,000 pound thrust class. These will be

similar to the above-mentioned TF-34 in flow requirements, and test

facility requirements will be similar as well.

Future weapons system acquisition will have a bearing on air-craft design, and therefore on engine design. Work is presently being done to develop laser weapons for aircraft use. For some missions, the effectiveness of this weapon is proportional to the power which can be generated in the transporting aircraft and such systems may require a platform as large as the Lockheed C-5A [Ref. 8]. If the Navy were to acquire such a system for strategic defense, it would find itself in possession of turbofan engines in the 50,000 pound thrust category, having airflow requirements of 1,500 pounds per second and requiring a test facility capable of handling 3,000 pounds per second airflows.

Consideration also must be given to the testing of turboshaft engines used in large rotary-wing aircraft. Facilities must be available for the measurement and absorption of the shaft energy generated by such engines. Similarly, turbine engines used for surface ship propulsion systems will require complex gearing and energy absorbing systems [Refs. 9 and 10].

Other trends in engine/airframe mating techniques will require some modification of test cell design and operation. The F-14 aircraft will utilize non-interchangeable left hand and right hand engines. This may mean that reversible mountings, slave accessories and so forth will be required in cells.

In order to minimize drag associated with nozzle and airframe interaction, non-axisymmetric nozzles may be employed in the future.

This possibility implies a requirement for an augmenter tube designed to permit replacement of the receptor bellmouth.

Knowledge of systems on the horizon which may eventually become operational is essential to provide flexibility and long life for projected test facilities. Prior to test cell design initiation, the update of each subject must be accomplished.

III. SUMMARY OF TEST FACILITY REQUIREMENTS

Figure 1 is the most accurate summary of test cell requirements available from current sources. As with any forecast, it includes some uncertainty; but the information included is as authoritative as possible, having been collected from engine manufacturers, Department of Defense planning agencies, published reports of service sponsored research, and interviews with facilities planners for several test cell operators. These data makes it clear that the decision as to facility capacity will restrict usage plans for extended periods and that the operator will require guidance by policy level managers to determine final construction requirements.

Gerend [Ref. 11] provides a simple method of predicting turbine engine weights and dimensions. This method has been used to check the credibility of this summary information. These projections are specifically confined to facilities for sea-level testing only. Forecasts of requirements for altitude test facilities are available in Refs. 12 and 13.

Figure 1.

Test Facility Requirements 1975 — 1995

(A) — Full Service Facilities

(B) — Facilities Limited to Fighter/Attack A/C

Thrust at Sea Level

Total Air Flow

(9)
134
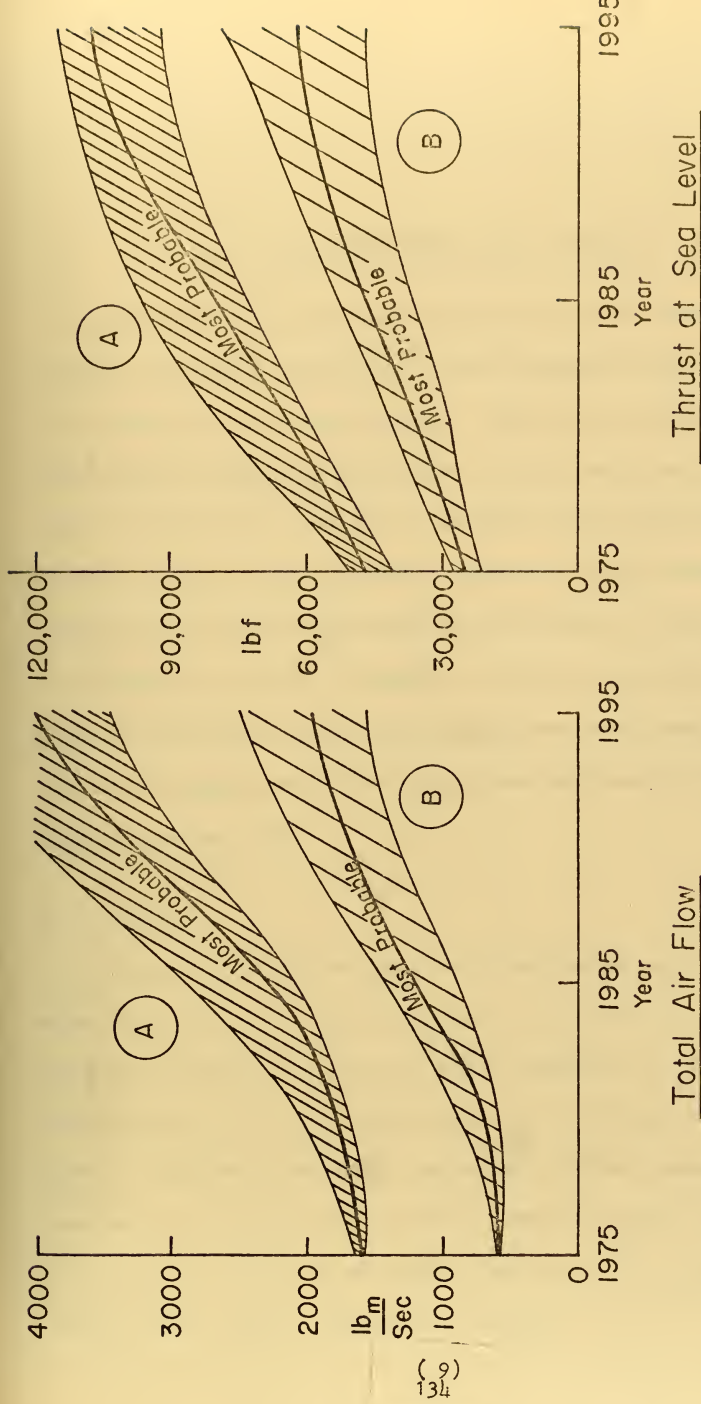
IV. PRESENT TEST CELL DESIGNS

Many currently operational jet engine test cells, both in the military and civilian communities, were designed and built to test the early generations of turbojet engines. These may be defined as the state of the art engines of the 1950's. In other instances, some even older test cells are in existence. The Naval Air Rework Facility at NAS North Island, California has several operational cells which were initially built to test reciprocating aircraft engines. These are still in use testing J-57 and J-79 engines, but their performance is marginal now and will be aerodynamically and environmentally unsatisfactory for the engines which will reach operational status in the next twenty years [Ref. 14].

A.   INLETS

Many of the oldest test cells were engineered so as to take maximum advantage of existing construction and to minimize costs. This practice is illustrated in Figure 2 which schematically illustrates the characteristics of the two oldest turbojet test facilities at NAS North Island. Of primary interest is the design of the inlet and the lack of consideration given to requirements for uniform airflow into the engine. The large block shown in the plenum chamber was the original test stand for the testing of reciprocating engines.

(10)

The next generation of test cells was designed with some added sophistication. It was realized that the test section itself should be long enough to provide for some flow straightening forward of the engine bellmouth. Such cells are typified by the installation shown in Figure 3 which depicts the general design of NARF North Island's depot level test cells designed and built in the late 1950's.

The cell aerodynamics are obviously cleaner than those pre-viously shown, and in operational use with present afterburner equipped engines they have been satisfactory. In all such installations certain compromises are made between the desired operational characteristics and economic constraints.

Modern turbine engines, particularly turbofan engines, have proven highly sensitive to aerodynamic distortion in poorly designed test cells. Large engines such as the General Electric CF6 and the Pratt & Whitney JT9D are built without inlet guide vanes, and, as a result, any distortion in the inlet flow field can have an effect on engine operation. General Electric considers total pressure distortion greater than two inches of water above or below the mean measured at the fan or compressor face unacceptable, and endeavors to reduce this difference to less than one inch H_2O [Ref. 15].

Modern test facilities built to test these large fan engines, as well as any future engines, have been designed to reduce inlet distor-tion as much as possible. United Air Lines' overhaul facility in San Francisco exhibits one of the simplest inlet designs. Air enters through
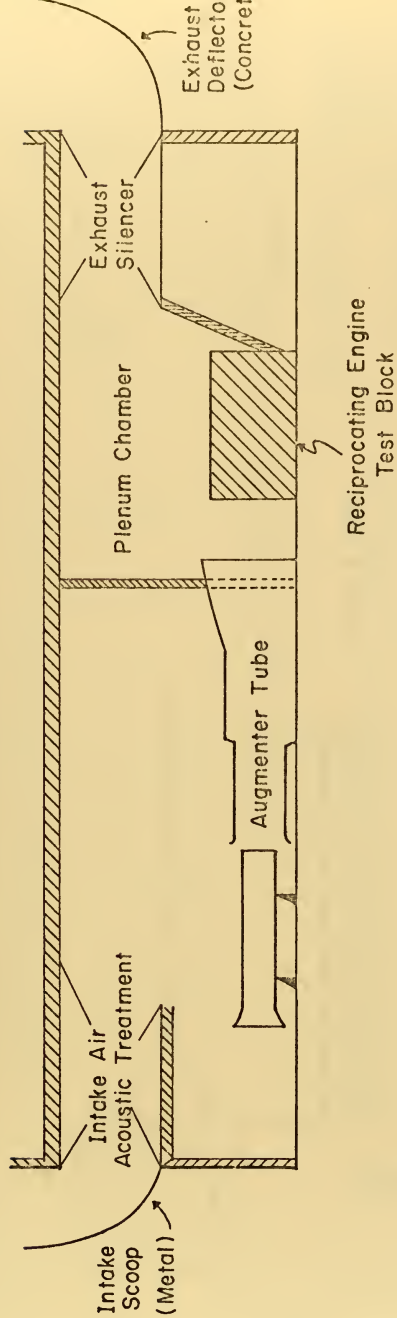
Test Cells 13, 14 Nas North Island.

Figure 2.

(12)

137
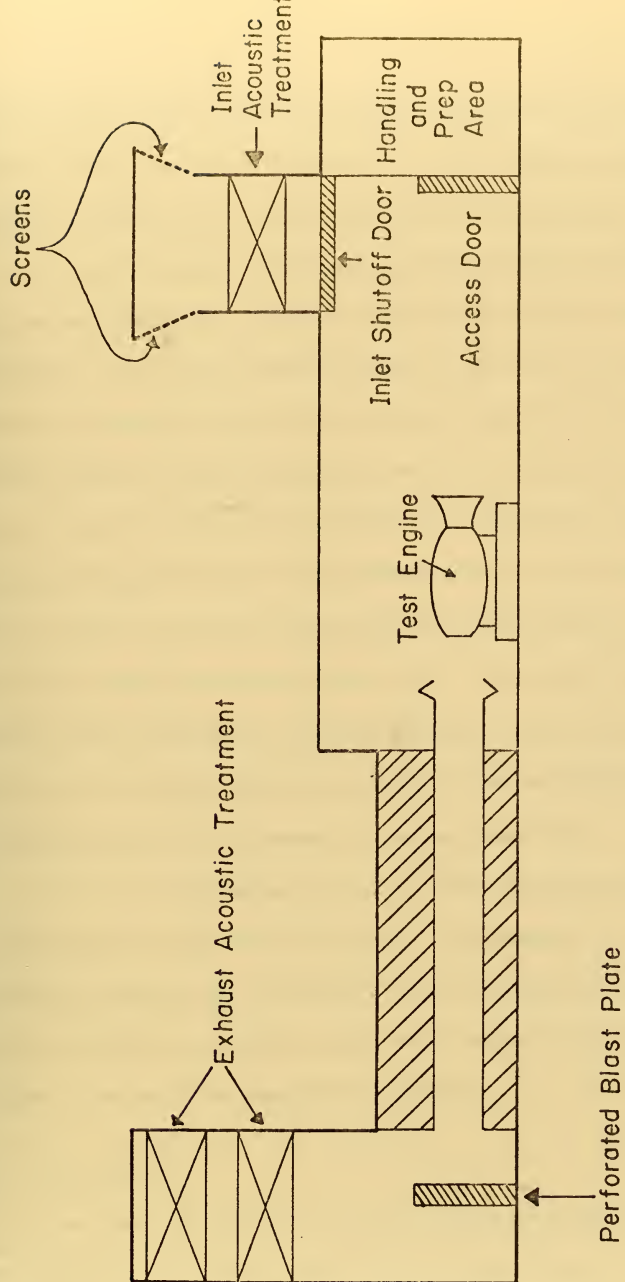
Figure 3. Test Cells 19 and 20, Nas North Island.

the horizontal inlet, passes the acoustic treatment and enters the test section without encountering any turns. This design is obviously easier to construct than one having a large vertical inlet.

A second example of modern design philosophy is exhibited in the test cell operated by Pacific Airmotive Corporation in Burbank, California. The vertical inlet is flush with the roof structure; turning vanes are installed to minimize the losses caused by the 90° turn. Turning vanes or flow straighteners will become increasingly neces- sary as test cell airflow design limits are approached. Some modern cells are designed so that turning vanes may be added in the future. The installation operated by AiResearch Manufacturing Co., in Torrance, California, has a vertical inlet. The only present require- ment for flow treatment is a corner fairing to reduce separation at the inlet bend, but designs have been drawn up for the addition of turning vanes when future requirements so dictate [Ref. 16].

A prime consideration in the use of flow treatment is the method of installing the engine in the test cell. The simplest and cheapest method of construction is to build a front-loading cell. However, if flow treatments are installed, this design requires that they be movable or that a portion of the treatment be hinged.

B.   EXHAUSTS

The basic philosophy of present exhaust treatments is to remove the majority of the kinetic energy from the jet exhaust, to cool the exhaust by mixing with secondary air or water, and to lower the noise

level of the exhaust. Removing the kinetic energy is also a method of acoustic treatment. The most common method of accomplishing the first two objectives is to utilize the kinetic energy of the exhaust to pump secondary air through the cell and into the exhauster or augmenter tube where mixing of the two streams occurs. Augmentation ratio, defined as the ratio of secondary air mass flow to engine air mass flow, is an important consideration in determining overall cell design. With an excessive augmentation ratio the depression limits of the cell may be exceeded; with too small a ratio, desired cooling may not be accomplished, and temperature limits of test cell exhaust components such as installed acoustic treatment may be exceeded. Present design goals for augmentation ratios are 2:1 for turbojet engines and 0.25:1 to 0.5:1 for high bypass turbofan engines [Refs. 5, 12, and 15]. Some facilities, however, still have augmentation ratios as large or greater than 1:1 for large turbofan engines [Ref. 17]. Turbulent mixing phenomena are not well understood, and much work remains to be done in analyzing the ejector system.

Water cooling is usually required for an engine operating in afterburner; the augmentation ratio required to cool the exhaust without water is greater than 6:1. The minimum amount of water usage is desirable in order that water supplies be preserved. Many cells utilize spray rings mounted inside the augmenter. These operate very inefficiently because of the difficulty of pentrating the hot, high speed core of the exhaust [Ref. 18]. Several attempts have been made to

Figure 4.

Static Exhaust Temperature
vs.
Augmentation Ratio

Stoichiometric Engine

J-79, A-B

J-79, Dry

Typical Turbofan

Stack Temperature (°F)

Augmentation Ratio

(16)
141
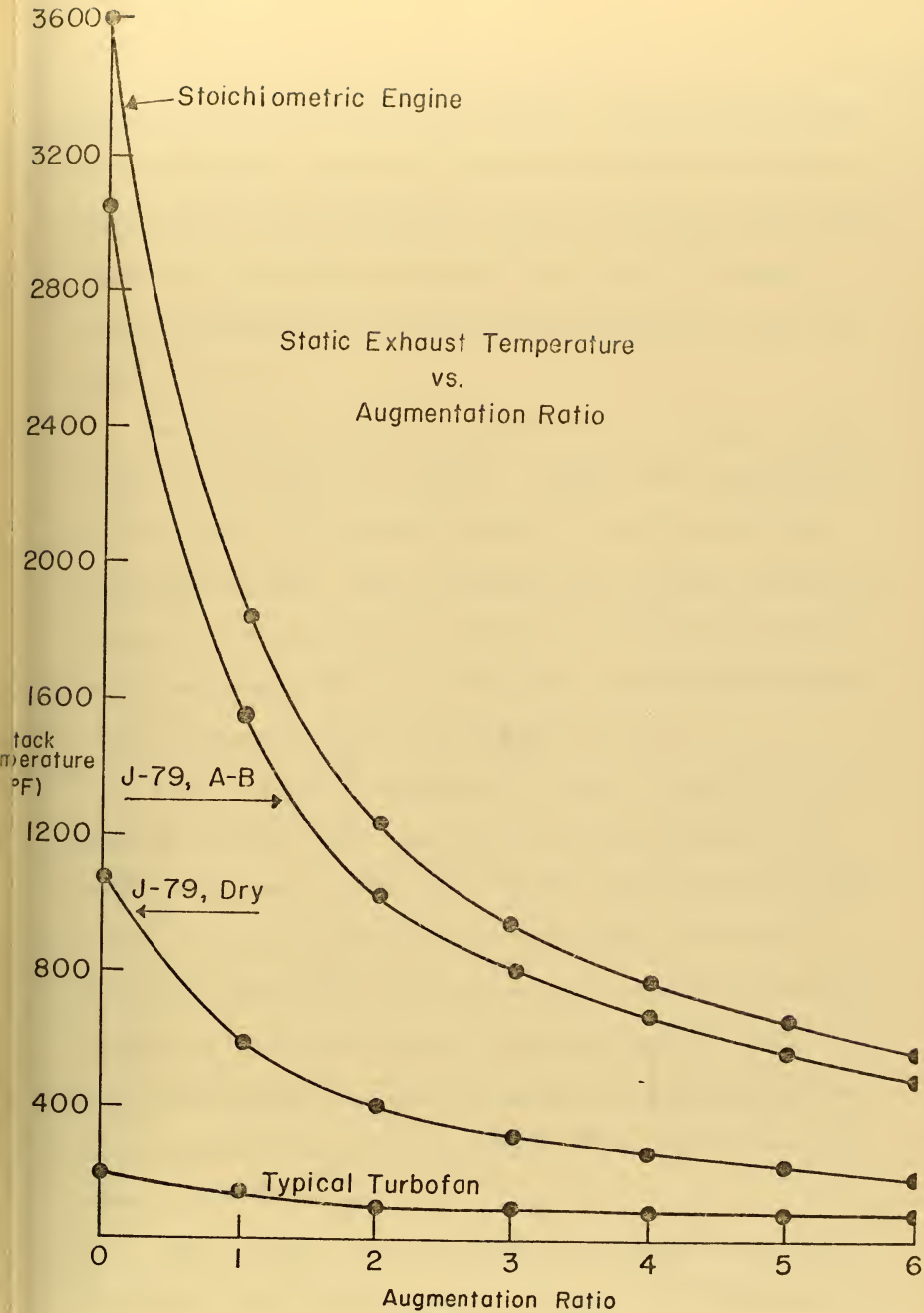
inject the water from within the core itself. The water sparger [Ref. 19] is an example. Care must be taken in the design of such items, since they can produce undesirable acoustic phenomena if their natural frequencies correspond to the driving frequencies of the exhaust. Further development of water injection is a necessity for economical future operation.

One method available for removing the kinetic energy of the jet exhaust is the "brute force" method. At NARF North Island in cells 13 and 14 [Fig. 2], the exhaust impinges on a solid concrete block, lined with steel plate. This is effective in destroying the continuity of the stream, but has failed to prevent serious damage to the walls of the plenum chamber [Ref. 14]. In the newer cells at North Island the exhaust impinges on a perforated steel plate [Fig. 3].

A newer method of treating the flow, one coming into more general use [Refs. 16, 17, 20, and 21], involves a colander in the form of a cylinder or a cone. The colander is the last section of the ejector tube, and is perforated with holes, usually on the order of 1-1/4" in diameter [Ref. 15]. This serves to break up the flow and changes the low frequency noise of the exhaust into more easily atten- uated higher frequencies. Work remaining in this area involves the study of placement and sizing of the holes so that uniform flow in the exhaust stack is attained.

Other methods of exhaust treatment will become necessary in the future. Environmental protection standards will require pollution

abatement systems for engine test facilities. These systems will require close matching between the engine nozzle and the exhauster, because any excess mass flow will unnecessarily load the abatement equipment. Also, in some cases, the flow needs to be properly conditioned before it reaches the abatement system [Ref. 22].

C.   GENERAL

Because of the relatively small flow rates, older turbojet engines could be tested in close proximity to cell boundaries. The larger engines now coming into use must be tested with adequate clearance from floors, walls and ceilings to reduce velocity distortions. This clearance can only adequately be provided by overhead thrust bed systems. Because thrust measuring devices above the engine are subject to conductive heat transfer they must either be monitored for temperature changes or kept at a constant temperature. United Air Lines' facility in San Francisco has both such systems installed [Ref. 17]. Current thrust measurement accuracy is typically $\pm$ 56 lbs. for an engine thrust of 41, 100 lb. [Ref. 23].

Overhead mounting systems have introduced a new problem to test operations in that the height of the engine when mounted in the cell makes accessibility difficult. United Air Lines has installed a hydraulically lifted platform beneath the mounting system. During actual testing the platform is lowered to a position flush with the floor, providing smooth passage for the secondary air past the engine [Ref. 17]. Another solution to this problem was developed for the previously

mentioned   AiResearch facility [Ref. 16]. The work platforms are suspended from the overhead at a convenient height, and are swung up and locked next to the ceiling during engine operation.

In many older cells considerable time is used in preparing and mounting the engine for test. If this time is kept to a minimum, total cell running time can be maximized. Modern design philosophy reduces the man-in-cell time by allowing much of the preparatory work to be done in the handling area rather than in the cell itself. In the handling area the engine is fitted to a specially designed adapter. Necessary engine connections for starting air, fuel, instrumentation leads, and external power are made to the adapter. The entire assembly is then moved to the cell area, and is hoisted to the thrust bed by a winch assembly in the thrust bed itself [Refs. 16, 17, and 20].

Means of handling and transporting the engine are also varied. Many facilities use wheeled dollies for transporting the engine and related assemblies [Refs. 16 and 17]. Some newer facilities utilize overhead monorail systems both in the handling and preparation areas and in the cell itself [Refs. 19 and 24]. Some problems have developed with monorail systems, however, and complete flow analysis must be accomplished before utilizing such a handling system. In one situation [Ref. 19], it has been found that vortices are formed by flow interaction with the monorail, causing serious flow distortion in a cell designed to test large turbofan engines.

Recently, attempts have been made to improve operator visual

contact with the interior of the cell. The usual method of providing
this contact is to provide a window between the control room and the
cell. Whenever the cell structure is penetrated, additional acoustic
problems are created; in order to provide minimum noise levels
within the control room there should be no direct connection between
the cell and the control room. One alternative to windows has been
to install closed circuit television. NARF North Island has installed
three black and white cameras in their large cells. These cameras
have no zoom or pan capability, and have not met with complete opera-
tor approval. Also, they do not obviate the need for entrance into the
cell by technicians to check for fuel or oil leaks when the engine is
operating.

Because of the varied engines which must be tested in one cell,
consideration must be given to the ease with which cell hardware can
be adjusted for various engine sizes. NARF North Island utilizes the
movable augmenter concept. The United Air Lines facility uses a
jackscrew arrangement to adjust the thrust bed position. The range
of adjustment will depend on the size of engines projected to be tested
and the means of providing adjustment is up to the option of the designer.

Modern test facilities are being equipped with automatic data
acquisition and processing capability. AiResearch Manufacturing Co.
has an excellent example of a system designed for developmental
engine testing and United Air Lines possesses a system designed for
production testing of overhauled and repaired engines [Refs. 16 and 17].

Most of the above information is applicable to depot level test cells for large overhaul facilities. Other proposals have been made for developing smaller test cells for use in intermediate level maintenance facilities. The Ground Support Equipment division of the Naval Air Engineering Center, Philadelphia, Pa., has designed the cell shown in Figure 5. This design differs greatly from those discussed in this section. A primary difference is the construction technique utilized. The cell shown is constructed from pre-fabricated sections and is designed to be demountable if the need should arise. The flow design is different in that separate intakes are provided for the primary (engine) and secondary (augmentation) airflows. Complete aerodynamic analysis is required for this and other major design alternatives.

A listing of some persons and firms conversant with current test cell design philosophy is given in Appendix B.

EXHAUST STACK

PRIMARY INLET

ROADWAY (REF.)

RAMP

WALKWAY (REF.)

FIRE EXTINGUISHING SYSTEM

SERVICE AIR

EMERGENCY ELECTRICAL SUPPLY

TEST CHAMBER

THRUST FRAME

ACOUSTIC SUPPRESSOR

AUGMENTER

DIESEL GENERATOR

SECONDARY INLET

INSTRUMENT AND CONTROL CAB ASSY.

WATER PUMP ASSY.

WATER TANK

FUEL TANK

FUEL PUMPING AND METERING ASSY.

DIKE
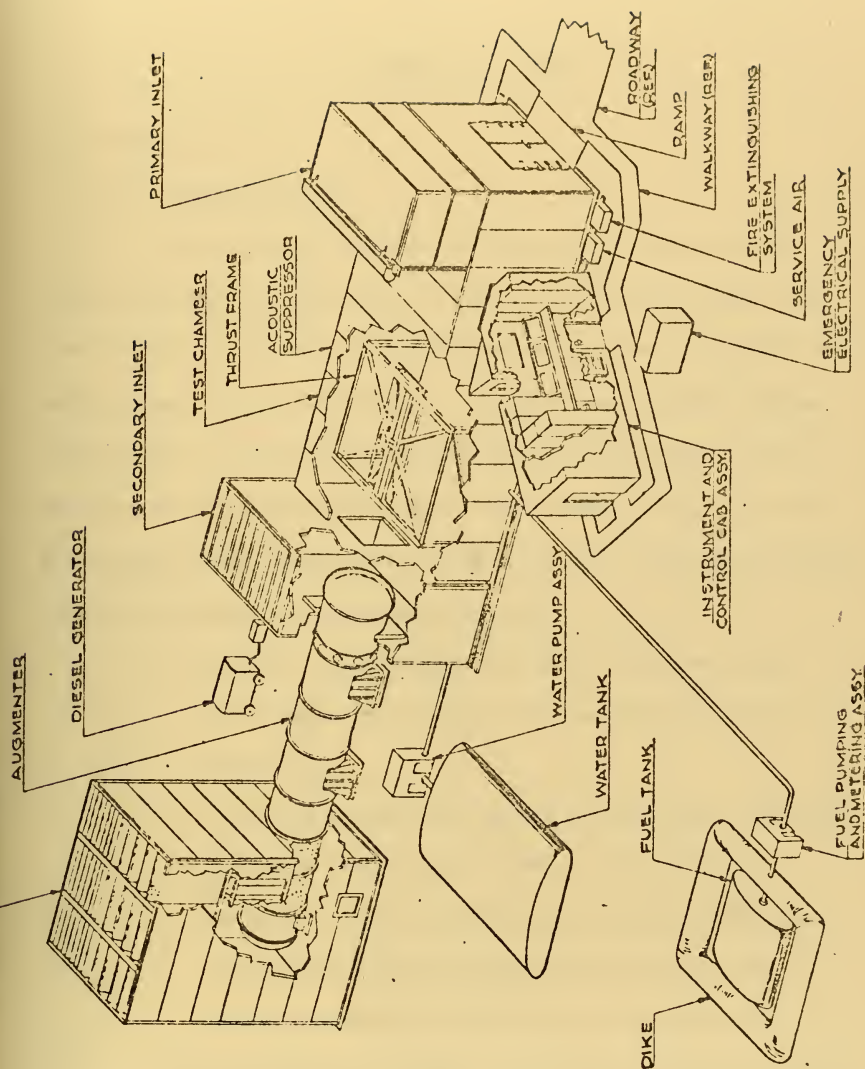
Figure 5. Demountable Test Cell.

V. DESIGN OPTIONS

A.   INLET

   1.   Acoustic Control

   The current development of commercial STOL aircraft
and increasingly stringent airport noise level restrictions [Ref. 25],
have resulted in extensive on-going research directed at reduction of
engine generated acoustic power. It is reasonable to expect that the
engines now in service will be the noisiest, per pound thrust, with
which new test cells must cope [See Fig. 6], [Refs. 26, 27, and 28].
It is equally certain that new test cells will require some form of inlet
acoustic treatment for the following reasons:

   a.   Current, noisy engines will still be in service after
        the anticipated introduction of the replacement cells
        [Ref. 28].

   b.   Turbofan engines increase the acoustic power directed
        upstream into the inlet [Refs. 27, 29, and 30].

   c.   Military aircraft will continue as the least restricted
        in required acoustic abatement by virtue of their
        mission and environment [Refs. 31, 32, and 33].

   d.   The test cell structure alone will not be able to absorb
        the acoustic power produced by even the quietest of
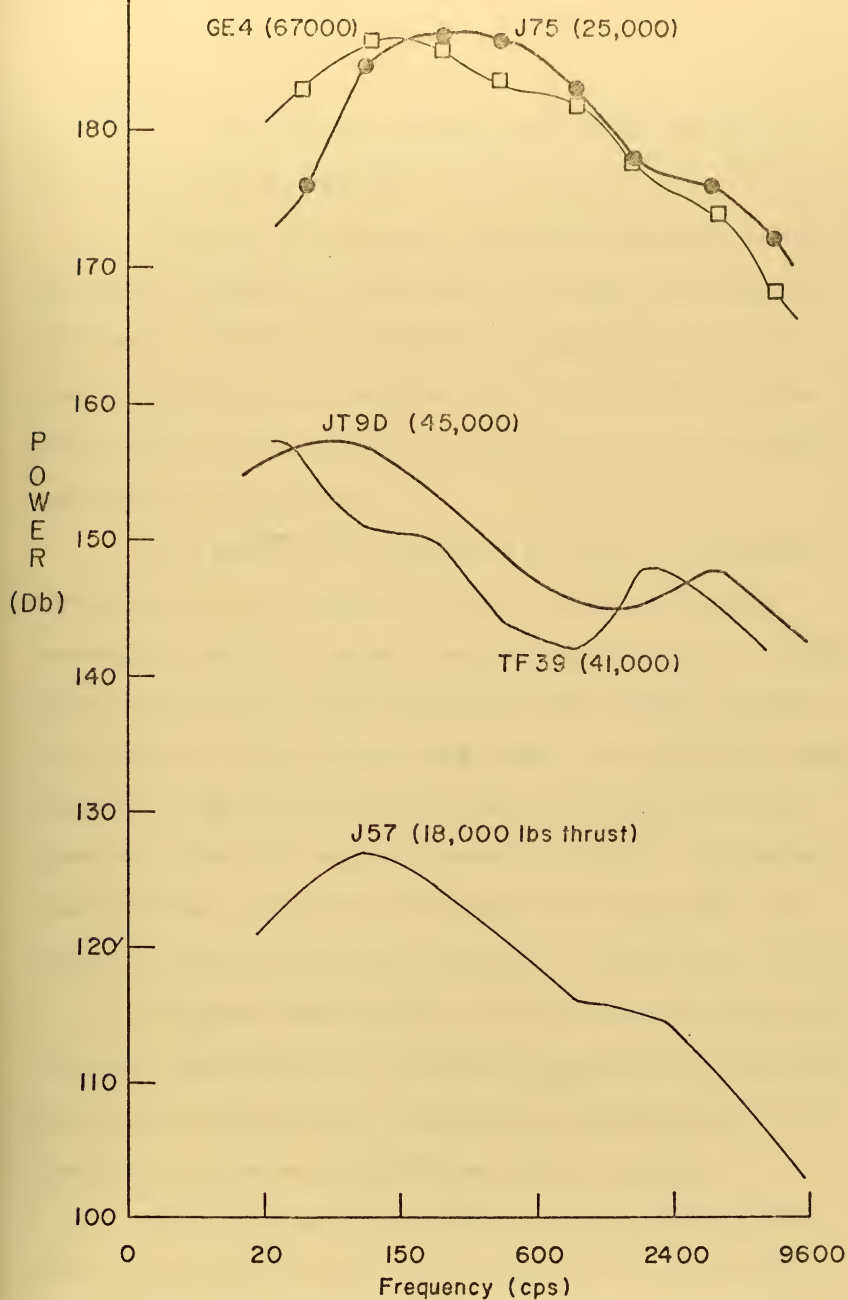
Figure 6. The effect of engine type and thrust on sound power levels.

projected future engines [Refs. 12, 25, 26, 27, 28, 31, 32, and 33].

Accepting the necessity of including specific acoustic treatment several options are available [Fig. 7]. Many of the designs for which performance data are available are proprietary ones and the cost of acquisition must be weighted against that of locally produced designs which must be oversized to compensate for the less complete information on effectiveness.

Flat baffles are the simplest of the duct obstruction types. Of sheet metal and fiberglass composition they can, with careful streamlining, provide acceptably low levels of flow distortion. Adjustment of length, thickness and spacing can match acoustic absorption characteristics to specified frequency ranges. The overall flow length required to meet both acoustic and aerodynamic limits may be the greatest for this option and the increased cell length or stack height must be off-set by simplicity of installation and replacement. Both proprietary and non-proprietary designs are available [Refs. 12 and 28].

Staggered baffles require less total flow length for the same absorption and produce less aerodynamic distortion than the flat types. They are also more difficult to construct and replace though reduced total size may ease handling difficulties [Refs. 28 and 34].

The sinuous passage treatment requires a length and produces a distortion level intermediate to those of the two baffle types. Construction and installation is more difficult and expensive than

(25)
150
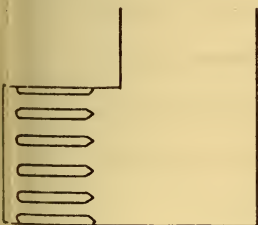
1 Flat Baffle

2 Staggered Baffle
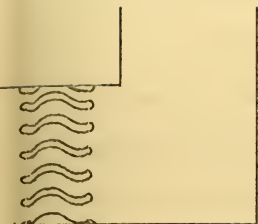
3 Sinuous Passage
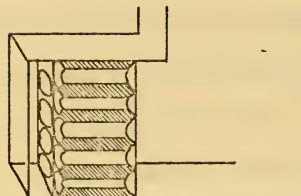
4 Tubular
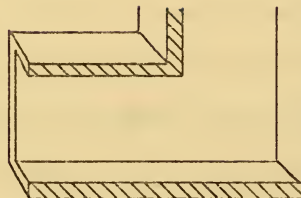
5 Lined Walls

1-4 may be used
with Horizontal
Inlets.

Figure 7. Inlet Acoustic Treatment Options.

either of the baffles, but proprietary designs are available which
permits single panel replacement [Refs. 28 and 33].

The acoustic performance of the tubular treatment reduces
the total flow length required below that of the other options but the
distortion level in some operating conditions may demand an increase
in mixing length which offsets this gain. Additionally they may prove
incompatible with good turning vane performance when used in a
vertical inlet. The available designs with adequately documented
performance levels are proprietary in nature [Refs. 25 and 29].

Another option which is not in current use and which remains
to be fully evaluated as to effectiveness is the lined wall concept. By
lining the considerable wall/overhead area foreward of the engine
inlet with suitable foam and lead septum material it may be possible
to entirely eliminate the need for duct obstructing devices with conse-
quent simplification of distortion control. Since considerable absorb-
ing thickness could be provided at low cost in a test cell, this option
must be considered. Preliminary analysis by the treatment manu-
facturer indicates that this method would be restricted to a vertical
inlet arrangement. The lining material is available from commercial
sources and it would be necessary to obtain their assistance in deter-
mining the type and quantity required [Ref. 29].

Any of these alternatives can provide the required acoustic
control and except as noted do not restrict the selection of inlet
position. Detailed investigation is required to evaluate the possible

trade-offs in cost, size, service life, and distortion. The construction

contractor will require the services of a qualified acoustic engineer,

but satisfactory inlet acoustic treatment can be provided at reasonable

cost. Doelling and Bolt [Ref. 35], provide an excellent summary of

calculation procedures for design use. Before final selection can be

made the designer must, of necessity, consider compatibility with the

aerodynamic requirements detailed in the next section.

2.   Aerodynamics

Comprehensive design criteria are not available for this

aspect of the inlet design. No general method is available for the

prediction of streamline, pressure, or velocity patterns though these

may limit the total test cell in its compatibility with future engines.

Reference 12 is an example of a completed construction specification

which ignores this requirement entirely and depends on luck for satis-

factory operation. The designer has available the choice of:

  a.   Inlet shape: horizontal, vertical, inclined, open

       ended or capped;

  b.   Number of turns, radii and flow lengths;

  c.   Shape of the flow dividers used in acoustic control;

  d.   Duct shape: expanding, contracting, constant area;

       open or vane guided turns,

  e.   Duct wall finish: protrusion streamlining, the shroud-

       ing of fittings and the installation of boundary layer

       trips or vortex generators [Ref. 36].

The following diverse factors must be considered in selecting from these options.

a. Cost and availability of real estate at the proposed site.

b. Effect of inlet stack height and position on the reingestion of exhaust gas.

c. Required cell air flow capacity.

d. Allowable pressure and velocity distortion of the flow at the engine inlet [Ref. 37].

e. Allowable cell depression.

f. Requirements for emergency airflow shut off to permit CO_2 flooding.

g. Local weather conditions, especially winds.

h. Construction cost per square foot of cross sectional area and foot of length.

Of these factors, a, g, and h, may be accurately determined following the selection of the construction site. Analysis of the effect of stack height and position requires that the exhaust treatment type and pollution control system be identified. In general, with exhaust directed vertically, increasing the inlet height and reducing inlet-to-exhaust separation distance reduces the probability of avoiding recirculation problems. A horizontal inflow naturally reduces the likelihood of exhaust gas capture [Refs. 38 and 39]. The references provide reasonably accurate prediction methods for proposed design susceptibility to recirculation.

Determination of the total inlet flow capacity requires identification of maximum projected engine requirements and facility type. With this available [Fig. 1], it is necessary to select the augmentation ratio for the cell. Again, this can not be freely chosen but is fixed by choice of exhaust treatment system since the various types have widely different requirements for excess air. Since a continuing trend toward higher exhaust temperature is evident in Section II excess air to cool this exhaust will go the same way. Since this capacity may limit the facility growth potential and excess capacity is low in maintenance cost, it should be maximized consistent with construction costs. References 37, 28, 32, 12, and 40 illustrate typical current and anticipated augmentation requirements. From these a total airflow capacity three times the maximum engine requirement can be justified.

Since test cell operation ideally simulates free atmosphere engine performance the approach velocity is limited in modern facilities to a maximum of 50 feet per second [Refs. 28, and 37]. This is an arbitrary limit, but is reasonable since increasing velocity above this point rapidly increases the cost of distortion control, increases cell depression and decreases the accuracy of thrust measurement data. Accepting this limit, cross-sectional area required is available and depression per foot of flow length may be accurately estimated using the standard duct flow loss techniques of Refs. 41, 42, and 43. Various depression limits have been used in design of current facilities but general agreement is found in considering the depression to

be a free variable and altering the design to change it only in the most extreme cases; i.e., those in which pressure loads approach the structural load limit [Refs. 37 and 40]. The effect of greatly increased mass flows on depression and required cross sectional areas is demonstrated in Fig. 8.

In the past, with these estimates, the designer could produce construction blueprints for the inlet. Prior to the introduction of the turbofan engine the production test cell was required to produce a specified quantity of air at a reasonable velocity at the engine inlet. Only the grossest mismatch of engine/cell sizes or the ingestion of objects other than air molecules could produce compressor stall, flow reversal, overtemp or unstable engine oscillation. Today, test cells can be and are built which have more than sufficient inlet flow capacity but which can not be used to test the engines for which they were designed [Refs. 37 and 10]. The condition responsible is non-uniformity of pressure or velocity distribution at the engine inlet. Turbofan engines, both high and low bypass, and special-use, lift type engines are the most sensitive to this distortion [Ref. 44], but when it exists it affects every engine tested to an unpredictable extent. Its sources are numerous and effectively include everything in the cell between the open atmosphere and the engine face which is in other than a straight smooth-walled duct [Refs. 37, 45, 46, 47, and 48].

The design of distortion free inlets is an empirical matter with even the most experienced contractors in the field [Ref. 34]. Until
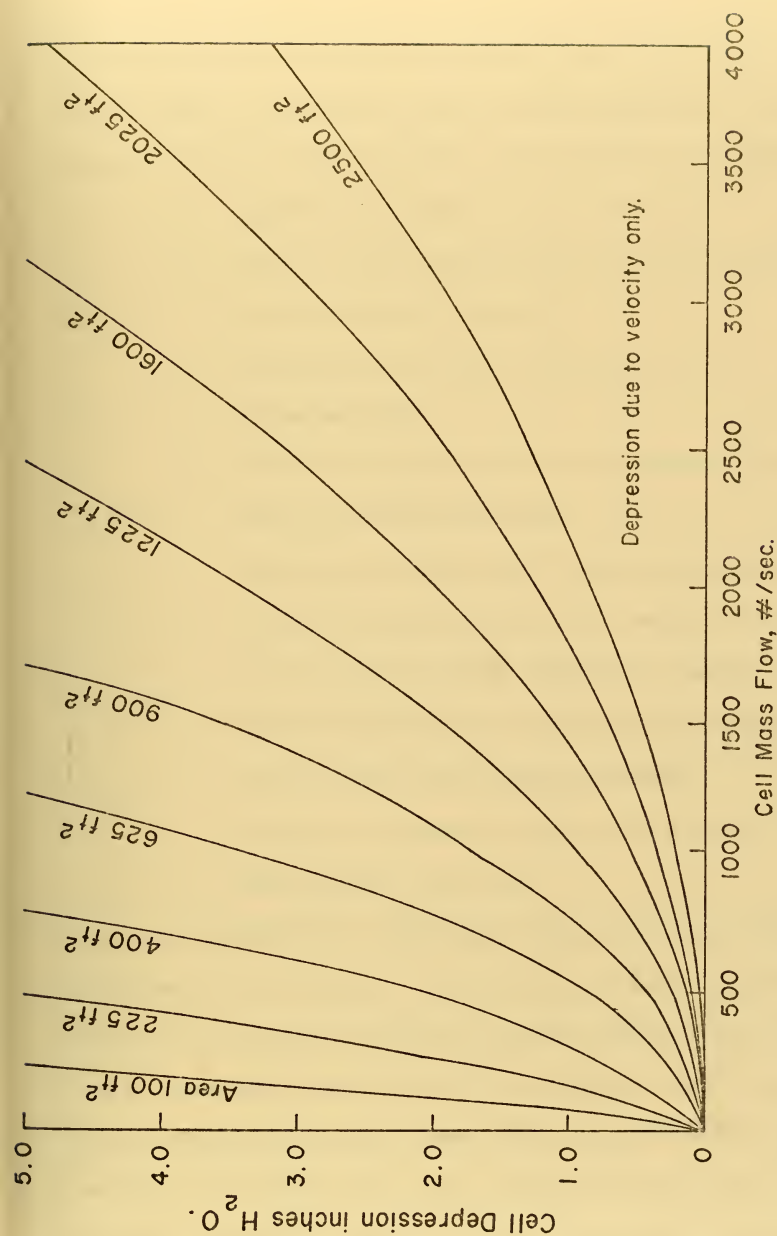
Figure 8. Effect of Increased Mass Flow on Cell Depression and Required Area.

a method becomes available to predict the flow distortion for a pro-
jected engine in a proposed cell with variable augmentation ratio, the
designer must accept the necessity of the following restrictions:

      a.   Minimize the number of turns in the inlet.

      b.   Place no flow dividing surfaces in the inlet which
              are not absolutely necessary.

      c.   Streamline all surfaces confining the flow or
              immersed in it.

      d.   Provide flow length forward of the engine for vortex
              and wake damping [Ref. 33].

      e.   Construct and test models of proposed designs [Ref. 49].

      f.   Provide turning vanes [Ref. 34], and flow straighteners
              for cell operations near design flow capacity.

      g.   Test the finished cell with reasonable completeness at
              all flow levels and augmentation ratios.

      h.   Employ aerodynamic methods in the design of duct
              curves [Refs. 50 and 51].

Reference 33 indicates an empirically determined pressure distortion
maximum of ± 0.25 in H_2O. The persistance of wakes generated by
flow obstructions may be estimated with the methods of Refs. 52, 53,
and 54. However, total distortion can not be accurately predicted and
no fixed limits have yet been established by test cell operators or
designers. Distortion indices have been published by many manufac-
turers for production engines. Definitions vary but each index may be

measured by pressure survey rakes located forward of the compressor face. The variation with engine speed of this index may be measured for a given engine type in a particular cell and the limit which will cause engine surge or stall is then available. Unfortunately, there is no method for predicting the value of the distortion index for a proposed cell design. Extensive investigation has also failed to establish useful correlations between test cell stall margin and that of the same engine installed in an aircraft [Ref. 55]. Therefore, the best the designer can now do is to conform to the above guidelines and include provisions for repeated aerodynamic monitoring of cell performance throughout the service life of the facility. Current research may vastly simplify this aspect of design and increase confidence in the final performance of future high capacity cells [Ref. 56]. For current installations distortion caused by inlet vortices may be reduced after discovery by the employment of wall or deck fences or aspirated plates [Ref. 36].

3. Maintenance and Safety

Aside from basic structural integrity of all components, the contribution of inlet design to safe cell operation has been in the provision for airflow shut off and filtering for fire fighting and protection of the engine from foreign object damage. This latter requirement is universally accepted and is met by various combinations of wire mesh duct screens and bellmouth covers. The designer may locate these screens as convenient but placement aft of distortion-producing

acoustic treatment will provide a bonus of a reduced requirement for flow mixing length. References 42 and 50 may be used to calculate pressure loss due to screening.

Though CO_2 flooding systems are available in many present test cells, there is less than complete agreement about the necessity of their incorporation in future facilities. Increased size and the greater CO_2 capacity required to effectively flood large cells has escallated the associated installation costs. Larger cross sections also imply longer operating times for hatch shut-offs and further reduce system effectiveness. Operator experience indicates that the Cardox flood system may itself be more of a hazard than the fires it is intended to prevent due to casualties possible from accidental actuation. Many aircraft powered by turbojet engines now incorporate quick shutdown systems and local application of extinguishing agents. Similar provisions in test facilities may eliminate the requirement for a quick-acting inlet shutoff. This is worth detailed investigation since it would remove the only inlet component requiring regular maintenance and would represent a considerable savings in construction cost [Refs. 16 and 34].

The cell access doors and their actuation systems are the other inlet components with maintenance requirements in a side loaded configuration. If the front loaded layout is selected, it may be necessary to include articulated acoustic treatment and flow straighteners which will increase loading time somewhat and be sources of

additional maintenance requirements. In either case, sliding or out-
ward opening doors provide designed-in safety.

Inlet design can make a substantial contribution to overall
cell performance and to reduction of operating costs by the inclusion
of a mounting frame for air filtration panels. Passing the flow through
a ten micron filter will increase the life of all cell components from
acoustic sheet metal to temperature probes [Ref. 16]. These panels
are low in cost and are reuseable; the increase in cell depression is
minimal. The air quality at nearly all facility sites is now poor
enough to make this a profitable addition to new designs; this quality
is not likely to improve much in the future.

B.   TEST SECTIONS

    1.   Engine Handling and Access

Efficient operation of production type test cells require that
the non-running time of the engine in the cell be minimized. The
engine-test bed adapter system is the best means of reducing this
time and has demonstrated satisfactory performance at many modern
facilities. Since the adapter is attached to the engine in the prepara-
tion area the handling system must transport the completed unit.
Selection of the optimum handling method requires consideration of
the following factors:

        a.   Tracked dollies prevent damage to concrete decking
           and eliminate traffic accidents that can occur with
           free dollies, but they are relatively inflexible in

accepting widely varying engine sizes. They are
also reasonably complex when used with engine-cell
adapters and may require more maintenance then
overhead handling systems of equal capacity.

b. Free dollies may require special high cost decking for
use with large, heavy engines and, when designed to
handle the engine/adapter combination, they may not
be suitable for general use elsewhere in the repair
facility.

c. Bridge cranes lack the ability to serve both the test
cell and a large preparation area. They also require
larger and more expensive cell access doors.

d. The overhead monorail, either powered or free,
minimizes access door size, can be tracked to multiple
prep area stations, is suitable for the engine/adapter
combination, can incorporate the hoisting unit required
for cell loading, is flexible in size and shape capacity,
and allows required maintenance to be performed out-
side the cell. This system is in operation [Ref. 11],
in present facilities; the only difficulty has been the
effect of the rail on inlet aerodynamics. A streamlined
track shroud or submersion in the overhead surface
may reasonably be expected to eliminate unacceptable
flow distortion.

Access to the installed engine must be convenient and safe. The access structure must not produce flow distortion or recirculation during test operation and must be adjustable in height and lateral position. Current systems utilize access structures which retract into the interior cell surfaces [Refs. 16 and 33]. Deck mounted service stands will be continually subject to corrosion damage from spilled engine fluids and cleaning solvents, and they must support transport dollies if an overhead system is not employed. A valuable addition to operational efficiency can be made by the designed inclusion of storage space for servicing and troubleshooting equipment which is convenient to the work area. Adequate lighting of the side and bottom engine surfaces is essential and at some sites the installation of radiant heating units can greatly increase efficiency and safety.

2. Acoustic

In current test cells it is the acoustic portion of the engine environment which is least similar to that of the aircraft-installed engine. Reflection from the smooth concrete surfaces surrounding the engine subjects the engine casing and external accessories to acoustic power levels several times those present in an aircraft. No reliable data on damage caused by this is available but it is certain that it is not beneficial. Some operators subjectively estimate that a 10-15% reduction in component life is attributable to this source. New cells should be designed to minimize the acoustic energy reflected onto the test engine either by absorbing it at the wall surface or directing it away

(38)
163

from the test section. Reference 57 illustrates the substantial reduction possible with commercial absorbent materials. The effectiveness of directionally reflective surfaces is illustrated in Ref. 39; this option has the advantage of nominal cost in new construction.

3. Aerodynamics

The primary requirement for the test section is that the flow remain unidirectional and without recirculation of engine exhaust. Aft of the engine bellmouth there is no further necessity for streamlining or shrouding equipment except that even small variations of pressure along the engine casing may produce variation in the measured thrust. This will be minimized by keeping the exposed surface area between the engine and the thrust bed to a minimum and, if constant, it can be included in cell correlation factors [Refs. 8 and 37].

When the augmentation ratio is high, there is little likelihood of recirculation. When little or no augmentation air is used, the control of recirculation is more difficult and, to be flexible, new facilities must be designed for possible operation in the zero augmentation mode [Ref. 37]. Figure 9 illustrates the primary alternatives for recirculation control. The septum wall provides positive control but must be considered as a last resort due to the mechanical complexity involved in making it removable, useable with different engine inlets, and strong enough to resist the considerable pressure loading which is possible. The second alternative requires that excess air be drawn past the engine even when it is not required for exhaust cooling or
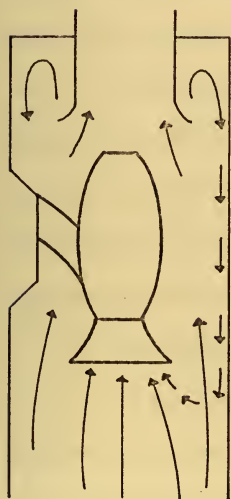
Septum Wall

Augmentation
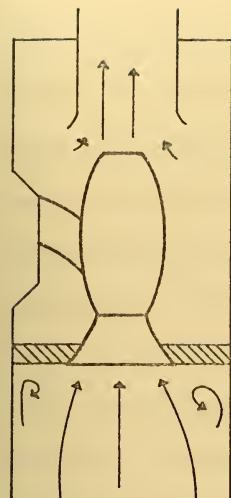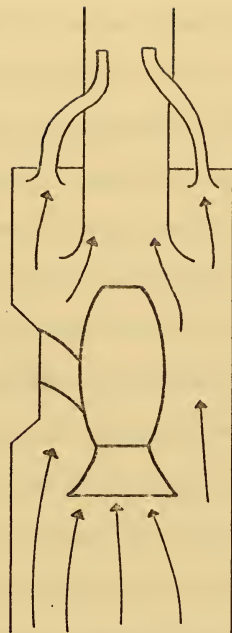
Passive Exauster

Figure 9. Recirculation Control Options.

mixing. Since this is needed only while the engine is in operation, it is logical to make the engine exhaust the power source and design the system to be entirely passive. An active exhauster powered by a separate electric motor is possible, but the flow capacity required and the additional cost and maintenance make it less than attractive. The drawback to inclusion of the passive venturi powered system is that the initial motivation for operation with a low augmentation ratio may be reduction of the flow volume to be handled by a pollution control system. If the afterburner method of pollution control is to be used the exhauster air could be added to the exhaust aft of the secondary combustion zone. In any system, if the volume flow required for control of recirculation is low enough, inclusion of the passive exhauster must be considered since it has the advantages of low initial cost and minimum maintenance requirements [Ref. 33].

Installation of cell instrumentation with the capacity to detect recirculation is a design feature which will return an excellent profit on a small initial investment by ensuring test reliability and preventing the accumulation of explosive mixtures when future engine-augmenter positions are varied.

4. Instrumentation and Mounting

A key feature of the instrumentation design is flexibility. Effective use of the engine adapter system requires that the permanent test cell portion of the equipment require little or no modification when new engines are introduced. Each adapter will be customized to a

particular engine but all must appear identical to the test bed. This demands that the original design have sufficient capacity to accept the number and type of data transmission chanels required by future engines and refined test techniques. References 12, 16 and 28 illustrate current estimates of this requirement; recent experience indicates that the savings possible by limiting this capacity will almost certainly be temporary ones, since excess capacity is free of maintenance cost and can, in fact, greatly reduce cell down-time by permitting rapid shift to alternate channels when malfunctions occur. Maintenance can then be performed at scheduled times. The importance of this capability cannot be overemphasized since most operators report that the majority of cell down-time results from instrumentation malfunctions.

Though cell accessibility may be complicated by the use of the overhead thrust bed, its advantages more than compensate for this, and it is now recognized as the best design for future test cells. Among these advantages are: natural similarity to aircraft engine mounting methods, ready compatibility with monorail handling, freedom from corrosion by collected fluids, flexibility in engine positioning, and the availability of advanced design experience. It is possible to utilize a single step plug-in of the adapter to the test bed but experience indicates that separating the connection of the physical support from the plug-in of the instrumentation leads enhances system reliability [Ref. 16].

For facilities required to anticipate a wide spectrum of

thrust levels, it is possible to improve thrust measurement accuracy by using a three component system: test frame, thrust bed and engine adaptor. With this arrangement the thrust bed may be changed to one having flexures with maximum sensitivity in the desired range [Ref. 16]. Investigation of the possibility of eliminating the direct thrust measurement system has shown that while it is technically feasible, the savings in engineering complexity are small and are offset by increased requirements for other types of instrumentation. In the view of most users, deletion of the direct thrust measurement system is not justified [Refs. 12, 16, and 39].

5.   Auxiliary Subsystems

One of the most persistent failures in test cell design has been lack of subsystem growth potential. Rapidly increasing fuel consumption rates have made extensive rework of some facilities necessary and restricted the operation of others [Refs. 12 and 16]. At several installations the supply of starting air has proven inadequate almost before the cell was placed in operation [Ref. 12]. For facilities requiring water for exhaust gas cooling or scrubbing it is imperative that future capacities be determined since they may well be double or triple those required to test current engines. In all these subsystems, doubling the design capacity increases initial cost only about 20 per cent while a similar change in an existing system may easily double the original cost and require extended facility closures.

(43)
168

In addition to sufficient capacity, the fuel system should be designed to permit future expansion to at least a two fuel operation [Refs. 2, and 58]. Again, providing this flexibility during design will cost far less than adding it later. Design of all subsystem controls should include maximum utilization of advanced control and monitor technology. The number and criticality of the subsystems which must be included in a turbojet test cell demand that careful attention be given to design of interlock controls providing fail-safe operation. There is no reason for operator error or an undetected malfunction to cause major damage to the engine or test facility. The electrical power dissipation, dynamometer and fire extinguishing systems should also be routed through a master interlock control.

C. CONTROL CENTER

The choice of data acquisition method will establish the require-ments for the design of this area. In a facility requiring manual data recording, 25-30 per cent of the total engine running time is occupied solely by data acquisition. Additionally, two to three minutes may elapse between the first and last data reading at each operating condi-tion. Thus the justification for the higher cost of automatic data acquisition systems includes reduced cell time per engine (with accompanying reduction for fuel, utility and pollution abatement loads) and increased test credibility due to the simultaneity and accuracy of data.

Sufficient incentive exists for the inclusion of automatic data

scanning equipment in all future production test cells. It is possible
to automatically acquire data and simply supply it as a printed record.
But the nature of the data processing normally required is such that
its inclusion within the automatic equipment is simple and effective.
It can then be presented in a written format acceptable to the user
[Fig. 10], or as real-time operator assistance. Further extension of
data system sophistication is possible and may be justified in the
following areas:

    a.   Individual engine history records containing either rework/
            repair testing results or expanded to include in-service
            information [Ref. 59].

    b.   Safety monitoring capability to provide warning of impend-
            ing failure or to initiate shutdown or other corrective
            action.

    c.   Operator assistance in the form of step-by-step procedural
            instructions and malfunction analysis.

The computer centered data system can also be operated in a closed
loop mode with engines tested under fully automatic control [Refs. 58
and 16]. It is unlikely that this could be economically justified in
future production type facilities, however, since manpower savings
would be small (installation and repair still required) and the cost of
a reliable system high.

      Long range economy is best served by including in the initial
system design excess capacity to permit processing of additional data

```
GUARD SYSTEM DATA      ****** TFE - 731 ENGINE ******        DATE   2' 7/72
                              SERIAL NO. 7307                 TIME     .39-22
                                                              PAMB   14.76
CYCLE    1
IDLE FOR 1 MIN

** CALCULATIONS **
NIC2            5789.0      PT2                14.76     WFCOR          197.13
N2C2           16233.5      TT2               140.4      TSFC             0.9065
N2/N1              2.804    FNCOR             202.17     PWF             -0.574
GEN POWER          0.000    HYD PUMP NO.1 PW  397.328
TOTAL EXT POWER  513.647    HYD PUMP NO.2 PW  116.318

** MEASURED DATA **

SPEEDS-                     THRUST (LBS)      203.05     FUEL FLOW MAIN   198.00
N1 (RPM)        5789.0      POWER ANGLE        38.60     FUEL FLOW VERFY  199.13
N2 (RPM)       16233.5

PRESSURES - (PSI)
COMP DISCH        27.76     OIL TANK VENT       0.00     PT7 LPT DISCH     15.04
FUEL PUMP INLET   67.51     NO.6 BRG SCAV       0.00
F/O (OIL IN)       0.00     TOT ENG SCAV        0.00
FAN G/B(OIL IN)   47.07     OIL PUMP DISCH      0.00

TEMPERATURES - (DEG F)
FUEL              55.2      TT7 LPT DISCH 180   0.0      TT5 HPI DISCH    838.2
F/O (OIL IN)       0.0      TT7 LPT DISCH 181   0.0      HPC DISCH          0.0
FAN G/B(OIL IN)  135.4      TT7 LPT DISCH 184   0.0      SURGE VAL D 805   84.3
HYD PUMP IN      130.4      TT7 LPT D+SCH 185   0.0      SURGE VAL D 806    0.0

FAN G/B SCAV     124.1      NO 4 BEARING        0.0
NO 4-5 BRG SCAV  151.0      NO 5 BEARING      168.7

VIBRATION - (MILS)
TURB VERT          0.680    COMP VERT           0.590    B-FAN ORB VERT     0.000
TURB HORIZ         0.070    COMP HORIZ          0.770    B-FAN ORB VERT     0.000
```

Figure 10. Typical Data System Output.

(46)
171

without major remodeling. Removeable flooring in the control area is an excellent means of providing both maintenance access and ease of modification. The sensitivity of electronic data systems to inter- ference and damage from acoustic, vibrational, and electromagnetic energy exceeds that of the human operators and reinforces the necessity for the inclusion of appropriate types of shielding in the design of the control area [Refs. 12, 14, and 28].

Replacement of the viewing window by a closed circuit TV monitor simplifies the insulation problem and increases safety. To justify its cost, the video monitoring system must be capable of pro- viding resolution and discrimination comparable to that of an operator present in the cell. With carefully considered lighting and placement, accurate color reproduction, magnification to a one foot focal distance, and full articulation it will be possible to eliminate the necessity for in-cell operator inspection. This could reduce run times and allow leakage checks at other than idle power settings. For some facilities the addition of a video recording capability to the monitor system may be advisable. Having low initial cost, adaptable to fully automatic control, and requiring little maintenance, a video tape recorder could provide accurate records of malfunctions and permit continuing studies of cell efficiency. A recorder could also supply effective training material for operators when new engine models are introduced or new test procedures are initiated.

Modular design of the control station and provision of ready

access to the installed equipment should be of prime concern to the
designer [Refs. 16 and 28]. Some operators presently feel that
audio monitor capability should be provided, and an earpiece adapta-
tion of the required intercom system could be employed for this
purpose.

D. AUGMENTER AND EXHAUST TREATMENT

1. General

An efficient, flexible and reliable exhaust system is perhaps
the most critical segment in test cell design, yet the present level of
engineering sophistication in this area is still elementary. Justifica-
tion for the above statement is the recent change in the design criteria
of cell exhaust treatments. Early designs were primarily built to
lower exhaust temperatures to levels that would not unacceptably
shorten the life of installed noise abatement systems. This was
accomplished by mixing the jet exhaust with secondary air. Past
acoustic practices have been re-examined [Refs. 60, and 61], and in
many cases stricter requirements have been formulated [Refs. 15, 12,
25, and 58].

Additionally, attention is now being focused on reducing the
air pollution levels of jet engine test cells. Generally, test cells are
placed in a different regulatory category than are jet aircraft them-
selves. They are classed with other stationary sources [Refs. 62,
and 63].

2. Aerodynamics and Thermodynamics

A poorly designed augmenter system may be one that acts, as an unnecessarily powerful jet pump. In this situation too much secondary or cooling air is entrained with the engine exhaust, causing higher than designed cell airflows and cell depressions. Also, larger than design airflows will increase distortion levels and possibly disrupt smooth engine operation [Refs. 37, 15, and 6]. Large air flow can also cause errors in thrust measurement.

At the other end of the design spectrum is the system that fails to induce enough secondary airflow, and thereby fails to prevent the problem of recirculation of exhaust gases. Excessive exhaust temperature may also result.

The problem of excess secondary airflow has been encountered at several facilities. At North Island a flange has been added to the augmenter bellmouth, restricting the flow of secondary air. This is not a smooth design aerodynamically, and the capability of this facility to handle large bypass fan engines or other high flow rate engine types is severely limited with the present flow restriction. A second solution is to install orifice plates within the augmenter itself to reduce the available flow area [Ref. 20]. This type addition is slightly more flexible than the former since various size plates may be installed depending on the flow characteristics of the particular engine under test. These fixes are shown in Figure 11, a and b.

At the United Air Lines facility in San Francisco, secondary

airflow in their new large jet engine test facility has been estimated as being almost twice as high as was originally anticipated [Ref. 17]. This condition has not exceeded cell structural limits with the present engines being tested, (JT9D, CF6), but the cell performance with advanced technology engines which may reach the 100,000 pound thrust category will be marginal. This situation indicates the need for close attention to augmenter design and more thorough analysis of the ejector process.

Secondary air provides the necessary cooling of the engine exhaust and prevents recirculation. For a turbojet engine operating out of afterburner mode an augmentation ratio of 2:1 has been set as a reasonable design goal [Refs. 12 and 15]. Augmenter performance is a function of the area ratio of the augmenter and exhaust nozzle, the length of the augmenter, the position of the exhaust nozzle relative to the entrance of the ejector tube, and velocity ratio. Most recommended test cell augmentation ratios for fan engines vary from 0.25:1 to 0.5:1 for high bypass engines and up to 1:1 for low bypass types [Refs. 12, 15, 5, and 64]. Appendix A contains the standard definitions of augmentation ratio for turbojets and turbofan jets.

Besides its function of providing the means of mixing and cooling the engine exhaust, the ejector system must overcome the various pressure drops in the inlet and the exhaust systems. Figure 13 shows the general pressure pattern within the test cell. Basicly, momentum is transferred to the secondary air, thereby increasing its pressure.

(50)

Studies have been made to determine the mixing characteristics of jet pumps [Refs. 65 thru 74]. These indicate that for each characteristic exhaust and secondary airflow combination there is an optimum length and diameter mixing tube. However, because of the cost of construction of the exhaust facilities many trade-offs must be made, and a flexible design must be selected that will work reasonably well over the range of engines to be tested.

A second method of cooling the exhaust is to use water spray cooling. This method is mandatory for engines operating in the afterburner mode, but may be used in other modes as well. Studies have been carried out [Refs. 15 and 27], which indicate the amounts of air, water or both which are required to cool exhaust gas temperatures to acceptable levels. When suitable amounts of water cooling are used, secondary airflow can become negligible. However, compromises must be made to determine the amount of water used. At the present time most of the water used in spray cooling is lost through the stack. At several locations, including NARF North Island, fresh water supplies are at a premium; availability may dictate the design option chosen.

Where water cooling is necessary and available, difficulties remain in devising means whereby the high temperature jet core may be thoroughly penetrated by water streams. It is known [Ref. 18], that even high pressure water jets have little success penetrating into the core of a high speed flow. Various designs have been developed, including concentric rings, water spargers and bounce sprays [Refs.

20, 19, and 75]. These designs, however, have not been optimized for facilities required to test widely varying engine types.

Matching augmenter characteristics to individual engines will be difficult, particularly where low augmentation ratios are desired.

Variable area nozzles are common for afterburning engines. The exhaust from the fans of high bypass engines is at a relatively low energy level, and since it contains no products of combustion, separate ducting may be desirable. The Pegasus engine used in the Harrier aircraft requires complex ducting during test cell operation [Ref. 5].

Prevention of thermal damage to the augmenter must be considered. In the entrainment zone [Fig. 12], the walls are subject to radiant heating, while in the fully developed mixing zone they are heated by convection. Water jackets may be necessary during testing of afterburning or high turbine inlet temperature engines, particularly if the selected exhaust treatment system requires a low augmentation ratio.

3. Acoustic Treatment

Noise sources that must be treated by exhaust systems are: turbomachinery generated noise, combustion noise, turbulent noise generated by the interaction of the jet exhaust and the secondary air and the turbulence in the exhaust itself [Refs. 76-81]. In the entrainment zone the shear stresses are high and the turbulence level is relatively low, creating most of the high frequency noise emanating
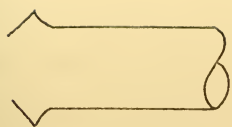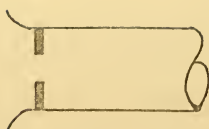
Figure 11.

Augmenter Flow Restrictions at Two Navy NARFs.

      (a)   Flange installation at NARF North Island

      (b)   Orifice installation at NARF Alameda
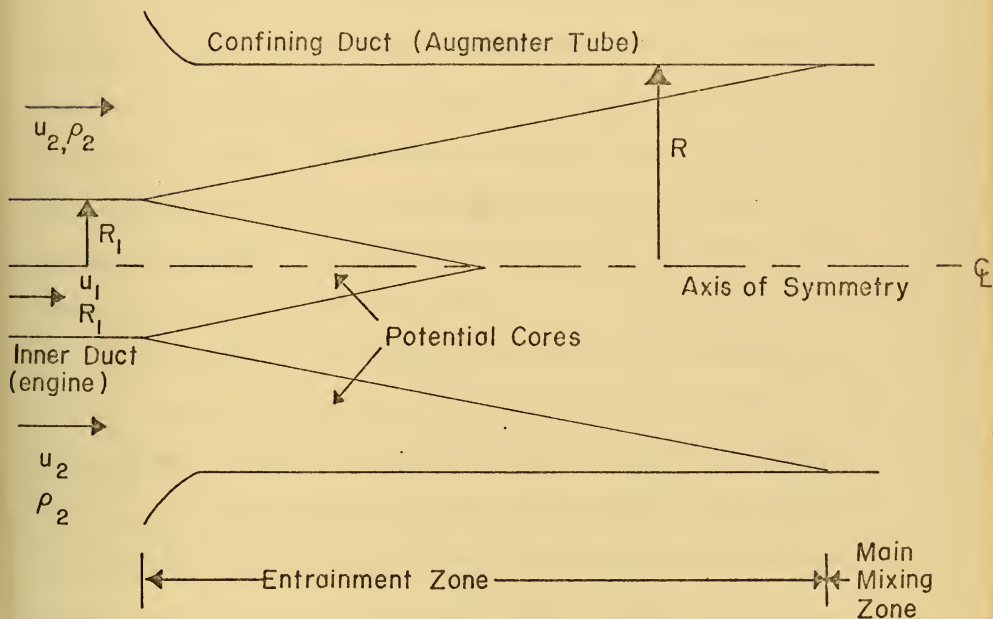
Figure 12. Jet Mixing Zones.

from the jet [Ref. 82]. Most of the low frequency sounds, those which contribute the most to the overall sound level, come from the portion of the exhaust beyond the potential core; the peak of this sound is at a wavelength about three times the diameter of the jet [Ref. 82]. It is this low frequency sound that is most difficult to attenuate. The higher frequency noise of machinery is easily abated with standard techniques which include baffles of all types, lined passages and bends, and tubular exhaust passages [Refs. 15, 33, and 37].

The properly designed augmenter can contribute to the overall reduction of noise; experimental results [Ref. 83], have shown that jet noise can be reduced by a factor of 5 (7db) in an ejector noise suppressor. It was also shown that the initial mixing conditions and the length of the injector are more important factors in obtaining this attenuation than the area ratio of the tube and jet or the position of the primary jet relative to the ejector inlet.

Methods of breaking up the continuity of the jet and increasing the frequency of the exhaust noise are discussed in Section IV. The utilization of a colander in the form of a cone or a cylinder is presently preferred over other options in modern cell designs. It has been found by experience that a hole size 1-1/4 inch in diameter is the smallest practical size [Ref. 15]. Holes smaller than this tend to be easily blocked due to impurities in cooling water as well as particulate matter present in the engine exhaust. Standard practice has been to uniformly space the holes over the surface of the colander, with total hole area
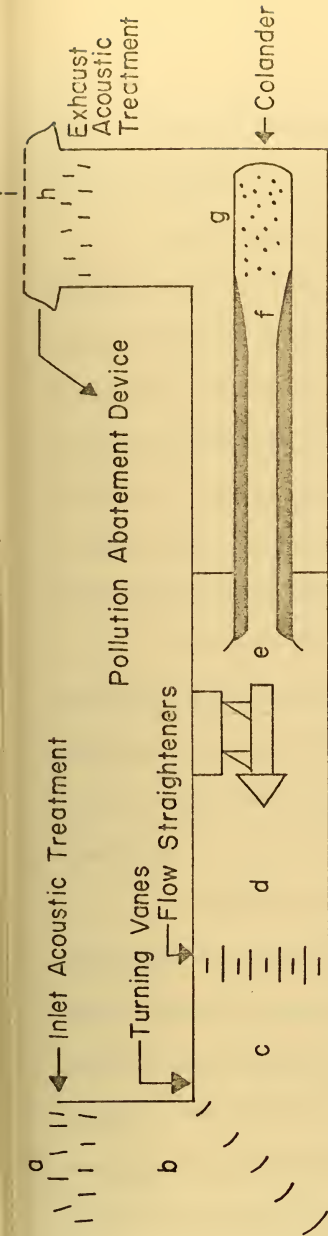
Figure 13. Test Cell Pressure Profile.

40 to 60 per cent in excess of the cross sectional area of the augmen-
ter tube itself [Refs. 21 and 15].

An exception to this practice has been introduced in some
smaller Navy "C" cells [Ref. 21 and Fig. 5]. In these cells holes
were placed only in the lower half of the colander. This design has
exhibited a serious shortcoming in that flow through the exhaust stack
is very non-uniform; in fact, some points in the stack exhibit zero
velocity. This causes portions of the acoustic treatment to be exposed
to higher than design flow rates, thereby shortening useful life and
decreasing overall performance.

Analysis must be done during design to ensure adequate flow
conditioning over the operational range of the proposed test cell. The
designer must ensure that enough pressure rise will be obtained to
overcome any flow blockage that may be present under all operating
conditions.

Unwanted acoustic energy may be generated by obstructions
present in the ejector assembly. These include spray rings or nozzles,
diffuser rings and any other hardware installations. These obstructions
increase the turbulence level of the flow, thereby increasing the noise
sources within the flow. The merits of each proposed installation must
be weighed according to the use intended for the individual test cell.
Care must be taken that natural frequencies of installed components
are not activated by the driving frequencies of the flow.

Possible exhaust stack treatments are as varied as those

intended for use in the inlet. Options include lined bends and passages, tubular mufflers, sinuous passages or straight passages [Refs. 28, 29, and 15]. Steel Helmholtz resonators have been investigated by General Electric [Ref. 15], and have been found to be unsatisfactory for their own use; this approach has been successfully taken by Aero Systems Engineering, however [Ref. 39]. Differences are in the cell utilization of the two operators, and in the acoustic characteristics of the engines tested.

A primary concern is to develop a system which will withstand a moderate range of temperatures and wide range of velocities. Most installations have been designed to withstand exhaust stack temperatures in the $450-550^{\circ}$ F range, with a maximum of 600° [Ref. 15]. At one time NARF North Island attempted to maintain temperatures below 200° in the non-afterburning mode by water cooling. However, it was impossible, with the existing water spray design, to operate the afterburner and maintain stack temperatures below 450°, and the installed acoustic treatments were subjected to such severe thermal shock that their useful life was drastically shortened. Within practical limits a constant stack temperature should be maintained in all test modes.

Because of the varied sizes and characteristics of engines that will be tested in new construction test cells, consideration should be given to the possibility of providing variable area exhaust stacks. Methods of accomplishing this vary from simply blanking unnecessary portions of the stack with pre-fitted metal shutters according to the

flow requirements of the engine under test to a movable cover over the stack opening which is programmed to provide optimum flow area (and available acoustic treatment) for a given engine power level. By designing the basic exhaust system to handle the largest forecast air-flow with the additional capability of efficiently handling much lower flows the problem of test cell obsolescence caused by advances in engine technology can be avoided.

4.   Emission Control Devices

In the future, major design effort must be devoted to pollu-tion abatement systems. It has been established by Executive Order 11282, May 26, 1966, that Federal installations comply with local environmental protection requirements. At the present time most emission requirements which are applicable to test facilities deal with the particulate emissions which cause visible pollution. Future legislation will limit emission levels of invisible noxious gases, carbon monoxide, oxides of nitrogen and sulfur dioxide. Studies have been conducted to determine exhaust emissions of gas turbine engines [Refs. 63, and 84-89], and although the exact emission levels are not agreed upon, most figures mutually agree on an order of magnitude basis.

The abatement system chosen for test cell operation must first remove visible particulate emissions. California legislation limits the deviation from a maximum of 20 per cent obscuration (#1 on the Ringleman scale) to three minutes out of every hour.

Except at idle, gas turbine engines emit very low levels of unburned hydrocarbons and CO, so that attempts to reduce these should concentrate on low flow rate conditions [Ref. 84].

By 1975 Los Angeles County will limit emission of oxides of nitrogen to 225 ppm [Ref. 62]. New developments in engine technology resulting in high pressure ratios and high combustion temperatures have raised the levels of these oxides in engine exhausts [Ref. 84]. The chosen abatement system must at the very least not add to these levels and ideally should reduce them.

The installed system must be able to remove unburned fuel from the exhaust flow. Estimates are that in the afterburner mode turbojets exhaust about 10 per cent unburned fuel. Also, the ability must be retained to purge unwanted fuel from the exhaust drainage system. Prior to light-off it is Navy practice to "dry run" the engine; that is, the engine is windmilled and the throttle fully opened to check for leaks. This results in relatively large amounts of fuel being dumped directly into the exhaust system.

Emissions of sulfur dioxide will not be a problem as long as the current restrictions on sulfur content of fuel are maintained. Present restrictions limit the sulfur content to .3 per cent, and most fuels contain even less.

Although advances have been made in combustor technology, completely clean jet engines are not yet a reality. NARF Alameda was recently cited in violation of local standards while testing a high

time engine configured with "clean" combustor cans. One source [Ref. 63], theorizes that reactions within the cell exhaust system change the character of particulate emissions, either in size or number, so that visibility obscuration is greater at the test cell exhaust stack than at the engine tailpipe.

Interim solutions for reducing smoke involve the use of fuel additives. United Air Lines in San Francisco utilizes CI-2 in their testing. Additives coat engine hot section parts, and the effect of adding heavy metallic vapors to the exhaust is under continuing investigation by the EPA.

Early studies of pollution abatement systems have resulted in the selection and development of a nucleation scrubber [Ref. 75]. Other devices analyzed include filtering devices, venturi scrubbers and electrostatic precipitators. These have been evaluated as unsatisfactory from considerations of safety, flexibility and economy in Ref. 75.

Filtering devices alone present problems because of their tendency to become clogged by particles entrained in the exhaust. Additionally, they require extremely low flow velocities, and are not effective in removing noxious gases.

The primary drawback to the venturi system is its inability to operate efficiently over greater than a 10 per cent interval away from its design point, which is an unacceptable restriction in light of the fact that air flows vary as much as sixty to seventy per cent from idle to full power setting. A possible solution to this would be the

installation of a bank of venturis, entailing high initial costs and complicated flow controls.

The present shortcoming of electrostatic precipitators is the inability to completely prevent fuel buildup on and around the electrodes; this condition creates the danger of an explosive discharge. Also, these systems cannot remove noxious gases or oxides of nitrogen.

Nucleation scrubbers work by process of creating large particles by condensation of vapor from a saturated vapor. The nucleates are the particulate matter already present in the exhaust. The enlarged particles are then removed by impaction in the scrubbing system. A prototype scrubber system developed by Dr. A. Teller (Pat. #3, 324, 630) has been installed by the Navy at NARF Jacksonville. This particular scrubber has the capacity to handle large changes in flow volume, can reduce noxious gases and unburned fuel and with modification can remove much of the oxides of nitrogen and sulfur if such action is required. Installation of this scrubber is also anticipated at NARF Norfolk. The primary drawback at present with the scrubber system is its high initial costs. At its present level of development this system is not considered the ideal solution, and investigation is being carried out in other areas as well.

The nucleation scrubber as well as the other alternatives discussed are all similar in that they function by physically removing particulates and unwanted gases; a second class of installations acts

by converting unwanted pollutants to harmless chemical species.
These include afterburners and catalytic converters.

Northern Research and Engineering Corporation has pro-
posed a thermal converter installation for test cells [Ref. 62]. This
reference is a comprehensive discussion of the feasibility of such an
installation and the justification for Navy procurement in light of
future requirements for pollution control. At the present time much
work remains to be done in conducting recommended studies and
testing.

The installation of a converter system will require close
matching of the test section, engine and exhauster itself since the
proposed system requires a low augmentation ratio.

The final selection of an abatement system will be based on
its flexibility and economy. It must be able to operate over a wide
range of exhaust velocities and temperatures. The initial cost of
procurement and installation must be low, as must the cost of opera-
tion and upkeep. The system must be reliable enough to allow firm
scheduling of cell down time with the minimum amount of unscheduled
maintenance. An additional factor will be the ease with which the
abatement system may be retrofitted to existing test cell structures.

The creation of secondary pollution must be avoided.
Thermal pollution of natural water supplies is a real possibility in
systems requiring heavy cooling. Also to be avoided is the creation
of additional, unwanted noxious gases or other undesirable products of
combustion if an additional combustion process is used.

Maximum allowable temperatures, pressures and velocities will dictate the level of required protection of hardware exposed to the jet exhaust. Because of the temperatures encountered during after-burner runs it may become necessary to water cool certain exposed parts. Refractory linings have been considered, but were rejected for economic reasons [Ref. 62].

Complete acoustic analysis must be completed to ensure that the natural frequencies of equipment exposed to the flow not be excited by the frequencies of turbulence generated noise.

Finally, the design of adjustable components should be kept as simple as possible. Operators are wary of too much gadgetry in test cell design [Refs. 17 and 20], and cell down time increases with the addition of mechanical sophistication. All facilities must be de-signed to operate with the minimum amount of required upkeep.

APPENDIX A

Equivalent Augmentation Ratio for Turbofans

Test Cell Augmentation ratio is defined as

$$A = \text{Augmentation ratio} = \frac{m_i - m_e}{m_e}$$

where m_i = total mass flow in the inlet stack

m_e = mass flow passing through engine

Bypass ratio for a turbofan is defined as

$$B = \frac{m_e - m_c}{m_c}$$

where m_c = mass flow through engine core

Cooling air for a turbojet is $m_i - m_e$. For a turbofan cooling air is $(m_i - m_e) + (m_e - m_c)$, if energy added by fan is neglected. Manipulation leads to

$$A_{eff} = A + B + AB = \frac{m_i - m_c}{m_c}$$

Appendix B

Firms with Experience in Test Cell Design

The following firms are known to have valuable expertise in
areas pertinent to test cell design. The list is by no means complete,
but it will give the potential operator an excellent starting point for
contacts regarding facility design. Additionally, the customer should
contact the large number of test cell operators to ascertain any prob-
lems which inevitably arise. These operators include airline overhaul
facilities, engine manufacturers and military rework facilities.

1. Aerodynamics and Engineering

Aero Systems Engineering Inc.
358 E. Fillmore Avenue
St. Paul, Minn. 55107

Burns and Roe Inc.
9800 South Sepulveda Blvd.
Los Angeles, California 90045

FluiDyne Engineering Corp.
5900 Olsen Memorial Highway
Minneapolis, Minn. 55422

Gustav Getter Associates
524 North Avenue
New Rochelle, New York 10801

Northern Research and Engineering
200 Vassar Street
Cambridge, Mass.

Price-Clark Industries
420 South Pine Street
San Gabriel, California 91776

Sverdrup and Parcel and Associates
800 North 12th Blvd.
St. Louis, Missouri 63101

(65)
190

2.   Acoustic Controls

Aeroacoustics Corp.
P. O. Box 65
Amityville, New York 11701

Bolt, Beranek and Newman Inc.
50 Molton Street
Cambridge, Mass.

Industrial Acoustics Company
380 Southern Blvd.
Bronx, New York 10454

Koppers Company Inc.
400 Commonwealth Avenue
Bristol, Va. 15219

R.I. Corporation
499 West 2nd Street
Ogden, Utah 84402

The Soundcoat Company, Inc.
175 Pearl Street
Brooklyn, New York 11201

REFERENCES

1. Yaffee, Michael L., "Continued Engine Market Shrinkage Seen,"
    Aviation Week & Space Technology, v. 96, no. 1, p. 40-41,
    3 January 1972.

2. Yaffee, Michael L., "USAF Propulsion Interests Detailed,"
    Aviation Week & Space Technology, v. 94, no. 9, p. 54-57,
    1 March 1971.

3. Yaffee, Michael L., "New Versions of TF41 Designed,"
    Aviation Week & Space Technology, v. 93, no. 16, p. 42-47,
    19 October 1970.

4. Yaffee, Michael L., "Hybrid Fighter Engine Designed,"
    Aviation Week & Space Technology, v. 95, no. 10, p. 40-42,
    6 September 1971.

5. Rolls-Royce Limited Technical Report No. TP 148/B.E.D.,
    Pegasus Facilities Planning Manual, 1970.

6. FluiDyne Engineering Corporation Proposal No. P-1084,
    Proposal for Development and Design Criteria and Model Tests
    of a Universal Test Cell, October 1967.

7. Hieronymus, William S., "Augmentor Wing Flight Tests Set,"
    Aviation Week & Space Technology, v. 94, no. 1, p. 48-50,
    4 January 1971.

8. Naval Air Rework Facility, NAS North Island, Technical Memo-
    randum No. E-41894, Aircraft Gas Turbine Test Cell Design
    Options, by A. E. Fuhs, August 1971.

9. "Aerojet Unveils Assault Vehicle," Aviation Week & Space
    Technology, v. 94, no. 3, p. 17, 18 January 1971.

10. IIT Research Institute Report IITRI-J6143-FR, Analysis, Test
    and Design of a Water Dynamometer, by William J. Courtney,
    October 1969.

11. The Boeing Company, Correlation of Gas Turbine Weights and Dimensions, by R. P. Gerend.

12. Air Force Systems Command Advanced Engine Research Facility, FY-71 MCP.

13. Arnold Engineering Development Center Report No. AEDC-TR-69-103, An Engineering Analysis of Facilities for Altitude Testing of Large Turbojet and Turbofan Engines During the 1973-1990 Era, by T. E. Beavers, July 1969.

14. Naval Air Rework Facility, NAS North Island, MCON P-135, Jet Engine Test Facility and Pollution Abatement; Facility Study and Present Value Analysis, 30 June 1971.

15. Flight Propulsion Division of General Electric, Airline Planning Guide: Test Facilities for Large Advanced Turbojet and Turbofan Engines, 1 April 1967.

16. Olive, R. L., Modern Jet Engine Development Facility, ASME Paper 71-WA/GT-6, August 1971.

17. Personal Communication with Mr. R. E. Totman, Staff Engineer, United Airlines Overhaul Facility, 17 December 1971.

18. Geery, E. L., and Margetts, M. J., Penetration of a High Velocity Gas Stream by a Water Jet, AIAA Paper No. 68-604.

19. Personal Communication with Mr. R. Boe, R.I. Corporation, Ogden, Utah.

20. Personal Communication with Mr. D. O'Dell, Naval Air Systems Command (Air 53431-D), Washington, D. C.

21. Personal Communication with Mr. G. Pulcher, Naval Air Propulsion Center, GSE Division, Philadelphia, Pa.

22. Personal Communication with Mr. G. Getter, Getter and Associates, New Rochelle, New York.

23. Arnold Engineering Development Center Report AEDC TR-68-152, Thrust Stand Certification for the TF 39, by E. S. Gall.

24. Personal Communication with Mr. C. F. Roscoe, Naval Air Systems Command, 04 Group, Washington, D. C.

25. Surowiec, M. W., Silencing Considerations for Large Gas Turbines, ASME Paper 71-GT-26, April 1971.

26. "Quiet Fan Test Promises Cut in Noise Levels," Aviation Week & Space Technology, v. 94, no. 14, p. 21, 5 April 1971.

27. "Lockheed Research Aims at 50% Attenuation in Turbofan Noise," Aviation Week & Space Technology, v. 95, no. 3, p. 54-55, 19 July 1971.

28. Naval Air Systems Command/Naval Facilities Engineering Command Committee, Report on Standard Navy Depot Turbofan/ Jet Engine Test Cell.

29. The Aeroacoustic Corporation, Bulletin B-31, R1, 1968.

30. Fink, M. R., Shock Wave Behavior in Transonic Compressor Noise Generation, ASME Paper 71-GT-7, April 1971.

31. NASA SP-189, Progress of NASA Research Relating to Noise Alleviation of Large Subsonic Jet Aircraft.

32. Yaffee, Michael L., "U.S. Efforts Pace Engine Advance," Aviation Week & Space Technology, v. 92, 22 June 1970.

33. Burns & Roe, Inc., Standard Test Cell Design Study for Joint Airline Committee.

34. "New Jet Engine Test Cells," Architectural Products Review, June 1971.

35. Bolt, Beranek and Newman, Inc., Noise Control for Aircraft Engine Test Cells and Ground Run-up Suppressors, Volume 2: Design and Planning for Noise Control, by Norman Doelling and Richard H. Bolt, November 1961.

36. Colehous, J. L., "Inlet Vortex," Journal of Aircraft, v. 8, no. 1, January 1971.

37. The Aeroacoustic Corporation Bulletin B-37, R1, 1968.

38. Leef, C. R., "Development of Nonrecirculating Wind Tunnel Configuration Insensitive to External Winds," Journal of Air- craft, v. 6, no. 3, May-June 1969.

39. Aero Systems Engineering, Inc., Letter of 10 February 1972 from L. B. Broberg, President.

40. Naval Air Rework Facility, NAS North Island, Memorandum, Test Cell Conversion for TF34 Engine, 18 May 1971.

41. Livesey, J. L., Duct Performance Parameter Considering Spatially non-Uniform Flow, AIAA Paper No. 72-85, presented at AIAA Tenth Aerospace Sciences Meeting, San Diego, California, 17-19 January 1972.

42. Carrier, W. H., and others, Modern Air Conditioning, Heating and Ventilating, Pitman Publishing Corporation, New York, 1959.

43. Hoerner, S. F., Fluid Dynamic Drag, published by the author, 1965.

44. NASA TM-X-1928, Experimental Investigation of the Effects of Pressure Distortion Imposed on the Inlet of a Turbofan Engine, by L. M. Wenzel, November 1961.

45. Yaffee, Michael L., "AEDC Facilities Busy, Despite Cuts," Aviation Week & Space Technology, v. 94, no. 17, p. 36-44, 26 April 1971.

46. Pope, A., Wind Tunnel Testing, Section 3:11, John Wiley & Sons, New York, 1964.

47. Vavra, M. H. Aero-Thermodynamics and Flow in Turbo Machines, Chapter 9, John Wiley & Sons, New York, 1960.

48. Schlichting, H., Boundary Layer Theory, Chapter XI, McGraw Hill, New York, 1968.

49. FluiDyne Engineering Corporation Project #0482, Aerodynamic Model Study of Test Cells 2, 5, 6, 7, Building 500, by J. J. Idzoref, August 1965.

50. NACA TN-4241, An Approximate Method for Design or Analysis of Two-Dimensional Subsonic-Flow Passages, by E. F. Valentine.

51. NACA TN-4384, Analysis of Turbulent Flow in non-Circular Passages, by R. G. Deissler.

52. NACA TN 4318, Analytical Relation for Wake Momentum Thickness and Diffusion Ratio for Low Speed Tuning Vanes, by S. Lieblein.

53. Burggaaf, O. R., "Analytic and Numerical Studies of the Structure of Steady Separated Flows," Journal of Fluid Mechanics, vol. 24, part 1, pp. 113-151, 1966.

54. Dwyer, H.A. "Rapid Calculation of Inviscid Flow Over Arbitrary Shaped Bodies," Journal of Aircraft, v. 8, no. 2, February 1971.

55. Naval Air Test Center Report No. ST-64R-69, J52-P8A Engine Stall Margin Investigation, by J. Matechak and L. A. Thomas, 20 August 1969.

56. Tower, P.W., Thesis Research, Thesis to be published October 1972, Naval Postgraduate School, Monterey, Calif.

57. The Soundcoat Company, Bulletins 701-704.

58. Allison Division of General Motors, Research and Development Facilities.

59. Pacific Airmotive Corporation Engineering Report, Reliability Program Support Services for Turbine Engines, 1 June 1971.

60. Parsons-Vonseb Report, Sound Study for Aeronautical Propulsion Laboratory, Naval Postgraduate School, May 1961.

61. Bureau of Aeronautics Specification XMA-51, Sound Measurement Tests for 30,000 Pound Thrust Capacity Turbojet Test Facility, January 1959.

62. Northern Research and Engineering Corporation Report 950-313, Preliminary Design, Model Testing and Installation of a Prototype of a Thermal Converter for the Control of Exhaust Emissions from Navy Jet Engine Test Cells, Technical Proposal.

63. Personal Communications with Mr. H. Lindenhofen, Naval Air Propulsion Center, Aero Engines Department, Philadelphia, Pa.

64. General Electric Report No. 4DG 0006B01, Supplemental Airline Planning Guide: Test Facilities for Large Turbojet and Turbofan Engines, 1 June 1968.

65. Pai, S.I. Fluid Dynamics of Jets, D. Van Nostrand Co., Inc., 1954.

66. Birkhoff, Garrett, Jets, Wakes and Cavities, Academic Press, New York, 1957.

67. Gurevich, M. I., The Theory of Jets in an Ideal Fluid, Translated by R.E. Hunt, Pergamon Press, 1966.

68. Abramovich, G. N., The Theory of Turbulent Jets, M.I.T. Press, 1963.

69. Arnold Engineering Development Center Report AEDC-TR-71-236,
    Summary Report: An Experimental Investigation of Subsonic
    Coaxial Free Turbulent Mixing, by D. E. Chriss and R. A. Paulk,
    February 1972.

70. AGARDograph 79, Jet Simulation in Ground Test Facilities, by
    M. Pindzola, November 1963.

71. Pai, S. I., "Axially Symmetrical Jet Mixing of a Compressible
    Fluid," Quarterly of Applied Mathematics, July 1952.

72. Ghia, K. N., Torda, T. P., Lavan, Z., "Laminar Mixing of
    Heterogeneous Axisymmetric Coaxial Confined Jets," AIAA
    Journal, v. 7, no. 11, p. 2072, November 1969.

73. Monroe, P.A., An Investigation of the Performance and
    Mixing Phenomena Associated with a Supersonic Exhauster
    Interacting with Subsonic Secondary Flow, Ae. E. Thesis,
    Naval Postgraduate School, Monterey, September 1967.

74. Wade, B.S., Parametric and Experimental Analysis of Ejector
    Performance, M.S. Thesis, Naval Postgraduate School,
    Monterey, July 1967.

75. Getter and Associates Report for the Naval Facilities Engineer-
    ing Command, Pollution Abatement Study and Systems Analysis
    for Jet Engine Test Cells.

76. Ribner, and others, Proceedings of a Short Course on Noise
    Generation and Suppression in Aircraft, 29 January-2 February
    1968, UTSI.

77. NASA SP-5093, Acoustics Technology, A Survey, 1970.

78. Aerodynamic Noise, Proceedings of AFOSR-UTIAS Symposium
    Held at Toronto, 20-21 May 1968, University of Toronto Press,
    1969.

79. Richards, E.J., Mead, D.J., Noise and Acoustic Fatigue in
    Aeronautics, John Wiley and Sons, Ltd., 1968.

80. Ferriss, D. H., Johnson, R.F., "Turbulence in the Noise Pro-
    ducing Region of a Circular Jet," Journal of Fluid Mechanics,
    v. 19, part 4, p. 591, August 1964.

81. Lighthill, M.J., "Jet Noise," AIAA Journal, v. 1, no. 7,
    p. 1507, July 1963.

82. Westervelt, P.J., in Ribner, and others, <u>Proceedings of a Short Course on Noise Generation and Suppression in Aircraft,</u> 29 January-2 February 1968, UTSI.

83. Aeronautical Research Council, Reports and Memoranda No. 3389, <u>The Noise of Ejectors,</u> by D. Middleton, October 1963.

84. Department of Mechanical Engineering, University of California, Berkeley, <u>Atmospheric Pollution by Aircraft Engines and Fuels--A Survey,</u> by R.A. Sawyer, 1 September 1971.

85. Cornell Aeronautical Laboratory, Report No. NA-5007-K-1, <u>Analysis of Aircraft Exhaust Emission Measurements,</u> 15 October 1971.

86. Northern Research and Engineering Corporation, Report No. 11684, <u>Assessment of Aircraft Emission Control Technology,</u> September 1971.

87. Heywood, J.B., Fay J.A., Linden, L.H., "Jet Aircraft Air Pollutant Production and Dispersion, " <u>AIAA Journal,</u> v. 9, no. 5, p. 841.

88. AFAEPL Technical Memorandum APTC-TM-69-11, <u>Turbo-Propulsion Exhaust Smoke and Smoke Abatement,</u> by R.E. Henderson, April 1969.

89. Study Group on Aviation Exhaust of the CRC Aviation Fuel, Lubricant and Equipment Research Committee, <u>Report on Analysis of Exhaust Gases from Current Commercial Jet Engines,</u> 23 July 1968.

BIBLIOGRAPHY

1. Bauer, R.C., "Characteristics of Axisymmetric and Two-
    Dimensional Isoenergetic Jet Mixing Zones," AEDC-TDR-63-
    263, December 1963.

2. Brunda, Donald F., "Evolution of a Circumferential Inlet
    Pressure Distortion Index for a TF-30-P12 Turbofan Engine,"
    NAPTC-ATD-193, July 1970.

3. Channapragada, R.S., "A Compressible Jet Spread Parameter
    for Mixing Zone Analysis (Part II)," CETEC Corporation,
    TM-14-63-U31.35, June 1963.

4. Donovan, L.F., Todd, C.A., "Computer Program for Calcu-
    lating Isothermal Turbulent Jet Mixing of Two Gases," NASA
    TN D-4378, March 1968.

5. Engel, M.O., "Some Problems in the Design and Operation of
    Jet Ejectors," Proc. Instn. Mech. Eng., vol. 177, no. 13, p. 347,
    1963,

6. Englert, G.W., Luidens, R.W., "Wind Tunnel Techniques for
    Simultaneous Simulation of External Flow Fields About Nacelle
    Inlet and Exit Airstream," NACA TN 3881.

7. Fabri, J., Paulon, J., "Theory and Experiments on Supersonic
    Air-to-Air Ejectors," NACA TM-1410, September 1958.

8. Fejer, A.A., Hermann, W.G., Torda, T.P., "Factors That
    Enhance Jet Mixing," ARL-69-0175, October 1969.

9. Ferri, A., Edelman, R., "Some Observations on Heterogeneous
    Mixing Inside Channels," ARL-67-0274, December 1967.

10. Fuhs, A.E., "Combustion Research Problems Associated with
    Advanced Air Breathing Engines," AIAA Paper 71-1, Ninth
    Aerospace Sciences Meeting, New York, N.Y., January 1971.

11. Garrett Company Report PE-8278-R, "AiResearch Engines for Remotely Piloted Vehicle Application in the 1975 and 1980 IOC Period," 1 December 1971.

12. Ghia, K.N., Torda, T.P., Lavan, Z., "Turbulent Mixing in the Initial Region of Heterogeneous Axisymmetric Coaxial Confined Jets," NASA CR-1615, May 1970.

13. Johnson, J.E., Astleford, W.J., "A Facility and Instrumentation for Studying Engine Control and Performance," Southwest Research Institute, San Antonio, Texas AWRI-RS-576.

14. Keenan, J.H., Neumann, E.P., Lustwerk, F., "An Investigation of Ejector Design by Analysis and Experiment," Journal of Applied Mechanics, September 1950.

15. Korst, H.H., Chow, W.L., "Non-Isoenergetic Turbulent $(P_{rt} = 1)$ Jet Mixing Between Two Compressible Streams at Constant Pressure," NASA CR-419, April 1966.

16. Krenkel, A.R., Lipowsky, H.H., "Design Analysis of Central and Annular Jet Ejectors," ARL 66-0210, October 1966.

17. Palmer, J.P., Parker, J., "Effect of Steady Inlet Distortion on the Stability and Performance Characteristics of an Augmented Turbofan Engine," NAPTC-ATD-193, July 1970.

18. Pratt & Whitney Aircraft Project No. NARF-1, "Reduction of Fallout at Norfolk NARF Engine Test Cells."

19. Schetz, J.A., "Unified Analysis of Turbulent Jet Mixing," NASA CR-1382, July 1969.

20. Victor, A.C., Buecher, R.W., "An Analytical Approach to the Turbulent Mixing of Coaxial Jets," NAVWEPS Report 9057, NOTS TP 4070, October 1966.

DATA SUMMARY

ORDERED BY CONFIGURATION NUMBER

CONFIG NUMBER	$\dot{M}$	ENG VEL	RADIAL DISTORT.	CIRCUM. DISTORT.	K_D	AUG. RATIO
1113.113222	0.659	101.860	0.0007 SAT	0.0428UNSAT	0.9248	0.0
1113.213111	0.669	103.373	0.0017 SAT	0.0428UNSAT	0.4761	0.0
1113.213223	0.518	80.038	0.0017 SAT	0.0430UNSAT	0.9272	0.0
1113.313222	0.673	104.047	0.0011 SAT	0.0427 SAT	0.2608	0.0
1113.413222	0.667	103.968	0.0038 SAT	0.0427 SAT	0.3635	0.0
1113.413222	0.691	106.846	0.0012 SAT	0.0397 SAT	0.4010	0.0
1113.413543	0.495	76.478	0.0019 SAT	0.0432UNSAT	1.5234	3.635
1121.113222	0.672	103.883	0.0006 SAT	0.0399 SAT	1.1141	0.0
1121.113342	0.493	76.219	0.0048UNSAT	0.0437UNSAT	1.8473	1.197
1121.213222	0.665	102.835	0.0031 SAT	0.0430UNSAT	0.9334	0.0
1121.213342	0.492	76.044	0.0037UNSAT	0.0435UNSAT	2.0933	1.210
1121.313222	0.672	103.800	0.0006 SAT	0.0428UNSAT	0.7879	0.0
1121.313342	0.489	75.664	0.0042UNSAT	0.0435UNSAT	1.0884	1.425
1121.413222	0.680	105.098	0.0016 SAT	0.0397 SAT	0.5731	0.0
1122.112222	0.665	102.840	0.0006 SAT	0.0397 SAT	0.6558	0.0
1122.113542	0.473	73.467	0.0049UNSAT	0.0473UNSAT	5.9342	2.871

CONFIG NUMBER	Ṁ	ENG VEL	RADIAL DISTORT.	CIRCUM. DISTORT.	K_D	AUG. RATIO
1131.113222	0.651	100.642	0.0012 SAT	0.0400 SAT	0.6798	0.0
1131.113223	0.517	79.938	0.0013 SAT	0.0429UNSAT	0.6386	0.0
1131.213222	0.665	102.824	0.0013 SAT	0.0428UNSAT	0.6107	0.0
1131.213442	0.478	74.592	0.0058UNSAT	0.0488UNSAT	7.2430	3.419
1131.213543	0.463	72.185	0.0056UNSAT	0.0479UNSAT	7.1440	4.374
1131.313222	0.666	103.011	0.0020 SAT	0.0428 SAT	0.8638	0.0
1131.413222	0.675	104.380	0.0012 SAT	0.0428UNSAT	0.5851	0.0
1131.413223	0.519	80.297	0.0009 SAT	0.0397 SAT	0.2304	0.0
1132.113222	0.673	104.042	0.0017 SAT	0.0427 SAT	0.4863	0.0
1132.113542	0.477	73.851	0.0043UNSAT	0.0448UNSAT	2.0010	2.994
1132.413222	0.662	102.366	0.0022 SAT	0.0427 SAT	0.7981	0.0
1141.213222	0.610	94.279	0.0048UNSAT	0.0432UNSAT	1.5663	0.0
1141.213223	0.489	75.636	0.0011 SAT	0.0434UNSAT	0.8138	0.0
1141.313222	0.606	93.694	0.0036UNSAT	0.0431UNSAT	3.9948	0.0
1141.413222	0.615	95.102	0.0040UNSAT	0.0429UNSAT	0.9320	0.0
1142.113222	0.592	91.516	0.0022 SAT	0.0405 SAT	1.2020	0.0
1145.113222	0.593	91.633	0.0025 SAT	0.0431UNSAT	1.5177	0.0
1152.113222	0.650	102.017	0.0012 SAT	0.0428UNSAT	0.7284	0.0
1213.113222	0.664	102.559	0.0005 SAT	0.0428UNSAT	0.7936	0.0
1213.113223	0.523	80.814	0.0017 SAT	0.0428 SAT	0.2303	0.0
1213.113543	0.511	79.355	0.0067UNSAT	0.0456UNSAT	6.3772	3.542
1213.213142	0.518	80.091	0.0012 SAT	0.0432UNSAT	0.8522	0.0
1213.213222	0.672	103.857	0.0017 SAT	0.0428UNSAT	0.8828	0.0

CONFIG NUMBER	M	ENG VEL	RADIAL DISTORT.	CIRCUM. DISTORT.	K_D	AUG. RATIO
1213.213223	0.519	80.217	0.0009 SAT	0.0430UNSAT	0.5880	0.0
1213.313222	0.676	104.564	0.0021 SAT	0.0428 SAT	0.7643	0.0
1213.313342	0.501	77.456	0.0019 SAT	0.0435UNSAT	1.6468	5.380
1213.413142	0.511	79.051	0.0019 SAT	0.0428UNSAT	0.7996	0.0
1213.413142	0.585	90.443	0.0038 SAT	0.0398 SAT	0.6386	0.0
1213.413222	0.669	103.394	0.0013 SAT	0.0426 SAT	0.4594	0.0
1213.413223	0.522	80.649	0.0015 SAT	0.0427 SAT	0.2015	0.0
1213.413543	0.501	77.469	0.0010 SAT	0.0398 SAT	0.4407	3.588
1221.113142	0.521	80.476	0.0008 SAT	0.0399 SAT	0.6512	0.0
1221.113222	0.670	105.574	0.0006 SAT	0.0399 SAT	0.7268	0.0
1221.113342	0.491	76.016	0.0040UNSAT	0.0441UNSAT	1.9822	1.201
1221.213222	0.667	103.083	0.0020 SAT	0.0427 SAT	0.6362	0.0
1221.213342	0.490	75.847	0.0035UNSAT	0.0436UNSAT	1.7254	1.213
1221.313222	0.674	104.160	0.0003 SAT	0.0428UNSAT	1.3878	0.0
1221.313342	0.492	76.086	0.0032 SAT	0.0438UNSAT	1.6497	1.417
1221.413222	0.679	104.966	0.0009 SAT	0.0397 SAT	0.4455	0.0
1222.112222	0.669	103.435	0.0014 SAT	0.0396 SAT	0.4508	0.0
1222.113222	0.660	102.017	0.0008 SAT	0.0426 SAT	0.2627	0.0
1222.113542	0.480	74.599	0.0075UNSAT	0.0450UNSAT	3.4913	2.871
1222.313142	0.490	75.805	0.0019 SAT	0.0400 SAT	0.6445	0.0
1222.313542	0.461	71.367	0.0055UNSAT	0.0437UNSAT	1.4443	3.120
1231.113222	0.651	100.653	0.0006 SAT	0.0399 SAT	0.7639	0.0

CONFIG NUMBER	$\dot{M}$	ENG VEL	RADIAL DISTORT.	CIRCUM. DISTORT.	K_D	AUG. RATIO
1231.113222	0.686	106.008	0.0000 SAT	0.0429UNSAT	1.2759	0.0
1231.113223	0.535	82.778	0.0005 SAT	0.0400 SAT	0.5463	0.0
1231.213222	0.668	103.203	0.0013 SAT	0.0427 SAT	0.5839	0.0
1231.313222	0.671	103.708	0.0009 SAT	0.0427 SAT	0.6156	0.0
1231.413222	0.677	104.620	0.0039 SAT	0.0397 SAT	0.6099	0.0
1232.113222	0.676	104.482	0.0017 SAT	0.0427 SAT	0.6962	0.0
1232.113223	0.526	81.275	0.0013 SAT	0.0428 SAT	0.5152	0.0
1232.313222	0.669	103.388	0.0015 SAT	0.0427 SAT	0.5738	0.0
1232.413222	0.665	102.731	0.0022 SAT	0.0427 SAT	0.5294	0.0
1232.413223	0.532	82.208	0.0016 SAT	0.0397 SAT	0.3593	0.0
1232.513222	0.665	102.793	0.0017 SAT	0.0427 SAT	0.7684	0.0
1241.413222	0.613	94.697	0.0053UNSAT	0.0429UNSAT	1.1393	0.0
1241.513222	0.616	95.226	0.0015 SAT	0.0432UNSAT	1.7527	0.0
1242.113222	0.588	90.914	0.0029 SAT	0.0406 SAT	1.5013	0.0
1245.113222	0.590	91.289	0.0023 SAT	0.0435 SAT	1.5154	0.0
1252.113222	0.660	102.085	0.0010 SAT	0.0398 SAT	0.5323	0.0
1313.113222	0.654	101.076	0.0009 SAT	0.0431UNSAT	1.4935	0.0
1313.213222	0.667	103.192	0.0022 SAT	0.0433UNSAT	1.3662	0.0
1313.313222	0.670	103.626	0.0017 SAT	0.0398 SAT	0.6598	0.0
1313.313342	0.458	73.841	0.0055UNSAT	0.0442UNSAT	1.3388	5.887
1313.413222	0.664	102.606	0.0017 SAT	0.0397 SAT	0.4789	0.0
1313.413543	0.481	74.334	0.0036UNSAT	0.0401 SAT	0.6303	3.740
1321.113142	0.519	80.231	0.0011 SAT	0.0430UNSAT	0.9013	0.0

CONFIG NUMBER	M	ENG VEL	RADIAL DISTORT.	CIRCUM. DISTORT.	K D	AUG. RATIO
1321.113222	0.663	102.559	0.0026 SAT	0.0401 SAT	1.1816	0.0
1321.213222	0.667	103.109	0.0024 SAT	0.0430UNSAT	1.2132	0.0
1321.313222	0.666	102.990	0.0021 SAT	0.0400 SAT	1.2651	0.0
1321.413142	0.511	78.997	0.0027 SAT	0.0431UNSAT	0.9284	0.0
1321.413222	0.676	104.553	0.0020 SAT	0.0428UNSAT	0.7551	0.0
1321.413223	0.519	80.297	0.0016 SAT	0.0428UNSAT	3.7567	0.0
1321.413543	0.483	74.749	0.0040UNSAT	0.0441UNSAT	2.6631	4.125
1322.313142	0.499	77.207	0.0027 SAT	0.0402 SAT	0.5707	0.0
1322.313542	0.445	68.824	0.0047UNSAT	0.0401 SAT	0.7908	3.234
1331.113222	0.647	100.030	0.0015 SAT	0.0427 SAT	0.8420	0.0
1331.113223	0.529	81.753	0.0005 SAT	0.0432UNSAT	0.9666	0.0
1331.213442	0.485	75.678	0.0072UNSAT	0.0488UNSAT	8.1328	3.367
1331.213543	0.461	71.769	0.0032 SAT	0.0484UNSAT	7.8237	3.761
1331.313222	0.662	102.283	0.0016 SAT	0.0427 SAT	0.8257	0.0
1331.413222	0.674	104.124	0.0007 SAT	0.0397 SAT	0.7611	0.0
1332.113222	0.670	103.538	0.0027 SAT	0.0428UNSAT	1.1891	0.0
1332.113542	0.465	71.940	0.0044UNSAT	0.0436UNSAT	1.4225	3.001
1332.413222	0.661	102.116	0.0020 SAT	0.0427 SAT	0.4180	0.0
1341.113142	0.485	74.948	0.0026 SAT	0.0401 SAT	0.7744	0.0
1341.113543	0.131	21.323	0.0019 SAT	0.0590UNSAT	1.2712	8.303
1341.213222	0.636	93.620	0.0045UNSAT	0.0430UNSAT	1.2245	0.0
1341.313222	0.606	93.626	0.0030 SAT	0.0431UNSAT	1.2006	0.0
1341.413222	0.610	94.291	0.0041UNSAT	0.0430UNSAT	1.1878	0.0

CONFIG NUMBER	Ṁ	ENG VEL	RADIAL DISTORT.	CIRCUM. DISTORT.	K_D	AUG. RATIO
1342.113222	0.615	95.141	0.0033 SAT	0.0430UNSAT	1.2081	0.0
1352.112333	0.656	101.413	0.0022 SAT	0.0428UNSAT	0.8028	0.0
1413.113222	0.655	101.255	0.0014 SAT	0.0429UNSAT	0.9861	0.0
1413.113223	0.521	80.569	0.0016 SAT	0.0427 SAT	0.3397	0.0
1413.213222	0.662	102.330	0.0026 SAT	0.0430UNSAT	0.8710	0.0
1413.313222	0.670	103.497	0.0025 SAT	0.0428 SAT	0.7493	0.0
1413.413142	0.516	79.737	0.0023 SAT	0.0397 SAT	0.4257	0.0
1413.413222	0.685	105.908	0.0019 SAT	0.0427 SAT	0.5130	0.0
1413.413223	0.518	80.071	0.0019 SAT	0.0397 SAT	0.2691	0.0
1421.113222	0.664	102.611	0.0012 SAT	0.0430UNSAT	1.3696	0.0
1421.213222	0.662	102.262	0.0017 SAT	0.0398 SAT	0.8665	0.0
1421.313222	0.665	102.772	0.0017 SAT	0.0428UNSAT	0.6173	0.0
1421.413142	0.511	79.058	0.0021 SAT	0.0397 SAT	0.2415	0.0
1421.413222	0.673	104.047	0.0016 SAT	0.0427 SAT	0.6543	0.0
1421.413223	0.519	80.191	0.0011 SAT	0.0397 SAT	0.1933	0.0
1421.413543	0.469	72.583	0.0027 SAT	0.0443UNSAT	1.8047	4.251
1422.112222	0.660	101.964	0.0019 SAT	0.0398 SAT	0.9058	0.0
1422.113222	0.651	100.589	0.0002 SAT	0.0399 SAT	0.9688	0.0
1431.113222	0.683	105.519	0.0015 SAT	0.0428UNSAT	1.1575	0.0
1431.113223	0.525	81.091	0.0003 SAT	0.0430UNSAT	0.8157	0.0
1431.213142	0.512	79.193	0.0024 SAT	0.0400 SAT	0.6932	0.0
1431.213222	0.663	102.006	0.0015 SAT	0.0429UNSAT	0.8362	0.0
1431.213442	0.430	66.593	0.0041UNSAT	0.0435UNSAT	0.7998	3.797

CONFIG NUMBER	Ṁ	ENG VEL	RADIAL DISTORT.	CIRCUM. DISTORT.	K D	AUG. RATIO
1431.213543	0.439	67.919	0.0036 SAT	0.0436UNSAT	1.5928	4.593
1431.313222	0.662	102.262	0.0025 SAT	0.0428UNSAT	0.7317	0.0
1431.413222	0.672	103.867	0.0015 SAT	0.0428UNSAT	0.5632	0.0
1431.413223	0.519	80.277	0.0014 SAT	0.0427 SAT	0.2674	0.0
1432.113222	0.666	132.881	0.0324 SAT	0.0428UNSAT	0.6691	0.0
1432.113223	0.521	80.516	0.0014 SAT	0.0397 SAT	0.2839	0.0
1432.313222	0.663	102.476	0.0034 SAT	0.0428UNSAT	0.5861	0.0
1432.413222	0.658	131.728	0.0023 SAT	0.0398 SAT	1.2544	0.0
1432.413223	0.519	80.237	0.0011 SAT	0.0397 SAT	0.2605	0.0
1432.513222	0.655	101.213	0.0019 SAT	0.0427 SAT	0.8127	0.0
1441.113142	0.486	75.162	0.0034 SAT	0.0437UNSAT	2.2344	0.0
1441.213222	0.601	92.899	0.0032 SAT	0.0435UNSAT	2.3310	0.0
1441.213223	0.497	76.832	0.0011 SAT	0.0430UNSAT	2.8497	0.0
1441.313222	0.602	93.129	0.0030 SAT	0.0430UNSAT	1.0353	0.0
1441.413222	0.613	94.692	0.0029 SAT	0.0429UNSAT	0.8877	0.0
1441.513222	0.598	92.468	0.0014 SAT	0.0436UNSAT	1.9607	0.0
1442.113222	0.590	91.242	0.0023 SAT	0.0407 SAT	1.5301	0.0
1445.113222	0.593	91.732	0.0026 SAT	0.0430UNSAT	1.4029	0.0
1452.113222	0.653	100.938	0.0023 SAT	0.0399 SAT	0.7254	0.0
1513.113222	0.660	102.011	0.0014 SAT	0.0397 SAT	0.8318	0.0
1513.413222	0.689	106.546	0.0014 SAT	0.0426 SAT	0.3537	3.3
1513.413543	0.478	73.945	0.0042UNSAT	0.0436UNSAT	1.7761	3.761
1521.413222	0.674	104.185	0.0010 SAT	0.0427 SAT	0.3770	0.0

CONFIG NUMBER	.M	ENG VEL	RADIAL DISTORT.	CIRCUM. DISTORT.	K D	AUG. RATIO
1531.113223	0.530	81.903	0.0010 SAT	0.0427 SAT	0.3465	0.0
5114.413222	0.660	101.985	0.0021 SAT	0.0432UNSAT	2.3709	0.0
1531.413222	0.673	104.078	0.0022 SAT	0.0427 SAT	0.3536	0.0
1532.113222	0.668	103.239	0.0044UNSAT	0.0429UNSAT	1.1711	0.0
1542.113222	0.597	92.416	0.0042UNSAT	0.0408 SAT	2.4297	0.0
2113.113222	0.666	103.306	0.0009 SAT	0.0426 SAT	3.3637	0.0
2113.173222	0.662	102.304	0.0013 SAT	0.0401 SAT	1.2379	0.0
2122.113222	0.658	101.755	0.0009 SAT	0.0396 SAT	0.2661	0.0
2132.113222	0.662	102.283	0.0026 SAT	0.0427 SAT	0.7569	0.0
2142.113222	0.607	93.797	0.0037UNSAT	0.0401 SAT	1.2660	0.0
2152.113222	0.660	101.980	0.0011 SAT	0.0428UNSAT	0.4849	0.0
3113.112122	0.930	144.040	0.0466UNSAT	0.0399 SAT	2.2277	0.0
3113.113122	0.671	103.692	0.0003 SAT	0.0396 SAT	0.2617	0.0
4113.213222	0.669	103.450	0.0029 SAT	0.0429UNSAT	1.5388	0.0
4113.313222	0.668	103.244	0.0034 SAT	0.0399 SAT	0.6376	0.0
4132.113222	0.661	102.231	0.0025 SAT	0.0427 SAT	0.5840	0.0
4132.413222	0.661	102.111	0.0021 SAT	0.0427 SAT	0.6446	0.0
5113.113142	0.514	79.408	0.0034 SAT	0.0434UNSAT	1.1222	0.0
5113.113222	0.659	101.933	0.0044UNSAT	0.0431UNSAT	1.4012	0.0
5113.113223	0.524	81.025	0.0010 SAT	0.0433UNSAT	1.3176	0.0
5113.213222	0.666	102.892	0.0020 SAT	0.0430UNSAT	1.3761	0.0
5113.213223	0.518	80.031	0.0015 SAT	0.0434UNSAT	1.1849	0.0
5113.413222	0.662	102.288	0.0028 SAT	0.0433UNSAT	1.7652	0.0

CONFIG NUMBER	Ṁ	ENG VEL	RADIAL DISTORT.	CIRCUM. DISTORT.	K_D	AUG. RATIO
5113.413223	0.520	80.397	0.0025 SAT	0.0432UNSAT	1.3538	0.0
5114.413223	0.523	80.867	0.0029 SAT	0.0435UNSAT	1.2837	0.0
5121.113632	0.500	77.269	0.0020 SAT	0.0398 SAT	0.2818	0.0
5121.713632	0.503	77.820	0.0015 SAT	0.0428UNSAT	0.6193	0.0
5121.813632	0.505	78.080	0.0031 SAT	0.0429UNSAT	0.5982	0.0
5121.913632	0.501	77.497	0.0021 SAT	0.0429UNSAT	0.8172	0.0
5124.113222	0.653	101.023	0.0026 SAT	0.0432UNSAT	1.9421	0.0
5124.113223	0.519	80.271	0.0029 SAT	0.0432UNSAT	1.3354	0.0
5124.213222	0.652	100.827	0.0047UNSAT	0.0432UNSAT	1.6720	0.0
5124.213223	0.515	79.657	0.0023 SAT	0.0430UNSAT	0.8582	0.0
5124.413142	0.513	79.381	0.0046UNSAT	0.0436UNSAT	1.4810	0.0
5124.413222	0.655	101.282	0.0017 SAT	0.0432UNSAT	1.8122	0.0
5124.413223	0.521	80.576	0.0027 SAT	0.0432UNSAT	1.2253	0.0
5124.413442	0.395	61.407	0.0047UNSAT	0.0453UNSAT	2.8919	3.770
5124.513442	0.373	58.359	0.0069UNSAT	0.0483UNSAT	5.1863	3.647
5131.113632	0.507	78.387	0.0024 SAT	0.0399 SAT	0.5632	0.0
5131.713632	0.503	77.772	0.0020 SAT	0.0430UNSAT	0.8742	0.0
5131.813632	0.506	78.162	0.0025 SAT	0.0399 SAT	3.6508	0.0
5131.913632	0.501	77.483	0.0025 SAT	0.0402 SAT	1.1054	0.0
5132.413542	0.371	57.484	0.0046UNSAT	0.0444UNSAT	1.0127	5.376
5132.713342	0.477	73.793	0.0043UNSAT	0.0428UNSAT	3.6498	3.493
5134.113222	0.658	101.718	0.0029 SAT	0.0431UNSAT	1.8226	0.0

CONFIG NUMBER	Ṁ	ENG VEL	RADIAL DISTORT.	CIRCUM. DISTORT.	K_D	AUG. RATIO
5134.113223	0.513	79.341	0.0038 UNSAT	0.0432 UNSAT	0.8659	0.0
5134.213222	0.651	100.700	0.0031 SAT	0.0431 UNSAT	1.6724	0.0
5134.213223	0.511	79.045	0.0006 SAT	0.0403 SAT	1.1970	0.0
5134.213442	0.367	56.812	0.0054 UNSAT	0.0439 UNSAT	1.5316	3.844
5134.513442	0.441	76.694	0.0512 UNSAT	0.0597 UNSAT	18.5831	3.074

DATA SUMMARY

ORDERED BY DISTORTION LEVEL

CONFIG NUMBER	M	ENG VEL	RADIAL DISTORT.	CIRCUM. DISTORT.	K_D	AUG. RATIO
3113.113122	0.671	102.692	0.0003 SAT	0.0396 SAT	0.2617	0.0
2122.113222	0.658	101.755	0.0009 SAT	0.0396 SAT	0.2661	0.0
1222.112222	0.669	103.435	0.0014 SAT	0.0396 SAT	0.4508	0.0
1131.413223	0.519	80.297	0.0009 SAT	0.0397 SAT	0.2304	0.0
1421.413223	0.519	80.191	0.0011 SAT	0.0397 SAT	0.1933	0.0
1221.413222	0.679	104.966	0.0009 SAT	0.0397 SAT	0.4455	0.0
1421.413142	0.511	79.058	0.0021 SAT	0.0397 SAT	0.2415	0.0
1331.413222	0.674	104.124	0.0007 SAT	0.0397 SAT	0.7611	0.0
1432.113223	0.521	80.516	0.0014 SAT	0.0397 SAT	0.2839	0.0
1122.112222	0.665	102.840	0.0006 SAT	0.0397 SAT	0.6558	0.0
1231.413222	0.677	104.620	0.0009 SAT	0.0397 SAT	0.6090	0.0
1113.413222	0.691	106.846	0.0012 SAT	0.0397 SAT	0.4010	0.0
1121.413222	0.680	105.098	0.0016 SAT	0.0397 SAT	0.5731	0.0
1432.413225	0.519	83.237	0.0011 SAT	0.0397 SAT	0.2605	0.0
1513.113222	0.660	102.011	0.0014 SAT	0.0397 SAT	0.8318	0.0
1252.113222	0.660	102.085	0.0010 SAT	0.0398 SAT	0.5323	0.0

CONFIG NUMBER	•M	ENG VEL	RADIAL DISTORT.	CIRCUM. DISTORT.	K_D	AUG. RATIO
1232.413223	0.532	82.208	0.0016 SAT	0.0397 SAT	0.3593	0.0
1313.413222	0.664	102.606	0.0017 SAT	0.0397 SAT	0.4789	0.0
1313.313222	0.670	103.626	0.0017 SAT	0.0398 SAT	0.6598	0.0
1413.413223	0.518	83.971	0.0019 SAT	0.0397 SAT	0.2691	0.0
1413.413142	0.516	79.737	0.0023 SAT	0.0397 SAT	0.4257	0.0
5121.113632	0.500	77.269	0.0020 SAT	0.0398 SAT	0.2818	0.0
1421.213222	0.662	102.262	0.0017 SAT	0.0398 SAT	0.8665	0.0
1422.112222	0.660	101.964	0.0019 SAT	0.0398 SAT	0.9058	0.0
1213.413543	0.501	77.469	0.0010 SAT	0.0398 SAT	0.4407	3.588
1432.413222	0.658	101.728	0.0023 SAT	0.0398 SAT	1.2544	0.0
1221.113142	0.521	80.476	0.0008 SAT	0.0399 SAT	0.6512	0.0
1213.413142	0.585	90.443	0.0008 SAT	0.0398 SAT	0.6386	0.0
4113.313222	0.668	103.244	0.0034 SAT	0.0399 SAT	0.5376	0.0
3113.112122	0.930	144.040	0.0466 UNSAT	0.0399 SAT	2.2277	0.0
1422.113222	0.651	100.589	0.0002 SAT	0.0399 SAT	0.9688	0.0
1121.413222	0.672	103.883	0.0006 SAT	0.0399 SAT	1.1141	0.0
5131.113632	0.537	78.387	0.0024 SAT	0.0399 SAT	0.5632	0.0
1231.113222	0.651	100.653	0.0006 SAT	0.0399 SAT	0.7639	0.0
1221.113222	0.670	103.574	0.0006 SAT	0.0399 SAT	0.7268	0.0
1452.113222	0.653	100.938	0.0023 SAT	0.0399 SAT	0.7254	0.0
5131.813632	0.506	78.162	0.0025 SAT	0.0399 SAT	0.6508	0.0
1231.113223	0.535	82.778	0.0005 SAT	0.0400 SAT	0.5463	0.0
1431.213142	0.512	79.193	0.0024 SAT	0.0400 SAT	0.6932	0.0

CONFIG NUMBER	$\dot{M}$	ENG VEL	RADIAL DISTORT.	CIRCUM. DISTORT.	K_D	AUG. RATIO
1131.113222	0.651	100.642	0.0012 SAT	0.0400 SAT	0.6798	0.0
1222.313142	0.490	75.805	0.0019 SAT	0.0400 SAT	0.6445	0.0
1321.313222	0.666	102.990	0.0021 SAT	0.0400 SAT	1.2651	0.0
2113.173222	0.662	102.304	0.0013 SAT	0.0401 SAT	1.2379	0.0
1322.313542	0.445	68.624	0.0047 UNSAT	0.0431 SAT	0.7906	3.234
1321.113222	0.663	102.559	0.0026 SAT	0.0401 SAT	1.1816	0.0
2142.113222	0.607	93.797	0.0037 UNSAT	0.0401 SAT	1.2660	0.0
1341.113142	0.495	74.948	0.0026 SAT	0.0401 SAT	0.7744	0.0
1313.413543	0.461	74.334	0.0036 UNSAT	0.0401 SAT	0.6303	3.740
5131.913632	0.501	77.483	0.0025 SAT	0.0402 SAT	1.1054	0.0
1322.313142	0.499	77.207	0.0027 SAT	0.0402 SAT	0.5707	0.0
5134.213223	0.511	79.045	0.0006 SAT	0.0403 SAT	1.1970	0.0
1142.113222	0.592	91.516	0.0022 SAT	0.0405 SAT	1.2023	0.0
1245.113222	0.590	91.289	0.0023 SAT	0.0405 SAT	1.5154	0.0
1242.113222	0.588	90.914	0.0029 SAT	0.0406 SAT	1.5013	0.0
1442.113222	0.590	91.242	0.0023 SAT	0.0407 SAT	1.5301	0.0
1542.113222	0.597	92.416	0.0042 UNSAT	0.0408 SAT	2.4297	0.0
2113.113222	0.666	103.036	0.0009 SAT	0.0426 SAT	3.3637	0.0
1513.413222	0.689	106.546	0.0014 SAT	0.0426 SAT	0.3537	0.0
1222.113222	0.663	102.017	0.0008 SAT	0.0426 SAT	0.2627	0.0
1113.313222	0.673	104.047	0.0011 SAT	0.0427 SAT	0.2608	0.0
1213.413222	0.669	103.394	0.0013 SAT	0.0426 SAT	0.4594	0.0
1232.313222	0.669	103.388	0.0015 SAT	0.0427 SAT	0.5738	0.0

CONFIG NUMBER	$\dot{M}$	ENG VEL	RADIAL DISTORT.	CIRCUM. DISTORT.	K_D	AUG. RATIO
1332.413222	0.661	102.116	0.0020 SAT	0.0427 SAT	0.4180	0.0
1113.413222	0.667	103.068	0.0008 SAT	0.0427 SAT	0.3635	0.0
1231.313222	0.671	103.708	0.0009 SAT	0.0427 SAT	0.6156	0.0
1521.413222	0.674	104.185	0.0010 SAT	0.0427 SAT	0.3770	0.0
1531.113223	0.530	81.903	0.0010 SAT	0.0427 SAT	0.3465	0.0
1531.413222	0.673	104.078	0.0022 SAT	0.0427 SAT	0.3536	0.0
1331.313222	0.662	102.283	0.0016 SAT	0.0427 SAT	0.8257	0.0
1413.113223	0.521	80.569	0.0016 SAT	0.0427 SAT	0.3397	0.0
1232.513222	0.665	102.793	0.0017 SAT	0.0427 SAT	0.7684	0.0
1132.113222	0.673	104.042	0.0017 SAT	0.0427 SAT	0.4863	0.0
1232.413222	0.665	102.731	0.0022 SAT	0.0427 SAT	0.5294	0.0
4132.413222	0.661	102.111	0.0021 SAT	0.0427 SAT	0.6446	0.0
1231.213222	0.668	103.208	0.0013 SAT	0.0427 SAT	0.5839	0.0
1413.413222	0.685	105.908	0.0019 SAT	0.0427 SAT	0.5130	0.0
1432.513222	0.655	101.213	0.0019 SAT	0.0427 SAT	0.8127	0.0
2132.113222	0.662	102.283	0.0026 SAT	0.0427 SAT	0.7569	0.0
1331.113222	0.647	100.030	0.0015 SAT	0.0427 SAT	0.8420	0.0
1213.413223	0.522	80.649	0.0015 SAT	0.0427 SAT	0.2015	0.0
1421.413222	0.673	104.047	0.0016 SAT	0.0427 SAT	0.6543	0.0
4132.113222	0.661	102.231	0.0025 SAT	0.0427 SAT	0.5840	0.0
1431.413223	0.519	80.277	0.0014 SAT	0.0427 SAT	0.2674	0.0
1232.113222	0.676	104.482	0.0017 SAT	0.0427 SAT	0.5962	0.0
1221.213222	0.667	103.083	0.0020 SAT	0.0427 SAT	0.6362	0.0

CONFIG NUMBER	M	ENG VEL	RADIAL DISTORT.	CIRCUM. DISTORT.	K D	AUG. RATIO
1132.413222	0.662	102.366	0.0022 SAT	0.0427 SAT	0.7981	0.0
1232.113223	0.526	81.275	0.0013 SAT	0.0428 SAT	0.5152	0.0
1213.113223	0.523	80.814	0.0017 SAT	0.0428 SAT	0.2303	0.0
1131.313222	0.666	103.011	0.0020 SAT	0.0428 SAT	0.8638	0.0
1213.313222	0.676	104.564	0.0021 SAT	0.0428 SAT	0.7643	0.0
1413.313222	0.670	103.497	0.0025 SAT	0.0428 SAT	0.7493	0.0
1131.413222	0.675	104.380	0.0012 SAT	0.0428UNSAT	0.5851	0.0
1131.213222	0.665	102.824	0.0013 SAT	0.0428UNSAT	0.6107	0.0
1431.313222	0.662	102.262	0.0025 SAT	0.0428UNSAT	0.7317	0.0
1332.113222	0.670	103.538	0.0027 SAT	0.0428UNSAT	1.1801	0.0
1432.313222	0.663	102.476	0.0034 SAT	0.0428UNSAT	0.5861	0.0
1121.313222	0.672	103.800	0.0036 SAT	0.0428UNSAT	0.7879	0.0
1152.113222	0.600	102.017	0.0012 SAT	0.0428UNSAT	0.7284	0.0
1431.413222	0.672	103.867	0.0015 SAT	0.0428UNSAT	0.5632	0.0
1321.413222	0.676	104.553	0.0020 SAT	0.0428UNSAT	0.7551	0.0
1432.113222	0.666	102.881	0.0024 SAT	0.0428UNSAT	0.6691	0.0
5132.713342	0.477	73.793	0.0040UNSAT	0.0428UNSAT	0.6498	3.493
1213.113222	0.664	102.559	0.0005 SAT	0.0428UNSAT	0.7936	0.0
1113.213111	0.669	103.373	0.0017 SAT	0.0428UNSAT	0.4761	0.0
1213.213222	0.672	103.857	0.0017 SAT	0.0428UNSAT	0.8826	0.3
1213.413142	0.511	79.051	0.0019 SAT	0.0428UNSAT	0.7996	0.0
1352.112333	0.656	101.413	0.0022 SAT	0.0428UNSAT	0.8028	0.0
1113.113222	0.659	101.850	0.0007 SAT	0.0428UNSAT	0.9248	0.0

CONFIG NUMBER	.M	ENG VEL	RADIAL DISTORT.	CIRCUM. DISTORT.	K_D	AUG. RATIO
1421.313222	0.655	102.772	0.0017 SAT	0.0428UNSAT	0.6173	0.0
1221.313222	0.674	104.160	0.0003 SAT	0.0428UNSAT	1.3878	0.0
2152.113222	0.660	101.980	0.0011 SAT	0.0428UNSAT	0.4849	0.0
5121.713632	0.503	77.820	0.0015 SAT	0.0428UNSAT	0.6193	0.0
1321.413223	0.519	80.297	0.0016 SAT	0.0428UNSAT	0.7567	0.0
1231.113222	0.686	106.008	0.0000 SAT	0.0429UNSAT	1.2759	0.0
1431.113222	0.683	105.519	0.0015 SAT	0.0428UNSAT	1.1575	0.0
5121.913632	0.501	77.497	0.0021 SAT	0.0429UNSAT	0.8172	0.0
1413.113222	0.655	101.255	0.0014 SAT	0.0429UNSAT	0.9861	0.0
1431.213222	0.660	102.006	0.0015 SAT	0.0429UNSAT	0.8362	0.0
4113.213222	0.669	103.450	0.0029 SAT	0.0429UNSAT	1.5388	0.0
1532.113222	0.668	103.239	0.0044UNSAT	0.0429UNSAT	1.1711	0.0
1441.413222	0.613	94.692	0.0029 SAT	0.0429UNSAT	0.8877	0.0
5121.813632	0.505	78.080	0.0031 SAT	0.0429UNSAT	0.5982	0.0
1141.413222	0.615	95.102	0.0040UNSAT	0.0429UNSAT	0.9320	0.0
1131.113223	0.517	79.938	0.0013 SAT	0.0429UNSAT	0.6386	0.0
1213.213223	0.519	80.217	0.0009 SAT	0.0430UNSAT	0.5880	0.0
1421.113222	0.664	102.611	0.0012 SAT	0.0430UNSAT	1.3696	0.0
5113.213222	0.666	102.892	0.0020 SAT	0.0430UNSAT	1.3761	0.0
1445.113222	0.593	91.732	0.0026 SAT	0.0430UNSAT	1.4029	0.0
1441.313222	0.602	93.129	0.0030 SAT	0.0430UNSAT	1.0353	0.0
1241.413222	0.613	94.697	0.0053UNSAT	0.0429UNSAT	1.1393	0.0
1341.213222	0.606	93.620	0.0045UNSAT	0.0430UNSAT	1.2245	0.0

216

CONFIG NUMBER	M	ENG VEL	RADIAL DISTORT.	CIRCUM. DISTORT.	K_D	AUG. RATIO
5131.713632	0.503	77.772	0.0020 SAT	0.0430UNSAT	0.8742	0.0
1321.213222	0.667	103.109	0.0024 SAT	0.0430UNSAT	1.2132	0.0
1121.213222	0.665	102.835	0.0031 SAT	0.0430UNSAT	0.9334	0.0
1341.413222	0.610	94.291	0.0041UNSAT	0.0430UNSAT	1.1878	0.0
1321.113142	0.519	80.231	0.0011 SAT	0.0430UNSAT	0.9013	0.0
1431.113223	0.525	81.091	0.0003 SAT	0.0433UNSAT	0.8157	0.0
1113.213223	0.518	80.038	0.0017 SAT	0.0430UNSAT	0.9272	0.0
5124.213223	0.515	79.657	0.0023 SAT	0.0430UNSAT	0.8582	0.0
1342.113222	0.615	95.141	0.0033 SAT	0.0430UNSAT	1.2081	0.0
1441.213223	0.497	76.882	0.0011 SAT	0.0430UNSAT	0.8497	0.0
1413.213222	0.662	102.330	0.0026 SAT	0.0433UNSAT	0.8719	0.0
1145.113222	0.593	91.633	0.0025 SAT	0.0431UNSAT	1.5177	0.0
1321.413142	0.511	78.997	0.0027 SAT	0.0431UNSAT	0.9284	0.0
5113.113222	0.659	101.933	0.0044UNSAT	0.0431UNSAT	1.4012	0.0
5134.213222	0.651	100.700	0.0031 SAT	0.0431UNSAT	1.6724	0.0
5134.113222	0.658	101.718	0.0029 SAT	0.0431UNSAT	1.8226	0.0
1141.313222	0.606	93.694	0.0036UNSAT	0.0431UNSAT	0.9948	0.0
1313.113222	0.654	101.076	0.0009 SAT	0.0431UNSAT	1.4935	0.0
1213.213142	0.518	80.391	0.0012 SAT	0.0432UNSAT	0.8522	0.0
5124.413222	0.655	101.282	0.0017 SAT	0.0432UNSAT	1.8122	0.0
5124.113222	0.653	101.023	0.0026 SAT	0.0432UNSAT	1.9421	0.0
5124.413223	0.521	80.576	0.0027 SAT	0.0432UNSAT	1.2253	0.0
1341.313222	0.696	93.626	0.0030 SAT	0.0431UNSAT	1.2006	0.0

CONFIG NUMBER	M	ENG VEL	RADIAL DISTORT.	CIRCUM. DISTORT.	K D	AUG. RATIO
1141.213222	0.610	94.279	0.0048UNSAT	0.0432UNSAT	1.5663	0.0
5124.113223	0.519	80.271	0.0029 SAT	0.0432UNSAT	1.3354	0.0
5134.113223	0.513	79.341	0.0038UNSAT	0.0432UNSAT	0.8659	0.0
1331.113223	0.529	81.753	0.0005 SAT	0.0432UNSAT	0.9666	0.0
1113.413543	0.495	76.478	0.0019 SAT	0.0432UNSAT	1.5234	3.635
1241.513222	0.616	95.226	0.0015 SAT	0.0432UNSAT	1.7527	0.0
5114.413222	0.650	101.985	0.0021 SAT	0.0432UNSAT	2.3709	0.0
5113.413223	0.520	80.397	0.0025 SAT	0.0432UNSAT	1.3538	0.0
5124.213222	0.652	100.827	0.0047UNSAT	0.0432UNSAT	1.6720	0.0
1313.213222	0.657	103.192	0.0022 SAT	0.0433UNSAT	1.3662	0.0
5113.113223	0.524	81.025	0.0010 SAT	0.0433UNSAT	1.3176	0.0
5113.413222	0.662	102.288	0.0028 SAT	0.0433UNSAT	1.7652	0.0
1141.213223	0.489	75.636	0.0011 SAT	0.0434UNSAT	0.8138	0.0
5113.113142	0.514	79.408	0.0034 SAT	0.0434UNSAT	1.1222	0.0
5113.213223	0.518	80.031	0.0015 SAT	0.0434UNSAT	1.1849	0.0
1441.213222	0.601	92.899	0.0032 SAT	0.0435UNSAT	2.3310	0.0
1213.313342	0.501	77.456	0.0019 SAT	0.0435UNSAT	1.6468	5.380
5114.413223	0.523	80.867	0.0029 SAT	0.0435UNSAT	1.2837	0.0
1121.313342	0.489	75.664	0.0042UNSAT	0.0435UNSAT	1.0884	1.425
1121.213342	0.492	76.044	0.0037UNSAT	0.0435UNSAT	2.0933	1.210
1431.213442	0.430	66.593	0.0041UNSAT	0.0435UNSAT	0.7998	3.797
1221.213342	0.490	75.847	0.0035UNSAT	0.0436UNSAT	1.7254	1.213
5124.413142	0.513	79.381	0.0046UNSAT	0.0436UNSAT	1.4810	0.0

CONFIG NUMBER	Ṁ	ENG VEL	RADIAL DISTORT.	CIRCUM. DISTORT.	K D	AUG. RATIO
1441.513222	0.598	92.468	0.0014 SAT	0.0436UNSAT	1.9607	0.0
1431.213543	0.439	67.919	0.0036 SAT	0.0436UNSAT	1.5928	4.593
1513.413543	0.478	73.945	0.0042UNSAT	0.0436UNSAT	1.7761	3.761
1332.113542	0.465	71.940	0.0044UNSAT	0.0436UNSAT	1.4225	3.001
1222.313542	0.461	71.367	0.0025UNSAT	0.0437UNSAT	1.4443	3.120
1441.113142	0.486	75.162	0.0034 SAT	0.0437UNSAT	2.2344	0.0
1121.113342	0.493	76.219	0.0048UNSAT	0.0437UNSAT	1.8473	1.197
1221.313342	0.492	76.085	0.0032 SAT	0.0438UNSAT	1.6497	1.417
5134.213442	0.367	56.812	0.0054UNSAT	0.0439UNSAT	1.5316	3.844
1221.113342	0.491	76.016	0.0040UNSAT	0.0441UNSAT	1.9822	1.201
1321.413543	0.483	74.749	0.0040UNSAT	0.0441UNSAT	2.6631	4.125
1313.313342	0.458	70.841	0.0055UNSAT	0.0442UNSAT	1.3388	5.887
1421.413543	0.469	72.583	0.0027 SAT	0.0443UNSAT	1.8047	4.251
5132.413542	0.371	57.484	0.0046UNSAT	0.0444UNSAT	1.0127	6.376
1132.113542	0.477	73.851	0.0043UNSAT	0.0448UNSAT	2.0010	2.994
1222.113542	0.480	74.599	0.0075UNSAT	0.0453UNSAT	3.4913	2.871
5124.413442	0.395	61.407	0.0047UNSAT	0.0453UNSAT	2.8919	3.770
1213.113543	0.511	79.355	0.0067UNSAT	0.0456UNSAT	6.3772	3.542
1122.113542	0.473	73.467	0.0049UNSAT	0.0473UNSAT	5.9342	2.871
1131.213543	0.463	72.185	0.0056UNSAT	0.0479UNSAT	7.1440	4.374
5124.513442	0.373	58.359	0.0069UNSAT	0.0483UNSAT	5.1863	3.647
1331.213543	0.461	71.769	0.0032 SAT	0.0484UNSAT	7.8237	3.761
1131.213442	0.478	74.592	0.0058UNSAT	0.0488UNSAT	7.2430	3.419

CONFIG NUMBER	Ṁ	ENG VEL	RADIAL DISTORT.	CIRCUM. DISTORT.	K_D	AUG. RATIO
1331.213442	0.485	75.678	0.0072UNSAT	0.0488UNSAT	8.1328	3.367
1341.113543	0.131	21.323	0.0019 SAT	0.0590UNSAT	1.2712	8.303
5134.513442	0.441	76.694	0.0512UNSAT	0.0597UNSAT	18.5831	3.074

```
************************************************************
**                                                    ** ** **
**   PROCESSING OF VERTICAL INLET VELOCITY SURVEY      ** ** **
**                                                    ** ** **
**          FOR TOTAL VOLUMETRIC FLOW RATE            ** ** **
**                                                    ** ** **
************************************************************

      RESERVE THE REQUIRED ARRAY AREAS

      DIMENSION P(2,27),W(26),AREA(27),AP(1,27),PTEMP(1,26),TOTAR(27)

      READ THE TEST DATA

   60 READ(5,1000) CONFIG
 1000 FORMAT(F12.6)
      IF(CONFIG.LT.0.0) GO TO 50
      DO 10 I=1,2
      DO 11 J=2,26
      READ(5,1001) P(I,J)
 1001 FORMAT(F12.4)
   11 CONTINUE
   10 CONTINUE

      INITIALIZE THE REQUIRED CONSTANTS

      AY=0.1
      W(1)=1.0/16.0
      W(26)=W(1)
      W(2)=7.0/16.0
```

```
      W(25)=W(2)
      DO 13 IJ=3,24
      W(IJ)=0.5003
13    CONTINUE

      SET THE VELOCITY TO ZERO AT EACH WALL

      DATA P(1,1),P(2,1),P(2,27), P(1,27)/4*0.0/

      DETERMINE THE STATIC PRESSURE AT THE INTERSECTION OF THE
      TRACES, BY AVERAGING THE FOUR SURROUNDING DATA POINTS

18    CONTINUE
      AVG1=(P(1,10)+P(1,11))/2.0
      AVG2=(P(2,10)+P(2,11))/2.0
      AY=AY+1.0
      AVG=(AVG1+AVG2)/2.0

      REPORT THIS AVERAGE

22    FORMAT(   ////F10.5,'   INTERSECTION AVERAGE   ')
      WRITE(6,22)AVG

      AREA(1)=0.0
      AREA(27)=0.0
      DO 14 L=2,26

      ADJUST THE REPORTED PRESSURE AT EACH POINT ON THE TRACE BY
      THE DIFFERENCE BETWEEN THE INTERSECTION AVERAGE AND THE
      SECOND TRACE DATA POINT. DO THIS FOR EACH OF THE NON ZERO
      POINTS ON THE SECOND TRACE

      FACTOR=P(2,L)-AVG
      AREA(1)=0.0
      AP(1,1)=0.0
      AP(1,27)=0.0
```

```
C     COMPUTE THE AREA UNDER THE ADJUSTED PRESSURE PROFILE
C     BETWEEN EACH PAIR OF DATA POINTS BY AVERAGING THESE POINTS
C     AND WEIGHTING THIS AVERAGE BY THE DISTANCE BETWEEN THEM
C
C     KEEP A RUNNING TOTAL OF THESE AREAS
C
      DO 15 M=2,26
      AP(1,M)=P(1,M)+FACTOR
      AREA(M)=AREA(M-1)+((AP(1,(M-1))+AP(1,M))/2.0)*W(M-1)
      DATA TOTAR(1),TOTAR(27)/0.0,0.0/
   15 CONTINUE
C
      TOTAR(L)=AREA(26)
      FORMAT(F10.5,' SLICE AREA   ')
   23 WRITE(6,23)TOTAR(L)
   14 CONTINUE
C
C     AFTER ALL SLICE AREAS ARE COMPUTED,AVERAGE EACH ADJACENT
C     PAIR OF SLICES AND WEIGHT THIS AVERAGE BY THEIR LATERAL
C     SEPARATION. KEEPING A RUNNING TOTAL OF THESE VOLUMES
C
      VOL=0.0
      DO 16 JK=2,27
      VOL=VOL+((TOTAR(JK-1)+TOTAR(JK))/2.0)*W(JK-1)
   16 CONTINUE
C
C     DIVIDE THE VOLUME TOTAL BY THE TOTAL FLOW AREA TO YIELD
C     THE AVERAGE DYNAMIC PRESSURE AND VOLUMETRIC FLOW RATE
C
      PAVG=VOL/144.0
      FLOW=66.119*(SQRT(PAVG))
C
C     PRINT OUT THESE RESULTS
C
   20 FORMAT(//,' CONFIGURATION      Q    ',
     C       VOL,' FLOW RATE',/)
   21 FORMAT( 5X,F7.2,6X,F8.4,' IN H2O ',F9.4,' CFS ')
      WRITE(6,20)
      WRITE(6,21)CONFIG,PAVG,FLOW
```

```
C     REVERSE THE POSITIONS OF THE DATA TRACES IN STORAGE AND
C     REPEAT THE COMPLETE AVERAGING PROCEEDURE

      DO 17 JL=2,26
      PTEMP(1,JL)=P(1,JL)
      P(1,JL)=P(2,JL)
      P(2,JL)=PTEMP(1,JL)
   17 CONTINUE

C     IF ALL DATA SETS HAVE BEEN PROCESSED....TERMINATE

      IF(AY.LT..5) GO TO 18
      GOTO 60
   50 CONTINUE
      STOP
      END
```

```
                    DISTORTION DATA
                     PROCESSING


      RESERVE THE REQUIRED STORAGE SPACE AND IDENTIFY THE
      VARIABLES WHICH REQUIRE DOUBLE PRECISION

      DIMENSION BCOV(10),SUBD(10),AUGRT(10)
      DIMENSION PTOT(25),PSTAT(2),DOTL(25),PTSEC(8),DPCTG(25),PTMWT(25)
C    ,ISECT(8),PRING(3),CON(10),CMF(10),CVT(10),DIS(10),DFC(10),CONDC(1
C0),PRIM(3),BJV(3),ACOV(10)
      REAL*8 DPRES,TWENT1,BNUM,BLIM,DFCIRM,CONFIG,CON


      SET THE INPUT AND OUTPUT FORMATS

41 FORMAT(////,'     CONFIGURATION NUMBER  ',F14.8)
42 FORMAT(//,'   DISTORTION NUMBER  ',F14.8)
43 FORMAT('   FACE DATA     ',':')
C  PERCENTAGE.
   '       PSTATIC       MASS FLOW    DISTORTION P
45 FORMAT(/4X,'     THE COMPRESSOR
   '       STATION    PTOTAL
49 FORMAT(4X,F7.4,2X,F7.4,2X,F6.4,9X,F8.4)
51 '   THE COMPUTED   COEFFICIENTS FOR THIS RUN:  ',' ENGI
   USING    '      AVG PTOTAL   AVG VELOCITY
C  NE MCOT=
52 FORMAT(,'    NUMERICAL AVG   2X,F8.4,7X,F8.4,10X,F8.4)
53 FORMAT(//,'    AREA WTD AVGS   2X,F8.4,7X,F8.4,13X,F8.4)
55 FORMAT(,'       SECTOR   '.13,
56 FORMAT(,'      COMPUTATION OF THE CIRCUMFERENTIAL DISTORTI
   'ON SECTOR   '.14,    TOTAL PRESSURES ARE REQUIRED:
C  ON INDEX=
   '      AVERAGED SECTOR IS CONSIDERED TO BE SPOILED   ')
57 FORMAT(/////.
59 FORMAT(////,'   THE AVERAGE TOTAL PRESSURE IN THESE SPOILED SECTORS
```

```
C  IS
   61 FORMAT(/,' ',F7.4)
C STORTION FACTOR IS',F5.7)
   62 FORMAT(/,' (PTMAVG-PTMIN)/PTMAVG = ',7.4,' (PTMAX-PTMAVT)
C/PTMAVG = ',7.4,' (PTMAVG-PTMIN)/PTMAVG = ',7.4,' (PTMAX-P
C/PTMIN)/PTMAVG = ',7.4,' ATMOSPHERIC
   63 FORMAT(//,' ATMOSPHERIC PRESSURE WAS',F10.2,' INCHES IF MERCURY')
 1001 FORMAT(2F12.6)
 1023 FORMAT(3F8.6)
 1033 FORMAT(3F8.4,F8.4,15)
  104 FORMAT(//' MASS FLOW WTS'
  151 FORMAT(//' CONFIG. CIRCUM    VELOCITY             FACE D
  299 FORMAT(//,' CIAL LEVEL                  SUB         AUGMENTATION.')
  300 FORMAT(//,' LEVEL                     DUCT           VELOCITY DIS
C TORTION                                           RATIO.',/,
  301 FORMAT(2X,F8.4,7X,F8.4,10X,F8.4)
  302 FORMAT(F12.4,.4,' UNSAT        2F12.4)
  303 FORMAT(F12.4,.4,' SAT         2F12.4)
  678 FORMAT(F12.4,.4,' UNSAT        2F12.4)
  860 FORMAT(4F14.7)
C     FACTOR  RADIAL DISTORTION TOLERANC
  861 FORMAT(//' NAPTC RADIAL DISTORTION TOLERANCE IS   ',F8.4,' M
C IDRING CORRECTED AVERAGE 'F8.4' OUTER RING',//,17X,F8.4,' AND THE DISTO
  862 FORMAT(//' CIRCUM     INNER RADIUS RATIO IS   ',F8.4,' AND THE DISTO
C RTION AMPLITUDE ',F14.7)
  869 FORMAT(//' ***** STALL WILL OCCUR IN TH
  871 FORMAT(//' ***** STALL AMPLITUDE EXCEEDS ',F8.4)
C IS CONFIGURATION.',/,' ***** STALL WILL OCCUR
  872 FORMAT(//' *****THE ASSUMPTION,THAT THE HUB
C UR AS THE STORED ENGINE ASSUMPTION WAS THE BLADE
C     ',/,' BECAUSE THE ENGINE DISTORTION,STANDARD ENGINE
  892 FORMAT(//' THIS STALL THIS WILL OCCUR DUE
  893 FORMAT(//' THE CORRECTED VALUE WILL
 1001 FORMAT(//' STANDARD DISTORTION ZONE ')    OPERATE SAT
C IS FACTOR CIRCJMFERENTIAL ACCURACY OF MEASUREMENT,    ',F10.2)
 1003 FORMAT(//' CIRCILLY DISTORTION.'                  WITH THE LEVEL
C XTENT OF DISTORTION IN ALL PRESSURE PSIA.',/,' NO CIRCUMFERENTIAL
 1099 FORMAT(//' THIS EXISTS     THE COMPRESSOR FACE MACH NUMBER IS   ',F9.5)
 1112 FORMAT(16)
 1234 FORMAT(5F12.6)
 9300 FORMAT(3F12.6)
 9303 FORMAT(3F12.6)

C     SET THE COUNTING INDICES AND READ THE FIRST DATA SET
```

00004770
00004780
00004790

```
      IROUN=0
      IJK=1
   99 CONTINUE

      READ(5,101) CONFIG,AUGAIR
      CON(IJK)=CONFIG

C     IF NO MORE SETS FOLLOW PROCEED TO THE SUMMARY LIST

      IF(CONFIG.LT.0.0)GOTO 50
      IROUN=IROUN+1
      READ(5,103) PATM
      WPATM=PATM/0.073554

C     CONVERT MANOMETER DISPLACEMENT DATA INTO ABSLOUTE
C     PRESSURES

      DO 10 I=1,25
      READ(5,103) TOT
      PTOT(I)= WPATM-TOT
   10 CONTINUE
      READ(5,103) TAT
      PSTAT(1)=WPATM-TAT
      READ(5,103) TAT
      PSTAT(2)=WPATM-TAT

C     INITIALIZE THE REQUIRED INDICES, THEN LOCATE THE
C     MAXIMUM AND MINIMUM TOTAL PRESSURE AND IDENTIFY
C     THE LOCATION OF THESE READINGS

      DON=0.0
      PTMAX=0.0
      PTMIN=1000.00
      DO 13 J=1,25
      DIFF== PTMAX - PTOT(J)
      IF(DIFF.LT.-0.005) GOTO 12
      GOTO 11
   12 PTMAX = PTOT(J)
      INDEX= J
   11 CONTINUE
      DIFFM= PTMIN - PTOT(J)
```

```
      IF ( DIFFM.GT.0.005) GOTO 14
      GOTO 13
14    PTMIN = PTOT(J)
      INDEXM = J
13    CONTINUE

C     NUMERICALLY AVERAGE THE TOTAL PRESSURE DATA

      SUM=0.0
      DO 15 K=1,25
      SUM = PTOT(K) + SUM
15    CONTINUE
      PTAVG = SUM/25.0

C     AVERAGE THE TOTAL PRESSURE DATA BY AREA WEIGHTING
C     THE RECORDED PRESSURES

      ASUM=0.0
      DO 16 L=1,8
      ASUM = ASUM + (PTOT(L) * 0.596433 )
16    CONTINUE
      ASUM2=0.0
      DO 17 II=9,16
      ASUM2 = ASUM2 + (PTOT(II) * 0.38935)
17    CONTINUE
      ASUM3=0.0
      DO 18 IJ=17,24
      ASUM3=ASUM3 + (PTOT(IJ) * 0.43997 )
18    CONTINUE
      PTAAVG=(ASUM+ASUM2+ASUM3+(PTOT(25)*0.77309))/12.17911

C     AVERAGE THE STATIC PRESSURES

      PSTAVG = (PSTAT(1) + PSTAT(2))/2.0

C     AVERAGE THE TOTAL PRESSURE DATA BY MASS FLOW
C     WEIGHTING THE RECORDED PRESSURE USING THE NEAREST
C     STATIC PROBE DATA OR THE AVERAGE OF THESE VALUES
C     FOR THE NUMBER 25 (CENTER) PROBE
```

```
      DO 19 JJ=1,3
      VLOCAL=(SQRT(PTOT(JJ)-PSTAT(1)))*66.119
      DOTL(JJ)=(VLOCAL*0.596433)*0.0765
19    CONTINUE
      DO 20 JK=4,7
      VLOCAL=(SQRT(PTOT(JK)-PSTAT(2)))*66.119
      DOTL(JK)=VLOCAL*0.596433*0.0765
20    CONTINUE
      DOTL(8)=((SQRT(PTOT(8)-PSTAT(1)))*66.119)*0.596433*0.0765
      DO 21 JM=9,11
      VLOCAL=(SQRT(PTOT(JM)-PSTAT(1)))*66.119
      DOTL(JM)=(VLOCAL*0.38935)*0.0765
21    CONTINUE
      DO 22 JN=12,15
      VLOCAL=(SQRT(PTOT(JN)-PSTAT(2)))*66.119
      DOTL(JN)=VLOCAL*0.38935*0.0765
22    CONTINUE
      DOTL(16)=((SQRT(PTOT(16)-PSTAT(1)))*66.119)*0.38935*0.0765
      DO 23 JO=17,19
      VLOCAL=(SQRT(PTOT(JO)-PSTAT(1)))*66.119
      DOTL(JO)=VLOCAL*0.43997*0.0765
23    CONTINUE
      DO 24 JP=20,23
      VLOCAL=(SQRT(PTOT(JP)-PSTAT(2)))*66.119
      DOTL(JP)=VLOCAL*0.43997*0.0765
24    CONTINUE
      DOTL(24)=((SQRT(PTOT(24)-PSTAT(1)))*66.119*.439973*0.0765
      DOTL(25)=((SQRT(PTOT(25)-PSTAVG))*66.119)*0.773090*0.0765
      DENOM=0.0
      TOTAL=0.0
      DO 25 JQ=1,25
      PTMWT(JQ)=PTOT(JQ)* DOTL(JQ)
      TOTAL=TOTAL+PTMWT(JQ)
      DENOM=DENOM+ DOTL(JQ)
25    CONTINUE
      PTMAVG=TOTAL/DENOM

C     USING THESE THREE AVERAGES, DETERMINE THE
C     CORRESPONDING AVERAGE VELOCITIES AND MASS FLOW
C     RATES

      CMFTR=DENOM/144.0
      CVTRU=(SQRT(PTMAVG-PSTAVG))*66.119
      CVEL=SQRT(PTAAVG-PSTAVG)*66.119
      CMOT==(CVEL*(12.179)12./144.0)*(0.0765)
      CVELL=SQRT(PTAVG-PSTAVG)*66.119
```

```
      CMDOT1=CVELL*(12.17911/144.0)*(0.0765)

C     DETERMINE THE MASS FLOW WEIGHTED AVERAGE TOTAL
C     PRESSURE FOR EACH 45 DEGREE SECTOR

      DO 26 JR=1,8
      PTSEC(JR)=(PTMWT(JR)+PTMWT(JR+8)+PTMWT(JR+16))/(DOTL(JR)+DOTL(JR+8
     C)+DOTL(JR+16))
   26 CONTINUE

C     LOCATE THE MINIMUM SECTOR AVERAGE

      ISUM=0
      PTSPL=1000.0
      DO 27 JS=1,8
      CG=PTSPL-PTSEC(JS)
      IF(CG.GE.0.0000) GOTO 28
      GO TO 27
   28 PTSPL=PTSEC(JS)
      INDK=JS
   27 CONTINUE

C     CHECK TO SEE IF THIS MINIMUM AVERAGE IS MORE THAN
C     ONE PERCENT BELOW THE AVERAGE TOTAL PRESSURE

      LX=1
      RADNUM=1.0
      DO 33 IKE=1,8
      SST=ABS(PTSEC(IKE)-PTSPL)
      IF(SST.GE.0.0005) GOTO 34
      CONTINUE
      GOTO 39
   33 CONTINUE
   34 CONTINUE

C     IF IT IS,CONSIDER THIS SECTOR TO BE SPLOILED AND
C     EXAMINE THE ADJACENT SECTORS TO DETERMINE THE
C     RADIAL EXTENT OF THE SPOILED AREA

      LX=2
      INM=1
```

```
      ISECT(1)=INDK
      WAIT=(PTMAVG-PTSPL)/2.0
      INDKT=INDK
   35 FNDL=INDKT+INM
      IF(FNDL.GT..8.5)    FNDL=FNDL-8.0
      IF(FNDL.LT.-0.5)    FNDL=FNDL+8.0
      INDL=FNDL
      GCS=A3S(PTSEC(INDL)-PTSPL)
      IF(GCS.LT.WAIT) GOTO 30
      GOTO 36
   30 CONTINUE
      ISECT(LX)=INDL
      LX=LX+1
      RADNUM=RADNUM+1.0
      INDKT=FNDL
      GOTO 35
   36 BOQ=INM
      IF(BOQ.GT.0.0) GOTO 37
      GOTO 38
   37 INM=-1
      INDKT=INDK
      GOTO 35
   38 CONTINUE
```

C   COMPUTE THE NAPTC CIRCUMFERENTIAL DISTORTION FACTOR

```
      DPRES=PTSPL-PSTAVG
      TWENTI=DSQRT(DPRES/PTSPL)
      IF(RADNUM.LE.1.5) GOTO 244
      BNUM=0.0425
      GOTO 245
  244 BNUM=0.0395
  245 CONTINUE
      DFCIRM=(BNUM)/(TWENTI/(SQRT((PTMAVG-PSTAVG)/PTMAVG)))
   39 CONTINUE
```

C   CALCULATE THE STANDARD DISTORTION RATIOS

```
      A=(PTMAX-PTMAVG)/PTMAVG
      B=(PTMAVG-PTMIN)/PTMAVG
      C=(PTMAX-PTMIN)/PTMAVG
```

```
      DETERMINE THE MASS FLOW THRU EACH PROBE AREA AND THE
      PERCENTAGE DISTORTION OF THE VELOCITY PROFILE IN
      EACH ONE

         DO 40 JU=1,25
         DPCTG(JU)=((PTOT(JU)/PTMAVG)-1.0)*100.0
   40    CONTINUE
         DO 77 KQ=1,25
         DOTL(KQ)=DOTL(KQ)/144.0
   77    CONTINUE

C        FIND THE AVERAGE PRESSURE OF EACH PROBE RING

         PRING(1)=0.0
         PRING(2)=0.0
         PRING(3)=0.0

C        FIND EQUAL FLOW RING DIMENSIONS AND DETERMINE THE
C        AEDC DISTORTION FACTOR

         DO 708 MM=1,3
         MQ=((MM-1)*8)+1
         MR=MQ+7
         PRIM(MM)=10000.0
         DO 707 MK=MQ,MR
         PRIM(MM)=PRING(MM)+PTOT(MK)
         IF(PTOT(MK).LT.PRIM(MM))GOTO 650
         GOTO 651
  650    PRIM(MM)=PTOT(MK)
  651    CONTINUE
  707    CONTINUE
         PRING(MM)=PRING(MM)/8.0
         BJK(MM)=0.0
         DO 652 IJL5=MQ,MR
         ELS=ABS(PTOT(IJL5)-PRIM(MM))
         IF(ELS.LE.WAIT) GOTO 653
         GOTO 654
  653    BJK(MM)=BJK(MM)+1.0
  654    CONTINUE
  652    CONTINUE
  708    CONTINUE
         CRING1=2.0/0.65625
         CRING2=2.0/1.3437
```

232

```
      CRING3=2.0/1.6875
      PNB=((PRING(1))-PRIM(1)))/PRING(1)))*(BJK(1)**45.0)*CRING1
      PNC=((PRING(2))-PRIM(2)))/PRING(2)))*(BJK(2)**45.0)*CRING2
      PND=((PRING(3))-PRIM(3)))/PRING(3)))*(BJK(3)**45.0)*CRING3
      AEDC=(100.0*(PNB+PNC+PND))/(CRING1+CRING2+CRING3)

C     EVALUATE THE NAPTC RADIAL DISTORTION FACTOR

      IF(PRING(1).LT.PRING(2))  GOTO 709
      IF(PRING(2).LT.PRING(3))  GOTO 710
      IF(PRING(1).LT.PRING(3))  GOTO 711
  709 PRMIN=PRING(3)
      IEX=3
      RDIF=1.3/16.0
      RBAR=1.0
      GOTO 712
  710 PRMIN=PRING(2)
      IEX=2
      RDIF=6.0/16.0
      RBAR=1.3750
      GOTO 712
  711 PRMIN=PRING(1)
      IEX=1
      RDIF=5.0/16.0
      RBAR=1.75
  712 CONTINUE
      RADRAT=(RBAR*RDIF)/(2.0/1.75)
      DISAMP=((PRMIN-PTMAVG)/PTMAVG)*40.0
      IF(DISAMP.LE.0.0) DISAMP=0.0000

C     MAKE THE REQUIRED UNIT CONVERSIONS AND PRINT THE
C     INDIVIDUAL PROBE AND AVERAGED VALUES

      WRITE(6,41) CONFIG
      WRITE(6,42)
      WRITE(6,43)
      AJJ=2.5
      JX=1
      PSTAT(1)=PSTAT(1)*0.036126
      PSTAT(2)=PSTAT(2)*0.036126
```

233

```
      DO 44 JV=1,24
      PTOT(JV)=PTOT(JV)*0.036126
      WRITE(6,45) JV,PTOT(JV),PSTAT(JX), DOTL(JV),DPCTG(JV)
      COUNT=JV
      IF(COUNT.GT.AJJ) GOTO 46
      JX=1
      AJW=1.0
      GOTO 44
46    JX=2
      IF(AJW.GT.3.1) GOTO 47
      AJW=AJW+1.0
      GOTO 44
      AJJ=AJJ+8.0
47    CONTINUE
44    JV=25
      PSTAVG=PSTAVG*0.036126
      PTOT(25)=PTOT(25)*0.036126
      WRITE(6,45) JV,PTOT(JV),PSTAVG, DOTL(JV),DPCTG(JV)
      WRITE(6,111)
      WRITE(6,49)
      WRITE(6,51)
      PTAVG=PTAVG*0.036126
      PTAAVG=PTAAVG*0.036126
      PTMAVG=PTMAVG*0.036126
      CMACH =SQRT((2.*O/O.4)*(((PTMAVG/PSTAVG)**(0.4/1.4))-1.0))
      WRITE(6,52) PTAVG,CVELL,CMDOT1
      WRITE(6,53) PTAAVG,CVELL,CMDOT
      WRITE(6,151) PTMAVG,CVTRU,CMFTR
      WRITE(6,1234) CMACH

C              PRINT THE RESULTS OF THE SECTOR AVERAGE CALCULATIONS

      WRITE(6,56)
      DO 54 KR=1,8
      PTSEC(KR)=PTSEC(KR)*0.036126
      WRITE(6,55) KR,PTSEC(KR)
54    CONTINUE

C     IDENTIFY THE SPOILED SECTORS AND PRINT THE CIRCUM-
C     FERENTIAL DISTORTION FACTOR WITH ITS EVALUATION AS
C     TO SAT-UNSAT AND THE RPM LIMIT TO WHICH IT WOULD
C     REMAIN SATISFACTORY

      CLX=LX-1
```

```
      IF(CLX.LT.0.5) GOTO 1110
      LX=LX-1
      ASSP=0.0
      DO 58 KS=1,LX
      WRITE(6,57)ISECT(KS)
      KIS=ISECT(KS)
      ASSP=ASSP+PTSEC(KIS)
 58   CONTINUE
      DAVS=LX
      PTSPL=(ASSP/DAVS)
      WRITE(6,59) PTSPL
      WRITE(6,61) DFCIRM
      IF(RADNUM.LE.1.5) GOTO 257
      BLIM=0.04278
      GOTO 258
257   BLIM=0.04250
258   CONTINUE
      IF(DFCIRM.GT.BLIM) GOTO 1020
      SLRPM=11650.0+2504.0*(DFCIRM/0.0425)
      WRITE(6,1001) SLRPM
      GOTO1002
1110  CONTINUE
      DFCIRM=0.0000
      WRITE(6,1099)
      GOTO1002
1020  WRITE(6,869)
      DON=1.0
      WRITE(6,1003)
1002  CONTINUE

      EVALUATE THE RADIAL DISTORTION FACTOR AND OUTPUT
      ITS VALUE AND THE RESULTING CONDITION OF OPERATION

      IF(RADRAT.GT.0.373) GOTO 850
      CDIF=0.373-RADRAT
      SLINE=0.055+(CDIF*0.083333)
      ADMAT=10.9
      GOTO 851
850   CDIF=RADRAT-0.3730
      SLINE=0.032+(CDIF*0.0353)
      ADMAT=0.0
851   CONTINUE
      WRITE(6,860)
      PRING(1)=PRING(1)*0.036126
      PRING(2)=PRING(2)*0.036126
      PRING(3)=PRING(3)*0.036126
```

235

```
      WRITE(6,861) PRING(1),PRING(2),PRING(3)
      WRITE(6,862) RADRAT,DISAMP
      IF(DISAMP.GT.SLINE) GOTO 870
      WRITE(6,872) SLINE
      GOTO 880
870   CONTINUE
      WRITE(6,869)
      DON=1.0
      WRITE(6,871) SLINE
      IF(ADMAT.GT.5.5) GOTO 890
      WRITE(6,892)
      GOTO 891
890   WRITE(6,893)
891   CONTINUE
880   CONTINUE

C     LIST THE OTHER DISTORTION FACTORS

      WRITE(6,62) A,B,C
      WRITE(6,678) AEDC
      WRITE(6,63) PATM

C     STORE SUMMARY DATA

      CONDC(IJK)=DON
      BCON(IJK)=BDON
      SUBD(IJK)=AEDC
      AUGRT(IJK)=AUGAIR/CMFTR
      CMF(IJK)=CMFTR
      CVT(IJK)=CVTRU
      DIS(IJK)=DISAMP
      DFC(IJK)=DFCIRM
      ACDV(IJK)=CVTRU*(12.17911/144.0)

C     WHEN THE LAST DATA SET HAS BEEN PROCESSED PRINT A
C     SUMMARY TABLE OF THE RESULTS FOR EACH CONFIGURATION

      IJK=IJK+1
      DON=0.0
      GOTO 99
50    CONTINUE
      WRITE(6,299)
      WRITE(6,300)
```

```
      DO 66 IJK=1,IROUN
      IF(BCON(IJK).GT.0.5) GOTO 9100
      IF(CONDC(IJK).GT.0.5) GOTO 9093
      GOTO 9090
 9100 IF(CONDC(IJK).GT.0.5) GOTO 9092
      GOTO 9091
 9093 WRITE(6,301) CON(IJK),CMF(IJK),CVT(IJK),ACDV(IJK),DIS(IJK),DFC(IJK
     C),SUBD (IJK),AUGRT(IJK)
      GOTO 66
 9090 WRITE(6,302) CON(IJK),CMF(IJK),CVT(IJK),ACDV(IJK),DIS(IJK),DFC(IJK
     C),SUBD (IJK),AUGRT(IJK)
      GOTO 66
 9091 WRITE(6,303) CON(IJK),CMF(IJK),CVT(IJK),ACDV(IJK),DIS(IJK),DFC(IJK
     C),SUBD (IJK),AUGRT(IJK)
      GOTO 66
 9092 WRITE(6,304) CON(IJK),CMF(IJK),CVT(IJK),ACDV(IJK),DIS(IJK),DFC(IJK
     C),SUBD (IJK),AUGRT(IJK)
   66 CONTINUE

      STOP
      END
```

237

```
                        PROGRAM TO SORT SUMMARY DATA
                        BY CONFIGURATION CODE AND PRINT
                        TABLES OF CONFIGURATIONS HAVING
                             COMMON COMPONENTS


      RESERVE THE REQUIRED STORAGE SPACE AND DESIGNAT
      THE DOUBLE PRECISION VARIABLES

      DIMENSION CON(300),CMF(300),CVT(300),DIS(300),DFC(300),CONDC(300),    00000020
     CACDV(300),SUBD(300),AUGRT(320),BCON(320),ZCVT(300),ZDIS(300),ZDFC(    00000030
     C300),CONDC(300),ZACDV(300),ZSUBD(300),ZAUGRT(300),ZBCON(300),ZSUBLO   00000040
     CIS(300),ZCMF(300)
      REAL*8 FCON,FCONDC,FSUBD,FCMF,FCVT,FDIS,FDFC,FACDV,FAUGRT,FBCON        00000060
      REAL*8 RICON,CCNHD                                                    00000070
      REAL*8 CON,SUBLIS,UPPER,LOWER                                         00000080

      READ IN SUMMARY DATA LINES UNTIL A NEGATIVE
      CONFIGURATION IS ENCOUNTERED

      DO 9301 I2=1,300                                                      00000090
      READ(5,9302) CON(I2),CMF(I2),CVT(I2),ACDV(I2),DIS (I2)                00000100
      IF(CON(I2).LT.0.0)GOTO 9973                                           00000110
      READ(5,9302) DFC(I2),SUBD(I2),AUGRT(I2),CONDC(I2),BCON(I2)            00000120
 9301 CONTINUE                                                              00000130
 9973 CONTINUE                                                              00000140

      SET THE REQUIRED INPUT AND OUTPUT FORMATS
```

```
9300  FORMAT(16)                                                       00000160
9302  FORMAT(5F12.6)                                                   00000170
9303  FORMAT(7/)                                                       00000180
299   FORMAT(1H1,//)                                                   00000190
      FORMAT(                                                          00000200
303   CIAL LEVEL    NUMBER      MDOT      VELOCITY  VELOCITY  RATIO  DISTO 00000210
CRTION                                                                 00000220
301   FORMAT(   ,F6.3,F7.4,'  SAT  ',F7.4,'  SAT  ',F7.4,2X,F5.3)
302   FORMAT(   ,F12.6,F6.3,F7.4,'  SAT  ',F7.4,'UNSAT',F7.4,2X,F5.3)
303   FORMAT(   ,F12.6,F6.3,F8.3,F7.4,'UNSAT',F7.4,'  SAT  ',F7.4,2X,F5.3)
304   FORMAT(   ,F12.6,F6.3,F8.3,F7.4,'UNSAT',F7.4,'UNSAT',F7.4,2X,F5.3)
1100  FORMAT(F6.2,//)
1104  FORMAT(1H1,//)
CDIGIT=' '

C     CONFIGURATIONS HAVING A ',I2,' AS THE NO- 'I2,'                  00000270

C     ESTABLISH A RETURN POINT AND SET COUNTING INDICES

      IROUN=I2-1                                                       00000150
      CHANGE=0.0                                                       00000100
511   CONTINUE
      IROUND=IROUN-1                                                   00000320

C     COMPARE THE FIRST TWO CONFIGURATION CODES.  IF THEY
C     ARE IN ASCENDING ORDER COMPARE THE SECOND. AND
C     THIRD CODES. CONTINUE UNTIL A PAIR IS FOUND TO
C     BE OUT OF ORDER

      DO 500 I3=1,IROUND                                               00000330
      IF(CON(I3).LE.CON(I3+1)) GOTO 502                                00000340

C     TRANSFER THE FIRST UNORDERED SET TO TEMPORARY
C     STORAGE

      FCON=CON(I3)                                                     00000350
      FCONDC=CONDC(I3)                                                 00000360
      FSUBD=SUBD(I3)                                                   00000370
      FCMF=CMF(I3)                                                     00000380
      FCVT=CVT(I3)                                                     00000390
      FDIS=DIS(I3)                                                     00000400
      FDFC=DFC(I3)                                                     00000410
      FACDV=ACDV(I3)                                                   00000420
      FAUGRT=AUGRT(I3)                                                 00000430
      FBCON=BCON(I3)                                                   00000440
```

```
C     REPLACE THE FIRST SET WITH THE SECOND
      CON(I3)=CON(I3+1)                                          00000450
      CONDC(I3)=CONDC(I3+1)                                      00000460
      SUBD(I3)=SUBD(I3+1)                                        00000470
      CMF(I3)=CMF(I3+1)                                          00000480
      CVT(I3)=CVT(I3+1)                                          00000490
      DIS(I3)=DIS(I3+1)                                          00000500
      DFC(I3)=DFC(I3+1)                                          00000510
      ACDV(I3)=ACDV(I3+1)                                        00000520
      AUGRT(I3)=AUGRT(I3+1)                                      00000530
      BCON(I3)=BCON(I3+1)                                        00000540
C     REPLACE THE SECOND DATA SET WITH THE FIRST FROM ITS
C     TEMPORARY STORAGE LOCATION
      CON(I3+1)=FCON                                             00000550
      CONDC(I3+1)=FCONDC                                         00000560
      SUBD(I3+1)=FSUBD                                           00000570
      CMF(I3+1)=FCMF                                             00000580
      CVT(I3+1)=FCVT                                             00000590
      DIS(I3+1)=FDIS                                             00000600
      DFC(I3+1)=FDFC                                             00000610
      ACDV(I3+1)=FACDV                                           00000620
      AUGRT(I3+1)=FAUGRT                                         00000630
      BCON(I3+1)=FBCON                                           00000640
C     INDICATE THAT A CHANGE HAS BEEN MADE DURING THIS PASS
      CHANGE=1.0                                                 00000650
  502 CONTINUE                                                   00000660
C     RETURN TO COMPARE THE SECOND OF THESE NOW ORDERED
C     SETS WITH THE NEXT CONFIGURATION NOT PROCESSED
```

240

```
500 CONTINUE

      IF NO CHANGES WERE MADE IN COMPARING EACH PAIR OF    00000680
      CONFIGURATION CODES TERMINATE SORTING; OTHERWISE     00000690
      RETURN AND REPEAT THE COMPARISON CHECK               00000700
                                                           00000710
      IF(CHANGE.LT.0.5) GOTO 510                           00000720
      CHANGE=0.0                                           00000730
      IROUND=IROUND-1
  510 CONTINUE
 1106 CONTINUE

      READ FROM A DATA CARD THE FIRST COMPONENT CODE       00000740
      DESIRED AND THE POSITION IN WHICH IT MUST OCCUR      00000750
      FOR INCLUSION IN THE SUMMARY TABLE. IF THE CODE      00000760
      IS NEGATIVE TERMINATE                                00000770

      READ(5,1100) POSIT,DES
      IPOSIT=POSIT
      IDES=DES
      IF(IPOSIT.LE.0) GOTO 1101

      SEPARATE FROM THE CONFIGURATION CODE THE DIGIT       00000780
      IN THE DESIRED POSITION                              00000790
                                                           00000800
      KES=1                                                00000810
      DO 1102 KEY=1,IROUN                                  00000820
      IXPON=IPOSIT-4                                       00000830
      UPPER=CON(KEY)*(10..0**IXPON)                        00000840
      ILOW=UPPER/10..0                                     00000850
      LOWER=ILOW
      LOWER=LOWER*10..0
      IDIF=UPPER-LOWER

      IF THIS SEPARATED DIGIT IS EQUAL TO THAT REQUIRED,
      STORAGE THE ASSOCIATED SUMMARY DATA IN THE TABLE
      STORAGE MATRIX. IF IT IS NOT, RETURN AND CONSIDER THE
      NEXT CONFIGURATION CODE
```

```
      IF(IDIF.EQ.IDES) GOTO 1103                                        00000860
      GOTO 1102                                                         00000870
1103  CONTINUE                                                          00000880
      SUBLIS(KES)=CON(KEY)                                              00000890
      CONDCD(KES)=CONDC(KEY)                                            00000900
      ZSUBD(KES)=SUBD(KEY)                                              00000910
      ZCMF(KES)=CMF(KEY)                                                00000920
      ZCVT(KES)=CVT(KEY)                                                00000930
      ZDIS(KES)=DIS(KEY)                                                00000940
      ZDFC(KES)=DFC(KEY)                                                00000950
      ZACDV(KES)=ACDV(KEY)                                              00000960
      ZAUGRT(KES)=AUGRT(KEY)                                            00000970
      ZBCON(KES)=BCON(KEY)                                              00000980
      KES=KES+1                                                         00000990
1102  CONTINUE                                                          00001000
C
C     PRINT THE TABLE HEADING AND IDENTIFY THE DIGIT
C     AND POSITION REQUIRED FOR INCLUSION
C
      WRITE(6,1104) IDES,IPOSIT                                         00001010
      WRITE(6,299)                                                      00001020
      WRITE(6,300)                                                      00001030
C
C     EXAMINE THE CONTENT OF EACH DATA LINE AND PRINT IT
C     IN TABLE FORM WITH THE PROPER FORMAT
C
      IF(KES.EQ.1) GOTO 1106                                            00001040
      IDED=IKES-1                                                       00001050
      DO 1105 KET=1,IDEDT                                               00001060
      BIGGER=DFC(KET)*10000.0                                           00001070
      ING=BIGGER                                                        00001080
      SMALL=ING                                                         00001090
      DFC(KET)=SMALL/10000.0                                            00001100
      IF(ZBCON(KET).GT.0.5) GOTO 6100                                   00001110
      IF(CONDCD(KET).GT.0.5) GOTO 6093                                  00001120
      GOTO 6090                                                         00001130
6100  IF(CONDCD(KET).GT.0.5) GOTO 6092
6093  WRITE(6,301) SUBLIS(KET),ZCMF(KET),ZCVT(KET),ZDIS(KET),          00001150
     CZDFC(KET),ZSUBD(KET),ZAUGRT(KET)                                  00001160
      GOTO 6661                                                         00001170
6090  WRITE(6,302) SUBLIS(KET),ZCMF(KET),ZCVT(KET),ZDIS(KET),          00001180
     CZDFC(KET),ZSUBD(KET),ZAUGRT(KET)                                  00001190
                                                                        00001200
```

```
      GOTO 6661
 6091 WRITE(6,303) SUBLIS(KET),ZCMF(KET),ZCVT(KET),   ZDIS(KET),      00001210
     CZDFC(KET),ZSUBD(KET),ZAUGRT(KET)                                00001220
      GOTO 6661                                                       00001230
 6092 WRITE(6,304) SUBLIS(KET),ZCMF(KET),ZCVT(KET),   ZDIS(KET),      00001240
     CZDFC(KET),ZSUBD(KET),ZAUGRT(KET)                                00001250
 6661 CONTINUE                                                        00001260
 1108 CONTINUE                                                        00001270
 1105 CONTINUE                                                        00001280
      GOTO 1106                                                       00001290
 1131 CONTINUE                                                        00001300
                                                                      00001310

      IF NO ADDITIONAL TABLES ARE REQUIRED, TERMINATE

      STOP                                                            00001320
      END                                                             00001330
```

243

REFERENCES

1. Burns & Roe, Inc., <u>Standard Test Cell Design Study for the Joint Airline Committee</u>, April 1971.

2. Olive, R. L., <u>Modern Jet Engine Development Facility</u>, ASME Paper 71-WA/GT-6, August 1971.

3. North American Rockwell Corp., NA-69-57, <u>An Investigation of Subsonic Duct Distortion</u>, MacMiller, C. J., March 1969.

4. Leef, C. R., "Development of Nonrecirculating Wind Tunnel Configurations Insensitive to External Winds," <u>Journal of Aircraft</u>, Vol. 6, No. 3, May-June 1969.

5. Heat Transfer Laboratory, Mechanical Eng. Dept., University of Minnesota, Contract No. AF 33(616)474, <u>Incompressible Friction Factor, Transition and Hydrodynamic Entrance-Length Studies of Ducts with Triangular and Rectangular Cross Sections</u>, Eckert, E. R. G., Irvine, T. F., February 1965.

6. Air Force Systems Command Wright-Pattern Air Force Base, <u>FY 1971 Military Construction Proposal</u>, February 1969.

7. Kays, W. M., <u>Convective Heat and Mass Transfer</u>, McGraw-Hill, New York, 1966.

8. Eckert, E. R. G. and Irvine, T. F., "Flow in Corners of Passages with Non-Circular Cross Section," <u>Transactions of the ASME</u>, Vol. 78, No. 4, p. 709, May 1956.

9. Industrial Acoustics Company, Bulletin 4.0001.0, <u>Noise Control for Gaseous Flow Systems</u>.

10. Flight Propulsion Division, General Electric Corp., <u>Airline Planning Guide; Test Facilities for Large Advanced Turbojet and Turbofan Engines</u>, 1 April 1967.

11. Smith, A. J. W., "Subsonic Adiabatic Flow in a Duct of Constant Cross Sectional Area," <u>Journal of the Royal Aeronautical Society</u>, Vol. 68, p. 117-127, February 1963.

12. Colehour, J. L. and Farquhar, B. W., "Inlet Vortex," <u>Journal of Aircraft</u>, Vol. 8, No. 1, January 1971.

13. Arnold Engineering Development Facility, TR-71-50, <u>Effect of Steady Inlet Distortion on the Stability and Performance Characteristics of an Augmented Turbofan Engine</u>, Palmer, J. D., Parker, J. R., and Schwall, J. R., April 1971.

14. Reid, C., The Response of Axial Flow Compressor to Intake Flow Distortion, ASME Paper 69-GT-29 presented at the ASME Symposium, 9-13 March 1969.

15. Northern Research and Engineering Corp., Compressor Sensitivity to Transient and Distorted Transient Flows, Jansen, W., Swarden, M. C., and Carlson, A. W., December 1969.

16. Vavra, M. H., Aero-Thermodynamics and Flow in Turbomachines, Chapter 9, John Wiley & Sons, New York, 1960.

17. Naval Air Test Center Report No. ST-64R-69, J52-P8A Engine Stall Margin Investigation, Matechak, J. and Thomas, L. A., 20 August 1969.

18. NASA TM-X-1928, Experimental Investigation of the Effects of Pressure Distortion Imposed on the Inlet of a Turbofan Engine, Wenzel, L. M., November 1961.

19. Air Force Propulsion Laboratory Technical Report AFPL-TR-69-113, Advanced Tactical Fighter Accommodation Control System Analysis, Bayati, J. E. and Tyson, R. M., February 1970.

20. The Boeing Company, Experimental Correlation of Installation Effects for Inlet/Airplane Integration, Ball, W. H. and Ross, P. A., August 1969.

21. Corrsin, S., "Turbulent Flow," American Scientist, Vol. 49, No. 3, pp 300-325, September 1961.

22. Dwyer, H. A., Doss, E. D., and Goldman, A., "Rapid Calculation of Inviscid and Viscous Flow over Arbitrary Shaped Bodies," Journal of Aircraft, Vol. 8, No. 42, February 1971.

23. Burggraf, O. R., "Analytical and Numerical Studies of the Structure of Steady Separated Flows," Fluid Mechanics, Vol. 24, part 1, pp. 113-151, 1966.

24. Dixon, T. N., A Study on Stability and Incipient Turbulence in Poiseuille Flow by Numerical Finite Difference Simulation, Ph.D. Thesis, Rice University, 1966.

25. NACA TN-4241, An Approximate Method for Design or Analysis of Two-Dimensional Subsonic-Flow Passages, Valentine, E. F., November 1952.

26. Benedict, R. P., Handbook of Generalized Gas Dynamics, Plenum Press, New York, 1966.

27. Ferguson, T. B., "Stagnation Pressure and Losses in Ducts," Bulletin of Mechanical Engineering Education, Vol. 1, pp. 99-103, 1962.

28. Livesey, J. L., Duct Performance Parameter Considering Spatially Non-Uniform Flow, paper presented at the AIAA Tenth Aerospace Sciences Meeting, San Diego, California, 17-19 January 1972.

29 Carrier, W. H., and others, Modern Air Conditioning, Heating and Ventilating, Pitman, New York, 1959.

30. Keuth, A. M. and Schelzer, J. D., Foundations of Aerodynamics, John Wiley & Sons, New York, 1969.

31. Schlichting, H., Boundary Layer Theory, McGraw-Hill, New York, 1968.

32. Robertson, J. M., Hydrodynamics in Theory and Application, Prentice-Hall, Englewood Cliffs, New Jersey, 1965.

33. Holt, M., (ed.), Basic Developments in Fluid Dynamics, Academic Press, New York, 1965.

34. Cornell, W. G., "Losses in Flow Normal to Plane Screens," Transactions of the ASME, Vol. 27, pp. 791-799, August 1957.

35. NACA RM L57G08, An Investigation of Screens for Removing Distortions in Ducted Flows at High Subsonic Speeds, Wood, C. C., and Knip, G., July 1954.

36. Arnold Engineering Development Center, AEDC-TR-69-171, Evaluation of a Rotating Screen System for Producing Distortion at the Inlet of Turbojet Engines, Christenson, R. J. and Parker, J. R.,

37. NASA Report, Experimental Investigation of Expanded Duct Sections and Screens for Reducing Distortion in Subsonic Flows, Chiccine, B. G. and Abdalla, K. L., May 1959.

38. FluiDyne Engineering Corp. Project 0482, Aerodynamic Model Study of Test Cells 2, 5, 6, 7, Building 500, Idzoref, J. J., August 1965.

39. Pratt & Whitney Aircraft Co., Contract Report F33516-67-C 1848, Experimental Evaluation of a Hypothesis for Scaling Inlet Turbulence Data, Sherman, D. A., Motycka, D. L., and Oates, G. C., July 1971.

40. Comte-Bellot, G. and Corrsin, S., "The Use of Contraction to Improve the Isotropy of Grid-Generated Turbulence," The Journal of Fluid Mechanics, Vol. 25, part 4, pp. 657-682, 1966.

41. Bailey, D. L., An Analytic and Experimental Analysis of Factors Affecting Exhaust System Performance in Sea Level Static Jet Engine Test Facilities, Ae. E. Thesis, Naval Postgraduate School, Monterey, California, 1972.

42. Brunda, D. F. and Boytos, J. F., A Steady State Radial Inlet Pressure Distortion Index for Axial Flow Compressors, paper presented at the Gas Turbine and Fluids Engineering Conference, San Francisco, March 26-30, 1972.

43. NACA TN 4318, <u>Analytical Relation for Wake Momentum Thickness and Diffusion Ratio for Low Speed Turning Vanes</u>, Lieblein, S.

44. Naval Air Propulsion Test Center Report NAPTC-ATD-193, <u>Evaluation of a Circumferential Inlet Pressure Distortion Index on a TF30-P-12 Turbofan Engine</u>, Brunda, D. F. and Boytos, J. F., July 1970.

45. Naval Ships Engineering Command, Contract NObs92176, <u>Testing of Gas Turbine High Velocity Duct Systems</u>, Kelchofer, W. J. and Smith, R. A., August 1966.

INITIAL DISTRIBUTION LIST

No. Copies

1. Defense Documentation Center   2
   Cameron Station
   Alexandria, Virginia 22314

2. Library, Code 0212   2
   Naval Postgraduate School
   Monterey, California 93940

3. Dean of Research Administration   1
   Naval Postgraduate School
   Monterey, California 93940

4. Professor A. E. Fuhs, Code 57Fu   15
   Department of Aeronautics
   Naval Postgraduate School
   Monterey, California 93940

5. Lt. David L. Bailey   1
   721 Jamica Ct.
   St. Louis, Missouri 63122

6. Lt. Philip W. Tower   5
   775 Santa Clara
   Alameda, California 94501

7. John Adams   1
   AIR-4147B
   Naval Air Systems Command
   Washington, D. C. 20360

8. Rollin Boe   1
   R-I Corporation
   499 W. 2$^{\text{nd}}$ Street
   Ogden, Utah 84402

9. J. S. Brody   1
   Chief Test Engineer
   Detroit Diesel Allison
   Division of General Motors Corp.
   P. O. Box 894, Mailstop s16
   Indianapolis, Indiana 46206

10. Howard F. Carter   1
    Supervisor, Propulsion Systems
    Vought Aeronautics Company
    P. O. Box 5907
    Dallas, Texas 75222

11. George Davies 1
    Price Clark Industries
    420 South Pine Street
    San Gabriel, California 91776

12. Frank Freeman 12
    Code 642, Bldg. 94
    Naval Air Rework Facility
    NAS North Island, California 92135

13. Gustav Getter 1
    Gustav Getter Associates
    524 North Avenue
    New Rochelle, New York 10801

14. Karl Guttman 1
    Code 330
    Naval Air Systems Command
    Washington, D. C. 20360

15. Capt. W. D. Harkins 1
    Commanding Officer
    Naval Air Rework Facility
    NAS North Island, California 92135

16. A. A. Heinisch 1
    Burns and Roe, Inc
    Suite 618
    9800 South Sepulveda Blvd.
    Los Angeles, California 90045

17. Dr. James S. Holdhusen 1
    FluiDyne Engineering Corporation
    5900 Olson Memorial Highway
    Minneapolis, Minnesota

18. D. F. Jamison 1
    General Electric Company
    3430 South Dixie Highway
    Dayton, Ohio 45439

19. Francis S. Kirschner 1
    The Souncoat Company, Inc.
    175 Pearl Street
    Brooklyn, New York 11201

20. Harry Lindenhofen 1
    Naval Air Propulsion Center
    AE Department, Bldg. 600
    Philadelphia, Pa. 19112

21. Barrett R. Lucas   1
     Marketing Engineer
     Pratt & Whitney
     Aircraft Division
     United Aircraft Corporation
     East Hartford, Conn.

22. Dennis O'Dell   2
     AIR-53431B
     Naval Air Systems Command
     1421 Jefferson Davis Highway
     Washington, D. C.

23. Robert L. Olive   1
     AiResearch Manufacturing Company
     2525 W. 190th Street
     Torrance, California   90509

24. Eugene T. Pulcher   2
     Naval Air Engineering Center
     GSE Division 76-1
     Philadelphia, Pa.   19112

25. Chet Roscoe   1
     04 Group
     Naval Air Systems Command
     Washington, D. C.   20360

26. Irv Silver   1
     Code 03A
     Naval Air Systems Command
     Washington, D. C.

27. Cyril S. Staub   1
     AIR-4147A
     Naval Air Systems Command
     Washington, D. C.

28. R. E. Totman   1
     Power Plant Engineering
     United Air Lines
     San Francisco International Airport
     San Francisco, California   94128

29. R. W. Bell   1
     Chairman, Department of Aeronautics
     Naval Postgraduate School
     Monterey, California   93940

30. D. F. Brunda   1
     Naval Air Propulsion Test Center
     Trenton, New Jersey   19112

DOCUMENT CONTROL DATA - R & D		
(Security classification of title, body of abstract and indexing annotation must be entered when the overall report is classified)		
1. ORIGINATING ACTIVITY (Corporate author) Naval Postgraduate School Monterey, California 93940	2a. REPORT SECURITY CLASSIFICATION Unclassified	
	2b. GROUP	

REPORT TITLE

The Dependence of Compressor Face Distortion on Test Cell Inlet Configuration

4. DESCRIPTIVE NOTES (Type of report and, inclusive dates)
Aeronautical Engineer; December 1972

5. AUTHOR(S) (First name, middle initial, last name)

Philip William Tower

6. REPORT DATE December 1972	7a. TOTAL NO. OF PAGES 252	7b. NO. OF REFS 45
8a. CONTRACT OR GRANT NO.	9a. ORIGINATOR'S REPORT NUMBER(S)	
b. PROJECT NO.		
c.	9b. OTHER REPORT NO(S) (Any other numbers that may be assigned this report)	
d.		

10. DISTRIBUTION STATEMENT

This document is approved for public release and sale; its distribution is unlimited.

11. SUPPLEMENTARY NOTES	12. SPONSORING MILITARY ACTIVITY Naval Postgraduate School Monterey, California 93940

13. ABSTRACT

The aircraft turbine engine has evolved to the point that current static test facility designs require modification to provide adequate service and growth potential. Current design procedures are inadequate in that they do not provide methods for the prediction of flow uniformity at the increased thrust and air flow rates now being required. Through the testing of a multiplicity of inlet models the effect of test cell inlet configuration on engine distortion level is evaluated. A method is developed for the correlation of inlet design characteristics with experimentally observed distortion levels. Together with the evaluation of augmentor performance in an associated thesis by Lt. David L. Bailey, this tentative correlation provides a basis for the development of a practical system for the prediction of the performance of proposed test cell designs.

DD FORM 1 NOV 65 1473 (PAGE 1)

S/N 0101-807-6811

A-31408

14 KEY WORDS	LINK A		LINK B		LINK C	
	ROLE	WT	ROLE	WT	ROLE	WT
Future jet engine development						
Jet engine test facilities						
Test cell design						
Environmental protection						
Duct flow						
Acoustic control techniques						
Jet mixing						
Industrial safety						
Automatic data acquisition						
Model tests						
Test facility construction						
Boundary layer growth						
Construction aerodynamics						

DD FORM 1473 (BACK)
1 NOV 65
S/N 0101-807-6821

252

UNCLASSIFIED
Security Classification

A-31409